



South Dakota
Department of Transportation
Office of Research



U.S. Department
of Transportation
**Federal Highway
Administration**

SD2013-01-F



Precast Bridge Girder Details for Improved Performance

**Study SD2013-01
Final Report**

Prepared by
South Dakota State University
Brookings, SD 57007

May 2017

DISCLAIMER

The contents of this report, funded in part through grant(s) from the Federal Highway Administration, reflect the views of the authors who are responsible for the facts and accuracy of the data presented herein. The contents do not necessarily reflect the official views or policies of the South Dakota Department of Transportation, the State Transportation Commission, or the Federal Highway Administration. This report does not constitute a standard, specification, or regulation.

The South Dakota Department of Transportation provides services without regard to race, color, gender, religion, national origin, age or disability, according to the provisions contained in SDCL 20-13, Title VI of the Civil Rights Act of 1964, the Rehabilitation Act of 1973, as amended, the Americans With Disabilities Act of 1990 and Executive Order 12898, Federal Actions to Address Environmental Justice in Minority Populations and Low-Income Populations, 1994. Any person who has questions concerning this policy or who believes he or she has been discriminated against should contact the Department's Civil Rights Office at 605.773.3540.

ACKNOWLEDGEMENTS

This work was performed under the direction of the SD2013-01 Technical Panel:

Dustin Artz	Research	Penny Goetz	Walworth County Highway Dept.
Ron Bren	Local Government Assistance	Brian Olson.....	Local Transportation Programs
Aaron Breyfogle	Research	Josh Olson	Aberdeen Region
Mark Clausen	FHWA	Jason Smith	Materials & Surfacing
Toby Crow	Associated General Contractors	Larry Weiss	SDLTAP
Barney Frankl	Bridge Design		

The authors would like to acknowledge Cretex Concrete Products, Inc. for their contribution throughout the project. Special thanks go to Corey Hader of Cretex West, Aaron Breyfogle of the Research Office at South Dakota Department of Transportation, and Zachary Gutzmer of South Dakota State University for their assistance and valuable contribution to the project.

TECHNICAL REPORT STANDARD TITLE PAGE

1. Report No. SD2013-01-F	2. Government Accession No.	3. Recipient's Catalog No.	
4. Title and Subtitle Bridge Girder Details for Improved Performance		5. Report Date 05/08/2017	
		6. Performing Organization Code	
7. Author(s) Nadim Wehbe and Michael Konrad		8. Performing Organization Report No.	
9. Performing Organization Name and Address South Dakota State University Crothers Engineering Hall/Box 2219 Brookings, SD 57007		10. Work Unit No. HRV301	
		11. Contract or Grant No. 311183	
12. Sponsoring Agency Name and Address South Dakota Department of Transportation Office of Research 700 East Broadway Avenue Pierre, SD 57501-2586		13. Type of Report and Period Covered Final Report November 2013 – May 2017	
		14. Sponsoring Agency Code	
15. Supplementary Notes An executive summary is published separately as SD2013-01-X.			
16. Abstract <p>Precast/prestressed double tee bridge girders are widely used for accelerated bridge construction on local roads in South Dakota. A common issue among existing double tee bridges in South Dakota is the rapid deterioration of longitudinal joints (shear keyways) between adjacent girders. Deteriorated joints allow moisture and deicing chemicals to reach the deck reinforcement, leading to premature corrosion of reinforcing steel and spalling of concrete.</p> <p>The structural performance of conventional and proposed longitudinal joints between precast double tee bridge girders was examined experimentally under cyclic and monotonic loading. Two 40-ft long full-scale bridge superstructure specimens, each consisting of two joined double tee girders, were tested at the Lohr Structures Laboratory at South Dakota State University (SDSU). Each specimen represented two adjacent interior girders of a two-lane bridge having a width of an approximately 31 ft. The proposed continuous joint with overlapping steel mesh reinforcement in a grouted shear keyway exhibited substantially improved serviceability and strength performance characteristics over the conventional grouted joint with discrete welded connections.</p>			
17. Keywords ABC, Bridge Deck, Double Tee, Fatigue, Shear Key		18. Distribution Statement No restrictions. This document is available to the public from the sponsoring agency.	
19. Security Classification (of this report) Unclassified	20. Security Classification (of this page) Unclassified	21. No. of Pages 121	22. Price

TABLE OF CONTENTS

DISCLAIMER	II
ACKNOWLEDGEMENTS.....	II
TECHNICAL REPORT STANDARD TITLE PAGE	IV
TABLE OF CONTENTS	V
LIST OF TABLES.....	VII
LIST OF FIGURES.....	VII
TABLE OF ACRONYMS.....	IX
1 EXECUTIVE SUMMARY	1
1.1 INTRODUCTION	1
1.2 PROBLEM DESCRIPTION	1
1.3 RESEARCH WORK	1
1.4 RESEARCH FINDINGS	2
1.5 RECOMMENDATIONS	4
1.5.1 Terminology	4
1.5.2 Discrete Welded Joint.....	4
1.5.3 Monolithic Joint.....	4
1.5.4 Future Research	5
2 PROBLEM DESCRIPTION.....	6
3 RESEARCH OBJECTIVES	8
3.1 IDENTIFY GIRDER DESIGN ALTERNATIVES.....	8
3.2 LOAD TEST ALTERNATIVE GIRDERS.....	8
4 TASK DESCRIPTIONS.....	9
4.1 MEET WITH TECHNICAL PANEL.....	9
4.2 REVIEW LITERATURE	9
4.3 CREATE AND ADMINISTER SURVEY	9
4.4 CONFER WITH PRECAST COMPANIES	9
4.5 PREPARE TECHNICAL MEMORANDUM	9
4.6 PREPARE TESTING PLAN.....	10
4.7 CONSTRUCT TEST GIRDERS.....	10
4.8 PERFORM LOAD TESTING	10
4.9 COMPARE GIRDER PERFORMANCE	10
4.10 RECOMMEND GIRDER DESIGN	11
4.11 PREPARE FINAL REPORT.....	11
4.12 MAKE EXECUTIVE PRESENTATION	11
5 LITERATURE REVIEW	12
5.1 JONES	12
5.2 LI, MA, AND OESTERLE.....	13
5.3 ZHU, MA, AND FRENCH	14
5.4 CONCLUDING REMARKS.....	15
6 SURVEY OF STATE DOT AND LOCAL HIGHWAYS OFFICIALS.....	16
6.1 BROOKINGS COUNTY, SOUTH DAKOTA	16

6.2	PENNINGTON COUNTY, SOUTH DAKOTA	16
6.3	CASS COUNTY, NORTH DAKOTA	16
6.4	NEBRASKA DEPARTMENT OF ROADS.....	16
6.5	MONTANA BRIDGE BUREAU	16
6.6	WASHINGTON DOT BRIDGE DESIGN OFFICE	17
7	TEST SPECIMENS.....	18
7.1	DESIGN OF THE TEST SPECIMENS	18
7.1.1	“Conventional” Specimen.....	19
7.1.2	“Proposed” Specimen.....	20
7.2	FABRICATION AND ASSEMBLY OF THE TEST SPECIMENS	22
7.2.1	“Conventional” Specimen.....	22
7.2.2	“Proposed” Specimen.....	24
7.3	TEST SETUP	26
7.4	INSTRUMENTATION.....	27
7.4.1	Strain Gages.....	27
7.4.2	Linear Variable Differential Transformers.....	28
7.4.3	Cable Extension Transducers.....	29
7.4.4	Load Cells	29
7.4.5	Data Acquisition System.....	30
7.5	TEST PROCEDURE	30
7.5.1	Fatigue Testing.....	30
7.5.2	Strength Testing.....	31
8	EXPERIMENTAL RESULTS AND ANALYSIS.....	32
8.1	MATERIAL PROPERTIES.....	32
8.1.1	Fresh and Hardened Concrete Properties.....	32
8.1.2	Fresh and Hardened Properties of the Grout Mix	33
8.1.3	Prestressing Strand Properties	33
8.2	TEST RESULTS – “CONVENTIONAL” SPECIMEN	34
8.2.1	Fatigue I Loading.....	34
8.2.2	Fatigue II Loading.....	36
8.2.3	Strength Test.....	38
8.3	TEST RESULTS – “PROPOSED” SPECIMEN	40
8.3.1	Fatigue II Loading.....	40
8.3.2	Fatigue I Loading.....	43
8.3.3	Strength Test.....	44
8.4	ANALYSIS OF EXPERIMENTAL RESULTS	46
8.4.1	Fatigue Life.....	46
8.4.2	Stiffness Degradation.....	47
8.4.3	Flexural Strength.....	47
8.4.4	Reactions at the Support.....	48
8.4.5	Effect of Shear Span on Reaction Force Distribution to the Girder Stems.....	50
8.4.6	Joint Shear.....	51
8.5	COST ESTIMATE FOR THE PROPOSED JOINT.....	54
9	FINDINGS AND CONCLUSIONS.....	55
9.1	FINDINGS.....	55
9.2	CONCLUSIONS.....	56
10	RECOMMENDATIONS	58
10.1	TERMINOLOGY	58
10.2	DISCRETE WELDED JOINT	58

10.3	MONOLITHIC JOINT	58
10.4	FUTURE RESEARCH	58
11	RESEARCH BENEFITS	60
12	REFERENCES.....	61
	APPENDIX A: KICKOFF MEETING.....	63
	APPENDIX B: SURVEY TOOL	68
	APPENDIX C: TECHNICAL MEMORANDA (TASKS 5 AND 6)	71
	APPENDIX D: PLANS AND DETAILS OF TEST SPECIMENS	84
	APPENDIX E: TECHNICAL DATA SHEET FOR THE GROUT MATERIAL.....	90
	APPENDIX F: CALCULATIONS	92
	APPENDIX G: MEASURED STRAINS	95
	APPENDIX H: FINITE ELEMENT ANALYSIS	97
	APPENDIX I: ADDITIONAL LITERATURE REVIEW	104

LIST OF TABLES

TABLE 1:	FRESH CONCRETE PROPERTIES.....	32
TABLE 2:	FRESH CONCRETE PROPERTIES.....	32
TABLE 3:	FRESH PROPERTIES OF THE GROUT MIX.....	33
TABLE 4:	MEASURED COMPRESSIVE STRENGTH OF THE GROUT MIX.....	33
TABLE 5:	STAGES OF JOINT DETERIORATION DURING FATIGUE I – “CONVENTIONAL” SPECIMEN	46
TABLE 6:	STAGES OF JOINT DETERIORATION DURING FATIGUE II – “CONVENTIONAL” SPECIMEN	46
TABLE 7:	STAGES OF JOINT FATIGUE – “PROPOSED” SPECIMEN	47
TABLE 8:	STIFFNESS DEGRADATION EFFECTIVE RATES	47
TABLE 9:	MEASURED REACTIONS AT THE STEMS OF THE NORTH END SUPPORT (P = 42 KIPS).....	48
TABLE 10:	REACTIONS BASED ON SIMPLIFIED STRUCTURAL ANALYSIS (P = 42 KIPS).....	49
TABLE 11:	EXPERIMENTAL AND ANALYTICAL REACTIONS (P = 21 KIPS) – “CONVENTIONAL” SPECIMEN	50
TABLE 12:	EXPERIMENTAL AND ANALYTICAL REACTIONS (P = 21 KIPS) – “PROPOSED” SPECIMEN WITH NO DIAPHRAGMS	50
TABLE 13:	SUMMARY OF ANALYTICAL REACTION FORCE DISTRIBUTION FOR DIFFERENT SHEAR SPANS	51

LIST OF FIGURES

FIGURE 2-1:	GROUTED SHEAR KEYWAY WITH DISCRETE WELDED CONNECTIONS	6
FIGURE 2-2:	REFLECTIVE CRACKING OF THE ASPHALT OVERLAY.....	7
FIGURE 2-3:	CONCRETE DETERIORATION IN THE DECK OVERHANG OF A DOUBLE TEE BRIDGE.....	7
FIGURE 5-1:	TXDOT JOINT DETAIL (JONES, 1998)	12
FIGURE 5-2:	PROPOSED SIMPLE DETAIL FOR TXDOT GIRDERS (JONES, 1998)	13
FIGURE 5-3:	JOINT DETAIL BY LI ET AL. (2010).....	14
FIGURE 5-4:	U-BAR JOINT REINFORCEMENT DETAIL.....	15
FIGURE 7-1:	HL-93 TRUCK (AASHTO 2012)	18
FIGURE 7-2:	CROSS SECTION OF HYPOTHETICAL BRIDGE FOR SIZING THE “CONVENTIONAL” SPECIMEN	19
FIGURE 7-3:	STANDARD 3 FT-10IN WIDE BY 23 IN. DEEP DOUBLE TEE SECTION.....	19
FIGURE 7-4:	DETAILS OF THE “CONVENTIONAL” SPECIMEN.....	20
FIGURE 7-5:	CROSS SECTION OF HYPOTHETICAL BRIDGE FOR SIZING THE “PROPOSED” SPECIMEN	20
FIGURE 7-6:	CROSS SECTION OF THE “PROPOSED” SPECIMEN (2 ND MESH NOT SHOWN)	21

FIGURE 7-7: JOINT DETAILS OF THE “PROPOSED” SPECIMEN (2 ND MESH NOT SHOWN)	21
FIGURE 7-8: FABRICATION OF THE GIRDERS FOR THE “CONVENTIONAL” SPECIMEN	22
FIGURE 7-9: UNLOADING AND POSITIONING OF THE GIRDERS	23
FIGURE 7-10: VARYING GAP AT BOTTOM OF LONGITUDINAL JOINT OF THE “CONVENTIONAL” SPECIMEN	23
FIGURE 7-11: CONNECTION AT LONGITUDINAL JOINT OF THE “CONVENTIONAL” SPECIMEN	24
FIGURE 7-12: STEEL SLEEVE AND SHEAR KEY TIMBER FORMWORK – “PROPOSED” SPECIMEN	24
FIGURE 7-13: JOINT FORMWORK FOR THE “PROPOSED” SPECIMEN	25
FIGURE 7-14: RESTRAINING DIAPHRAGM IN PLACE	25
FIGURE 7-15: ISOMETRIC RENDERING OF THE TEST SETUP	26
FIGURE 7-16: DETAILS OF THE TEST SETUP	26
FIGURE 7-17: SURFACE-MOUNTED AND EMBEDDED STRAIN GAGES	27
FIGURE 7-18: STRAIN GAGE PLACEMENT	27
FIGURE 7-19: LVDT SYSTEM FOR MEASURING VERTICAL DEFLECTION	28
FIGURE 7-20: LVDT SYSTEM FOR MEASURING JOINT TRANSVERSE ROTATION	28
FIGURE 7-21: LVDT FOR MEASURING RELATIVE VERTICAL DISPLACEMENT	29
FIGURE 7-22: CABLE EXTENSION TRANSDUCERS	29
FIGURE 7-23: LOAD CELL FOR MEASURING REACTIONS	30
FIGURE 8-1: CONCRETE STRENGTH GAIN	33
FIGURE 8-2: DETERIORATION OF THE JOINT IN THE “CONVENTIONAL” SPECIMEN	34
FIGURE 8-3: MEASURED STIFFNESS DURING FATIGUE I – “CONVENTIONAL” SPECIMEN	35
FIGURE 8-4: STIFFNESS DEGRADATION DURING FATIGUE I – “CONVENTIONAL” SPECIMEN	35
FIGURE 8-5: RELATIVE DEFLECTION AND JOINT ROTATION DURING FATIGUE I – “CONVENTIONAL” SPECIMEN	36
FIGURE 8-6: RELATIVE DEFLECTION AT THE JOINT – “CONVENTIONAL” SPECIMEN	36
FIGURE 8-7: MEASURED STIFFNESS DURING FATIGUE II – “CONVENTIONAL” SPECIMEN	37
FIGURE 8-8: STIFFNESS DEGRADATION DURING FATIGUE II – “CONVENTIONAL” SPECIMEN	37
FIGURE 8-9: RELATIVE DEFLECTION AND JOINT ROTATION DURING FATIGUE II – “CONVENTIONAL” SPECIMEN	38
FIGURE 8-10: MEASURED LOAD-DEFLECTION DURING STRENGTH TEST – “CONVENTIONAL” SPECIMEN	39
FIGURE 8-11: “CONVENTIONAL” SPECIMEN AT FAILURE	39
FIGURE 8-12: MEASURED RELATIVE DEFLECTION AND JOINT ROTATION – “CONVENTIONAL” SPECIMEN	39
FIGURE 8-13: MEASURED END REACTIONS – “CONVENTIONAL” SPECIMEN	40
FIGURE 8-14: MEASURED STIFFNESS DURING FATIGUE II WITH 7 DIAPHRAGMS – “PROPOSED” SPECIMEN	40
FIGURE 8-15: STIFFNESS DEGRADATION DURING FATIGUE II WITH 7 DIAPHRAGMS – “PROPOSED” SPECIMEN	41
FIGURE 8-16: RELATIVE DEFLECTION AND JOINT ROTATION DURING FATIGUE II WITH 7 DIAPHRAGMS – “PROPOSED” SPECIMEN	41
FIGURE 8-17: MEASURED STIFFNESS DURING FATIGUE II WITHOUT DIAPHRAGMS – “PROPOSED” SPECIMEN	42
FIGURE 8-18: STIFFNESS DEGRADATION DURING FATIGUE II WITHOUT DIAPHRAGMS – “PROPOSED” SPECIMEN	42
FIGURE 8-19: RELATIVE DEFLECTION AND JOINT ROTATION DURING FATIGUE II WITHOUT DIAPHRAGMS – “PROPOSED” SPECIMEN	42
FIGURE 8-20: MEASURED STIFFNESS DURING FATIGUE I – “PROPOSED” SPECIMEN	43
FIGURE 8-21: STIFFNESS DEGRADATION DURING FATIGUE I – “PROPOSED” SPECIMEN	43
FIGURE 8-22: RELATIVE DEFLECTION AND JOINT ROTATION DURING FATIGUE I – “PROPOSED” SPECIMEN	44
FIGURE 8-23: MEASURED LOAD-DEFLECTION DURING STRENGTH TEST – “PROPOSED” SPECIMEN	44
FIGURE 8-24: “PROPOSED” SPECIMEN AT FAILURE	45
FIGURE 8-25: MEASURED RELATIVE DEFLECTION AND JOINT ROTATION – “PROPOSED” SPECIMEN	45
FIGURE 8-26: MEASURED END REACTIONS – “PROPOSED” SPECIMEN	46
FIGURE 8-27: COMPARISON OF STIFFNESS DEGRADATION	47
FIGURE 8-28: FREE BODY DIAGRAM – “CONVENTIONAL” SPECIMEN	49
FIGURE 8-29: FREE BODY DIAGRAM – “PROPOSED” SPECIMEN	49
FIGURE 8-30: REACTION FORCE DISTRIBUTION TO THE GIRDER STEMS (P = 21 KIPS)	50
FIGURE 8-31: ANALYTICAL REACTION FORCE DISTRIBUTION FOR SHEAR SPANS OF L/2, L/3, AND L/6	51
FIGURE 8-32: SHEAR FORCE IN THE WELDED CONNECTIONS OF THE “CONVENTIONAL” SPECIMEN	52
FIGURE 8-33: SUGGESTED EFFECTIVE JOINT LENGTH FOR SHEAR STRENGTH DESIGN	53

TABLE OF ACRONYMS

Acronym	Definition
AASHTO	American Association of State Highway and Transportation Officials
ADT	Average Daily Traffic
ADTT	Average Daily Truck Traffic
BDS	Bridge Design Specifications
CIP	Cast-in-place
DBT	Decked-bulb-tee
DOT	Department of Transportation
DWR	Deformed Wire Reinforcement
FE	Finite element
FHWA	Federal Highway Administration
ft	Foot
in.	Inch
kip	Kilo pound = 1000 pounds
klf	Kip per linear foot
ksi	Kip per square inch
lbs	Pounds
LRFD	Load and Resistance Factor Design
LTAP	Local Transportation Assistance Program
LVDT	Linear Voltage Differential Transformer
mm	Millimeter
NCHRP	National Cooperative Highway Research Program
PCI	Precast/Prestressed Concrete Institute
PCSSS	Precast Composite Slab Span System
psi	Pound per square inch
PVC	Polyvinyl Chloride
SDDOT	South Dakota Department of Transportation
SDSU	South Dakota State University
TxDOT	Texas Department of Transportation
WWF	Welded Wire Fabric
3D	Three-dimensional

1 EXECUTIVE SUMMARY

1.1 Introduction

Precast bridge superstructure elements are essential for accelerated bridge construction. Due to their ease of construction and reduced construction time and cost, precast/prestressed double tee bridge girders are routinely used by local governments in South Dakota for rapid construction of bridges on local roads. Detailing of longitudinal joints between precast bridge girders for adequate shear transfer remains a major concern, especially in “decked” precast girders, such as double tee girders, which do not require cast-in-place bridge decks.

1.2 Problem Description

The conventional joint detailing used for double tee girder bridges in South Dakota consists of discrete welded connections spaced along a grouted longitudinal joint (shear keyway) between adjacent girders. A common issue among existing double tee bridges is that the longitudinal joints deteriorate with time, most likely due to inadequate shear connection between adjacent girders. It is only a matter of time before the grout begins to crack along the joint, creating a path for moisture and deicing chemicals to reach the steel reinforcement in the deck, and leading to corrosion, concrete spalling, and structural degradation of the bridge. Short-term maintenance such as asphalt overlays can temporarily seal longitudinal joints, but asphalt overlays are costly and have a tendency to form reflective cracks directly above the longitudinal joints.

Due to age, rapid deterioration and increased traffic demands, many bridges on the South Dakota local highway system need replacement. The desired rate of bridge replacement created a backlog of local bridges in need of replacement. Double tee bridge girders provide economic and rapid construction technique for bridge replacement. Although the service life of double tee girders used on local roads was expected to be 50 to 70 years, some double tee bridges built less than 40 years ago already need replacement due to premature deterioration caused by inadequate longitudinal joints. This experimental study was performed to develop and verify the performance of a simple joint detailing for enhanced serviceability and strength.

1.3 Research Work

Two 40-ft long full-scale bridge superstructure specimens, each consisting of two joined double tee girders, were tested at the Lohr Structures Laboratory at South Dakota State University (SDSU). Each specimen represented two adjacent interior girders of a two-lane bridge (approximately 31 ft wide). One specimen, labeled “Conventional”, incorporated the longitudinal joint detailing that has been traditionally used in South Dakota (grouted keyway with discrete welded steel connections). The other specimen, labeled “Proposed”, incorporated a redesigned continuous longitudinal joint with a grouted shear keyway that is 4 in. wider than the conventional shear keyway. The redesigned joint did not require welded connections, but was reinforced with overlapping wire mesh layers that were extended out of the decks. The “Proposed” specimen was tested with and without a precast concrete diaphragm placed between stems of adjacent girders to restrain transverse rotation of the joint. The main objectives for the laboratory tests were to evaluate serviceability and strength of the

conventional and the proposed longitudinal joints when subjected to both fatigue (cyclic) and increasing monotonic loading.

Each specimen was subjected to cyclic loading representative of AASHTO's Fatigue I and Fatigue II load combinations, then tested to failure under increasing monotonic load. Fatigue I loading was included in this study to investigate the effects of maximum stress ranges that could result from potential overloads on agricultural routes. Based upon expected average daily truck traffic, the number of load cycles corresponding to 75 years of service was determined to be 411,000 load cycles. A strength test was performed for each specimen following the completion of the respective fatigue loading. It should be noted that damage to the specimens during fatigue loading were repaired prior to the start of the subsequent testing regimen.

1.4 Research Findings

The experimental results were examined and finite element analyses of the test specimens were conducted to assess the performance of the conventional and the proposed longitudinal joints. Following are the research findings.

- The proposed joint construction process was relatively simple and did not require special expertise or tools. The conventional joint required a certified welder to attach the welded connections.
- The proposed joint survived 800,000 of combined Fatigue II and Fatigue I load cycles (146 service years) without exhibiting any signs of failure. The conventional joint experienced structural failure at 62,000 load cycles (11.3 service years) under normal service loading conditions (Fatigue II).
- Water seepage through the conventional joint started at 19,500 load cycles (3.6 service years) and 15,000 load cycles (2.7 service years) for Fatigue II and Fatigue I loads, respectively. The proposed joint remained water tight under 800,000 cycles of combined Fatigue I and Fatigue II loading. It should be noted that non-shrink grout material specified by South Dakota DOT (described in this report) is adequate for the proposed joint. However, the joint must be cast in one continuous pour to eliminate cold joints that might allow for the passage of water.
- Under fatigue loading, the conventional joint deteriorated rapidly resulting in significant stiffness degradation, while the proposed joint remained essentially intact and had negligible effect on stiffness degradation. For Fatigue II loading, the stiffness degradation rate of the "Conventional" specimen was 26 times that of the "Proposed" specimen.
- The addition of rotation-restraining diaphragms to the proposed joint detail reduced the stiffness degradation rate by a factor of 2 (from 0.0046 kip/in/1000 load cycles to 0.0023 kip/in/1000 load cycles). However, even without diaphragms, the stiffness degradation rate was negligible and had no negative effects on the joint performance.
- The behavior of the conventional joint was close to that of a hinged connection while the behavior of the proposed joint was close to that of a rigid connection. The difference in

behavior had significant implications on flexural strength, distribution of the support reactions to the girder stems, and joint shear.

- The conventional joint allowed for the development of only 61.9% of the loaded and trailing girders combined flexural strength. The proposed joint was capable of engaging the trailing girder and developing 95.4% of the combined flexural strength.
- For the “Conventional” specimen, the measured reaction at the interior stem of the trailing girder constituted close to 50% of the system’s total support reaction, while the reaction at the interior stem of the loaded girder was only 31% of the total support reaction despite the fact that the load was applied almost on top of the stem. The combined reaction at the interior stems was approximately 60% of the total reaction for the “Proposed” specimen as compared to 80% for the “Conventional” specimen.
- The analytical results indicated that the shear span had a minor effect on the load distribution to the stems. For each of the three shear spans considered in this study, approximately one-third of the applied load was carried by each of the stems of the loaded girder and the first interior stem of the trailing girder of the “Proposed” specimen, while close to one-half of the applied load was carried by the first interior stem of the trailing girder of the “Conventional” specimen.
- The joint shear force, as calculated using the measured reactions, was 44% of the applied load for the “Conventional” specimen and 31% of the applied load for the “Proposed” specimen.
- The joint shear force was carried mainly by the welded connections in the conventional joint and by shear stresses in the proposed joint. A rational procedure based on an effective joint length and the ACI shear-friction equation was developed for the design of the proposed joint for shear.
- Implementing the proposed joint without diaphragms could increase the initial project cost by 3% to 4%.

Based on the research findings, the following conclusions were made.

- The proposed joint is feasible for field construction and does not require special skills.
- The proposed joint service life exceeds the desired bridge design life of 75 years while the conventional joint would fail during the early service years of a bridge.
- The proposed joint is successful in mitigating water seepage while the conventional joint is susceptible to water seepage at an early age.
- The proposed joint virtually eliminates stiffness degradation due to fatigue while the conventional joint would result in rapid stiffness degradation.
- The rotation-restraining diaphragms are redundant and do not provide tangible benefits to the performance of the proposed joint. Eliminating the diaphragms would reduce construction cost and time.

- The conventional joint behaves as a hinge which allows for shear transfer only. The proposed joint behavior is similar to a stiff link between the girders.
- Under the loading conditions considered in this study, the flexural strength of specimen with the proposed joint was more than 1.5 times that of the specimen with the conventional joint.
- The proposed joint allowed for a better spread of the support reactions over the girder stems.
- The analytical results indicate that the shear span had only a marginal effect on the load distribution to the stems.
- For the cases considered in this study, the proposed joint results in approximately 30% decrease in the joint shear demand.
- A rational procedure may be used for the shear design of stiff joints with shear-friction reinforcement similar to the proposed joint.
- The added initial construction cost for implementing the proposed joint is approximately 3% to 4% of the total bridge construction cost. The added cost is inconsequential when compared to potential savings obtained extending the joint service life to more than 75 years.

1.5 Recommendations

The following recommendations are based on the findings of this study.

1.5.1 Terminology

Future reference to the conventional joint and the proposed joint in double tee girder bridges should be “discrete welded joint” and “monolithic joint”, respectively.

The proposed terminology provides concise description of the anatomy and performance of the two joint types considered in this study.

1.5.2 Discrete Welded Joint

The discrete welded joint detailing should not be used for the construction of new double tee girder bridges.

The discrete welded joint is severely inadequate at both the serviceability and the strength limit states. Water seepage through the joints could occur within the first three years of service life, leading to moisture ingress and concrete deterioration. Failure of the welded connections could start at less than 15 years in service. Loss of the welded connections will compromise the structural integrity of the bridge and reduce its design load carrying capacity

1.5.3 Monolithic Joint

The monolithic joint detailing concept should be adopted for the construction of new double tee girder bridges.

The monolithic joint provides substantially improved serviceability and strength performance characteristics over the discrete welded joint at no significant increase in initial construction cost. The joint service life may well exceed the bridge design life of 75 years. The joint is water-tight, exhibits negligible stiffness degradation, leads to better distribution of the support reaction to the girder stems, and engages adjacent girders at the strength limit state

1.5.4 Future Research

A future study is needed to calibrate AASHTO's wheel load distribution factors, provide a simple method for determining the distribution of support reaction to the girder stems, and evaluate the joint shear demand in full bridge systems.

AASHTO LRFD Bridge Design Specifications provide live load distribution factors for determining the moment and shear demands in girders of double tee girder bridges. The AASHTO distribution factors are limited to joints that are “connected only enough to prevent relative vertical displacement at the interface.” Moreover, AASHTO does not provide methods for determining the live load shear force (reaction) at each stem or the critical shear force transferred at longitudinal joints.

The results of the current study clearly show that the joint behavior has significant influence on the support reaction at the girder ends, the distribution of the support reaction to the stems, and the value of the shear force transmitted through the joint. However, this study was limited to testing and analyzing a two-girder sub-assembly system using one of the standard double tee girder cross sections. The basic finite element models developed in this study can be expanded in a follow up parametric study to analyze full bridges with different spans and girder cross sections. The main objective of the future study would be to develop empirical equations that will enable the designer to determine load demands in different double tee bridge configurations.

2 PROBLEM DESCRIPTION

Precast bridge elements are routinely used for bridge construction in South Dakota. Currently one of the standard bridge types used for bridge replacement on the local road system is the precast/prestressed double tee girder. Double tee girder-type bridges are used because of their ease of construction and reduced construction time and cost. The precast double tee girders are joined to the adjacent girders to allow load sharing by means of longitudinal joint connections. Detailing of longitudinal joints between precast bridge girders for adequate shear transfer remains a major concern especially in “decked” precast girders, such as double tee girders, which do not require cast-in-place (CIP) bridge decks. The current longitudinal joint detailing used for double tee girder bridges in South Dakota consists of discrete welded connections and a grouted shear keyway between adjacent girders. Figure 2-1 shows joint details between standard 23 in. deep double tee girders used in South Dakota. The design life of these bridges was expected to be 50 to 70 years, but bridges less than 40 years old are showing signs of severe deterioration.

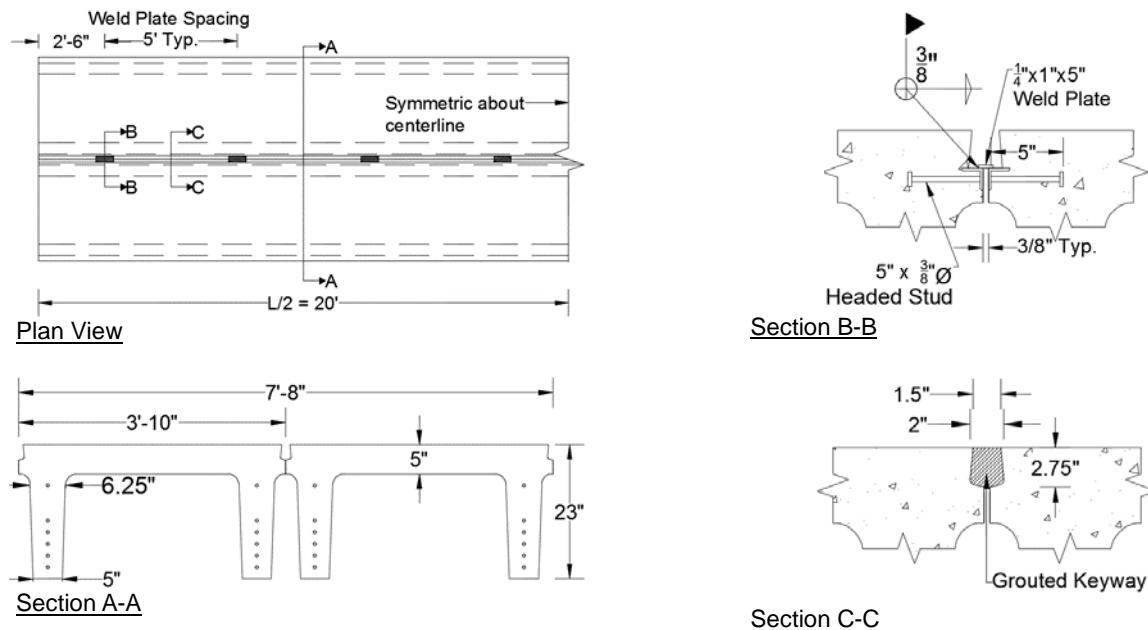


Figure 2-1: Grouted Shear Keyway with Discrete Welded Connections

A common issue among existing double tee bridges is that the longitudinal joints deteriorate with time, most likely due to inadequate shear connection between the adjacent girders. It is only a matter of time before the grout begins to crack along the joint length, creating a path for moisture and deicing chemicals to reach the steel reinforcement in the deck and leading to corrosion, concrete spalling, and structural capacity degradation. Deterioration of longitudinal joints can cause joined girders to separate from each other, resulting in reduced structural capacity.

Short-term maintenance such as asphalt overlays can temporarily seal the longitudinal joints. However, asphalt overlays are costly and have a tendency to form reflective cracks directly above the longitudinal joints. Reflective cracks allow water and deicing chemicals to penetrate the longitudinal joints. An example of reflective cracking and concrete deterioration at a double tee bridge is shown in figures 2-2 and 2-3, respectively.



Figure 2-2: Reflective Cracking of the Asphalt Overlay



Figure 2-3: Concrete Deterioration in the Deck Overhang of a Double Tee Bridge

Due to this rapid bridge deterioration and increased traffic demands, many bridges on the South Dakota local highway system need replacement. Double tee bridge girders provide economical and fast construction for bridge replacement; however, there is a need to develop a longitudinal joint detailing to mitigate the deficient performance exhibited by existing joints and enhance the service life of double tee bridges.

3 RESEARCH OBJECTIVES

The two main objectives of this study are listed below.

3.1 Identify Girder Design Alternatives

From literature review, determine whether alternatives to the double tee precast girder exist with improved details for shear transfer between longitudinal joints to alleviate joint degradation.

To meet this objective, a review of previous literature and a survey of current practices in South Dakota and neighboring states regarding longitudinal joints in decked precast/prestressed systems were conducted. The aims were to identify (1) alternative decked girder systems with adequate shear transfer at longitudinal joints and (2) improved joint detailing for potential implementation in the double tee girder system used in South Dakota. The researchers consulted with local precast companies to identify feasible options for alternative systems and improved joint detailing that would be submitted to the technical panel for discussion and approval. The technical panel selected an option that uses modified joint details for attaching adjacent double tee girders used in South Dakota. More details on the work to achieve this objective are presented under Tasks 2 to 5 of this report.

3.2 Load Test Alternative Girders

Perform load testing on alternative girder(s) and double tee girders, and compare results.

Two 40 ft long full-scale bridge superstructure specimens, each consisting of two joined double tee girders, were tested at the Lohr Structures Laboratory at South Dakota State University (SDSU). Each specimen represented two adjacent interior girders of a 33 ft wide prototype bridge. One specimen, labeled “Conventional”, was the control specimen and incorporated the longitudinal joint detailing that has been traditionally used in South Dakota (grouted keyway with discrete welded steel connections). The other specimen, labeled “Proposed”, incorporated a redesigned continuous longitudinal joint with a grouted shear keyway that is 4 in. wider than the conventional shear keyway. The redesigned joint did not require welded connections, but was reinforced with overlapping wire mesh that is extended out of the decks. The “Proposed” specimen was tested with and without precast concrete diaphragm placed between stems of adjacent girders to restrain transverse rotation of the joint. The main objectives for the laboratory tests were to evaluate serviceability and strength of the conventional and the proposed longitudinal joints when subjected to both fatigue (cyclic) and increasing monotonic loading and to compare the performance of the two specimens.

4 TASK DESCRIPTIONS

The research presented in this report comprised twelve Tasks. The following is a description of activities involved in each task.

4.1 Meet with Technical Panel

Meet with the technical panel to review the project scope and work plan.

A kick-off meeting with the technical panel was held on December 19, 2013. The researchers gave a presentation on the scope and work plan for the entire project. The presentation also covered an overview of decked girder systems and longitudinal joint detailing that had been identified through literature review. A copy of the presentation handout is presented in Appendix A.

4.2 Review Literature

Perform literature review of precast girder technologies with alternative shear transfer at the longitudinal joint.

A review of previous literature regarding the design and performance of longitudinal joints in decked precast/prestressed systems was conducted. The results are covered in Chapter 5 and Appendix I of this report.

4.3 Create and Administer Survey

Create and administer survey to other Departments of Transportation to identify other viable precast bridge girder designs.

A questionnaire regarding the use and performance of decked precast/prestressed girders was created and distributed to officials from several departments of transportation (DOTs) and Local Transportation Assistance Program (LTAP) contacts. The survey tool is presented in Appendix B. The responses to the survey are summarized in Chapter 6.

4.4 Confer with Precast Companies

Contact precast companies, describe problems with current design, and inquire about solutions to longitudinal joint details or entire sections.

The research team met with representatives from Cretex Concrete Products on March 4, 2014 and from Gage Brothers on March 13, 2014 to discuss performance issues of joints constructed according to current design and potential design alternatives to alleviate those performance issues. The results of the meetings are summarized in the technical memorandum discussed in Task 5.

4.5 Prepare Technical Memorandum

Prepare a technical memorandum and meet with the technical panel to discuss the improved joint details and precast girder designs gleaned from the literature review, surveys, and precast companies. Based on discussion, the technical panel will decide which option(s), if any, require structural testing to compare with the double tee.

On March 25, 2014 a technical memorandum was prepared by the research team and emailed to the technical panel for review. The memorandum is attached in Appendix C. Option 1, which included modifications to the joint connecting two double tee girders together, was tentatively selected by the technical panel pending a meeting to discuss available options. This meeting was held in Pierre on April 21, 2014, where the technical panel reaffirmed its decision to pursue the system proposed in Option 1 of the technical memorandum.

4.6 Prepare Testing Plan

If directed by the technical panel, prepare a technical memorandum describing a complete instrumentation, construction, and testing plan for technical panel review.

The research team prepared and submitted a technical memorandum (in combination with technical memorandum from Task 5) describing an instrumentation and testing plan for Option 1. The technical memorandum is attached in Appendix C. The plan was discussed with and approved by the technical panel. Detailed information on construction, instrumentation, and testing protocols is presented in Chapter 7 of this report.

4.7 Construct Test Girders

Upon approval of the plan by the technical panel, proceed with instrumentation and construction of test girders.

The test girders were fabricated at the Cretex facility in Mitchell, South Dakota. Fabrication of the test girders was completed on June 12, 2014 for the conventional joint specimen (control specimen) and on July 31, 2014 for the proposed joint specimen. The SDDOT project manager was present during the fabrication of the girders. Instrumentation and construction of the test girders are discussed in Chapter 7 of this report.

4.8 Perform Load Testing

Perform and provide the technical panel opportunity to observe ultimate and fatigue loading of alternate girder(s) and the traditional double tee girder.

The load testing of the conventional joint specimen started on June 30, 2014 and concluded on July 17, 2014. The load testing of the proposed joint specimen started on August 11, 2014 and concluded on September 18, 2014. The technical panel was notified ahead of time of the testing schedule. The SDDOT project manager and members of the technical panel witnessed part of the testing for each specimen. Detailed information on the experimental work is presented in Chapter 7 of this report.

4.9 Compare Girder Performance

Based on the results of testing, compare fatigue and shear transfer characteristics of the double tee and alternative section(s).

The experimental results from the two test specimens were analyzed and compared. The comparisons were based on joint performance (water tightness and joint deterioration) under AASHTO's Fatigue I and Fatigue II loading, joint shear transfer at the strength limit state, and load

distribution to the support reactions. Detailed information on the experimental results is presented in Chapter 8 of this report.

4.10 Recommend Girder Design

Develop a recommendation to the SDDOT based on cost and performance of the alternative girders compared to the double tee.

Based on the research work done in this study, the research team developed recommendations for joint detailing in newly constructed double tee girder bridges. The recommendations are presented in Chapter 10 of this report.

4.11 Prepare Final Report

Prepare a final report summarizing the research findings, conclusions, and recommendations.

This task is satisfied by this report.

4.12 Make Executive Presentation

Make an executive presentation to the SDDOT Research Review Board at the conclusion of the project.

A final presentation was given to SDDOT Research Review Board on September 7, 2016.

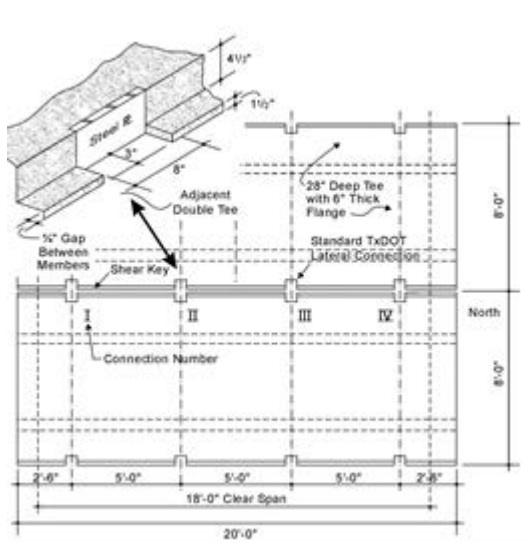
5 LITERATURE REVIEW

This chapter reviews previous studies regarding detailing and performance of longitudinal joints between precast decked bridge girders. The studies included in this review are limited to simple systems that can be constructed on local roads without the need for highly specialized bridge construction crews. Thus, studies of longitudinal joints that require post-tensioning or advanced concrete materials are not presented. Also absent from this review are studies that involve voided girder systems such as box girders and voided slabs. The technical panel for this project was not in favor of using voided girder systems due to concerns related to formwork that remains in place inside the girders after the completion of the bridge construction. Some of the studies that have been reviewed and are either not highly relevant to this study or include repeated information are presented in Appendix I (Zhu et al., 2012; Rouse et al., 2011; Culmo and Seraderian, 2010; Maguire et al., 2013; French et al., 2011).

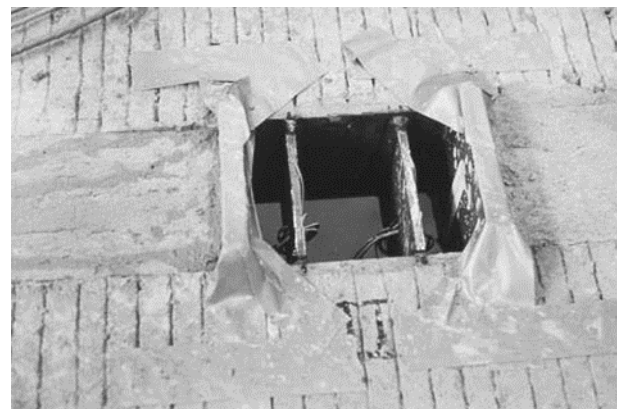
5.1 Jones

Jones (2001) performed full-scale load tests on a then “current” Texas Department of Transportation (TxDOT) detail and a proposed “simple” detail for joining the decks of double tee bridge girders. The objectives of the research were to develop, analyze, and test a new method for laterally connecting the flanges of double tee girders. Cyclic and monotonic loading protocols were used to assess the performance of the connections. Load distribution factors for the TxDOT bridges built with the “simple” detail were also addressed in the study.

The “current” longitudinal joint detail consisted of discrete welded steel connections and a grouted keyway. The connections consisted of 3/8 in. plates that were welded vertically between the adjacent girders. Steel plates with headed stud anchors were embedded into the girders at a constant interval along the girder length. Figure 5-1 shows details of the TxDOT connection.



Plan View



Steel Plates Connection

Figure 5-1: TxDOT Joint Detail (Jones, 1998)

The proposed “simple” detail consisted of discrete steel welded connections and a grouted shear keyway. The connection consisted of two steel plates, one in each girder, embedded into the deck concrete and a 1 in. diameter bar that was placed between and welded to the plates. This detail resulted in a narrow continuous grouted keyway that extended over the length of the girder. Figure 5-2 shows details of the “simple” joint.

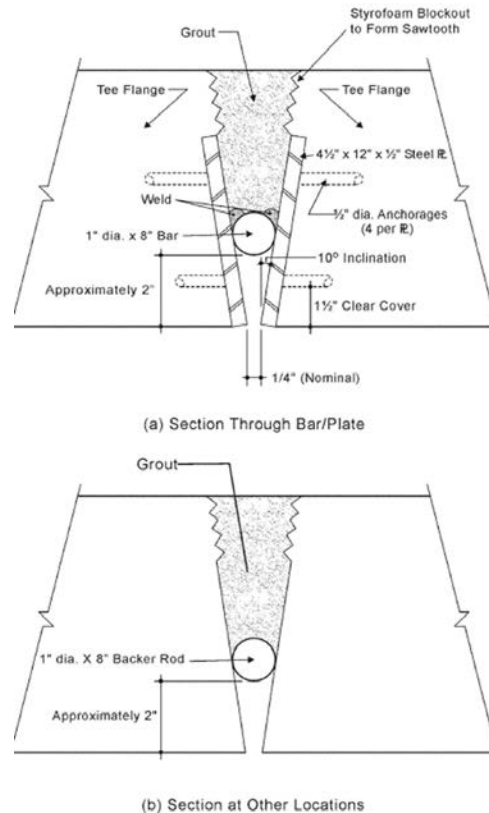


Figure 5-2: Proposed Simple Detail for TxDOT Girders (Jones, 1998)

The “current” and “simple” details were tested under cyclic and monotonic loadings to determine the long-term performance of the connections. The specimens consisted of two full-scale double tee girders joined with the “current” and “simple” details. The load position was varied during preliminary testing; however, during cyclic loading and strength tests, the load was applied at mid-span approximately one foot from the longitudinal joint.

Fatigue loads, used to represent vehicle live loads ranging from an initial 16 kips to a peak of 24 kips, were applied to the “simple” specimen at a rate of three cycles per second for a total of 1.5 million cycles. Monotonic load tests were performed at intervals ranging from 50,000 to 250,000 cycles to measure the stiffness of the system by applying a 20 kip load. Once cyclic loading was complete, the grout was removed around the steel joint and no signs of failure or degradation were visible.

5.2 Li, Ma, and Oesterle

Research completed by Li et al. (2010) investigated an improved continuous longitudinal joint connection detail for use in decked precast/prestressed bulb tee girders. Four full-scale slab specimens that represented joined bulb tee decks were tested under fatigue and monotonic loading.

The longitudinal joint was 8 in. wide at mid-depth and tapered to 6 in. at the top and the bottom of the deck. The joint reinforcement consisted of No. 5 headed bars that were staggered with an overlap of 6 inches in grouted keyway as shown in figure 5-3. Headed reinforcement was used rather than conventional reinforcement to develop the reinforcement in a relatively narrow joint width.

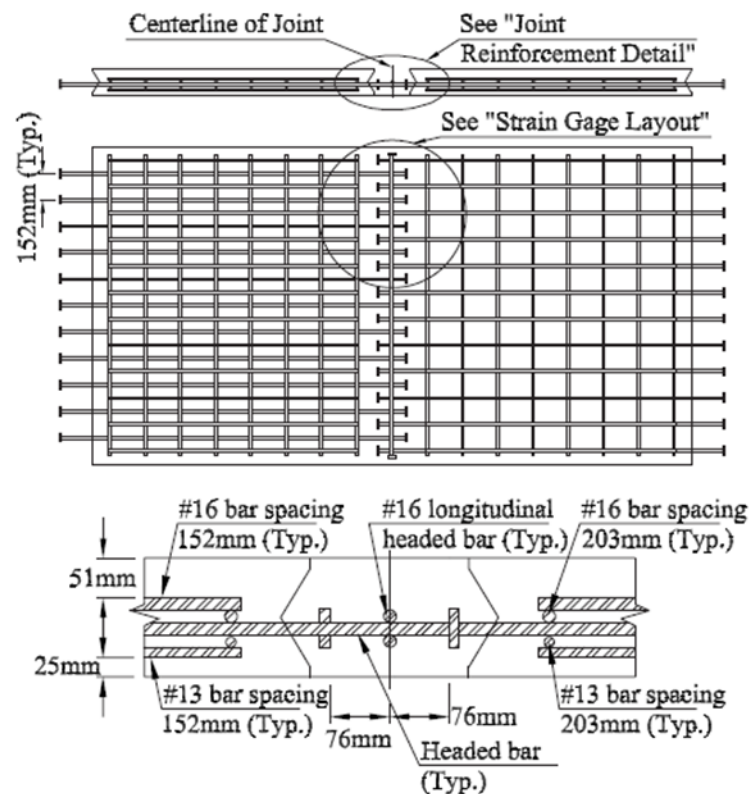


Figure 5-3: Joint Detail by Li et al. (2010)

The specimens were subjected to 2-million cycles of fatigue loading to determine the long-term performance of the joint. The fatigue loading protocol for the slab specimens was developed in a parametric study by Ma et al. (2007). Three-dimensional (3D) finite element (FE) models were created and field-verified to determine the shear force and moments at the longitudinal joints of the decked precast/prestressed bulb tee girders. AASHTO LRFD (2007) Fatigue II loading protocol was used in their study. The moments produced from the AASHTO LRFD fatigue truck in the 3D FE models were then used for the fatigue tests of the slab specimens. The slab specimens were instrumented to measure curvature, deflection, and steel strain.

Li et al. concluded that the fatigue loading had little influence on the structural behavior and strength of the longitudinal joint and that the improved longitudinal detail with headed reinforcement is a viable connection system for decked bulb tee girders.

5.3 Zhu, Ma, and French

Zhu et al. (2012) developed and tested U-bar joint details for use in decked bulb tee girders and bridge decks. Similar to the study by Li et al. (2010), four full-scale slab specimens with the U-Bar detail were tested under fatigue and monotonic loading.

The longitudinal joint was 8 in. wide at mid-depth and tapered to 6 in. at the top and the bottom of the deck. The joint reinforcement consisted of No. 5 U-bars that projected out of the deck and into a grouted keyway. An illustration of the U-bar detail is shown in Figure 5-4. No. 4 lacer bars were placed through the U-bars to develop the U-bars. The testing procedure and instrumentation were similar to those used in the study by Li et al. (2010).

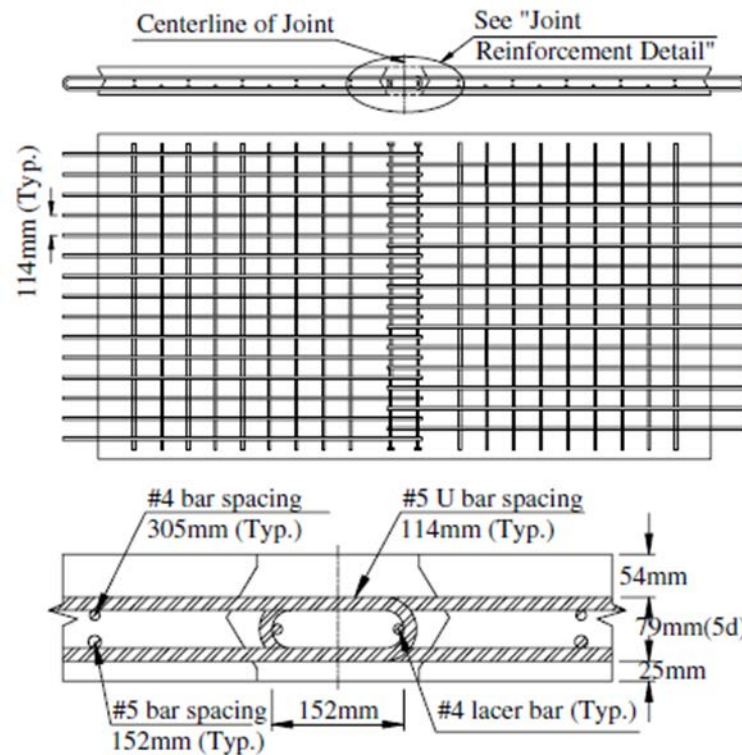


Figure 5-4: U-Bar Joint Reinforcement Detail

The results of the tests indicated that the fatigue loading had little impact on the U-bar joint behavior and strength. After the end of the 2-million cycle fatigue test, the slab specimen was successfully subjected to a ponding test with no leaks through the longitudinal joint. The U-bar detail was considered a viable connection system for the longitudinal joint between adjacent decked bulb tee girders.

5.4 Concluding Remarks

The “simple” joint detailing proposed by Jones (2001) is similar in concept to the joint detailing that has been in use for double tee girder bridges in South Dakota (described later in this report). The overlapping studded bars (Li et al., 2010) and overlapping U-bars (Zu et al., 2012) joints were developed for bulb tee decks that are in excess of 6 in. in thickness and may not be suitable for the thinner 5 in. and lightly reinforced decks of double tee girders used in South Dakota.

6 SURVEY OF STATE DOT AND LOCAL HIGHWAYS OFFICIALS

A questionnaire regarding the use and performance of decked precast/prestressed girders was distributed to officials from several DOTs and local governments. The survey instrument is presented in Appendix B. Several of the contacts that responded to the survey were not able to provide any information relevant to this study. Only the responses that were relevant to the study are summarized in this chapter.

6.1 Brookings County, South Dakota

Brookings County, SD, uses the double tee bridge girder system for the majority of bridges on local roads. The girders are joined using the conventional longitudinal joint detail with discrete welded connections described in Chapter 2. The County specifies non-shrink grout with a minimum strength of 3,500 psi. This strength is lower than the minimum 4,500 psi specified in Section 460.3S of South Dakota DOT Standard Specifications (2004). Reflective cracking was noted as a major concern in approximately 50% of the double tee bridges in the county.

6.2 Pennington County, South Dakota

Similar to Brookings County, Pennington County, SD, uses the double tee bridge girder system with the conventional joint detail described in Chapter 2. Although the response to the survey did not provide the percentage of double tee bridges that experience reflective cracking in Pennington County, corrosion from the formation of reflective cracks was noted as a major concern.

6.3 Cass County, North Dakota

Cass County, ND, does not typically use decked precast/prestressed girders; box girder bridges with cast-in-place (CIP) decks are more common. Few precast/prestressed double tee and quad stem girder bridges with welded steel connection and grouted keyway do exist in Cass County. Although reflective cracking was noticed on up to 20% of the decked girder bridges, it was more noticeable in the bridges with a concrete overlay as opposed to bridges with an asphalt overlay. The use of non-shrink grout with a 4 in. maximum slump for the shear keyway was the only specification reported by Cass County officials. No compressive strength was specified for the grout.

6.4 Nebraska Department of Roads

Nebraska primarily uses precast/prestressed voided or solid slabs that have section heights ranging from 10 in. to 12 in. The span lengths of the precast slabs is limited to 40 ft; CIP concrete decks are used for bridges with spans longer than 40 ft. The deck slabs are joined using grouted shear keyways filled with 4,000 psi non-shrink grout. The percentage of bridges with reflective cracking was not reported.

6.5 Montana Bridge Bureau

The Montana Bridge Bureau reported the use of decked bulb tee, triple stem, and quad stem bridge girder systems. The longitudinal joints between the decks of the three bridge girder systems are identical and consist of grouted keyways and welded steel connections. Montana also uses steel intermediate diaphragms to control movement of the girders relative to one another. Montana

Bridge Bureau reported reflective cracks on 100% of the bridges. They suggested making the longitudinal joint a moment connection to produce continuous curvature through the longitudinal joint.

6.6 Washington DOT Bridge Design Office

The Washington DOT uses the decked bulb tee girder for secondary roads systems with spans ranging from 60 ft to 120 ft. The decked bulb tee section is also commonly used by the SDDOT and has the same longitudinal joint with shear key and welded steel connections. The Washington DOT uses 5 in. thick CIP concrete topping with the decked bulb tee bridges. Reflective cracking was reported as a major issue with up to 60% of bridges experiencing reflective cracks above the longitudinal joints.

7 TEST SPECIMENS

An experimental program was conducted in this study to evaluate the structural performance of the conventional joint used in South Dakota and a proposed alternative joint for double tee bridge deck systems. This chapter covers design, fabrication, test setup, instrumentation, and test procedures for the test specimens.

7.1 Design of the Test Specimens

The technical panel and the research team of this project agreed to design the test specimens based on a two-lane, 40 ft span prototype bridge with 23 in. deep standard double tee girders. The prototype bridge was selected based on the configuration of a large number of existing double tee bridge systems in South Dakota and the ability to test full scale bridge sub-assemblages of this size in the J. Lohr Structures Laboratory at South Dakota State University (SDSU).

The bridge girders were designed for HL-93 live loading (AASHTO, 2012). HL-93 live loading consists of a design truck or a tandem, and a design lane load. The design truck comprises a pair of 32 kip axles and an 8 kip axle with axle spacing as shown in Figure 7-1. The design tandem comprises two 25 kip axles spaced 4 ft apart. The design lane load consists of a 0.64 klf load that is distributed along the bridge length and spread over a deck width of 10 ft. The bridge girders were designed by Cretex Concrete Products Inc. using the program PS Beam (Eriksson Technologies, 2011).

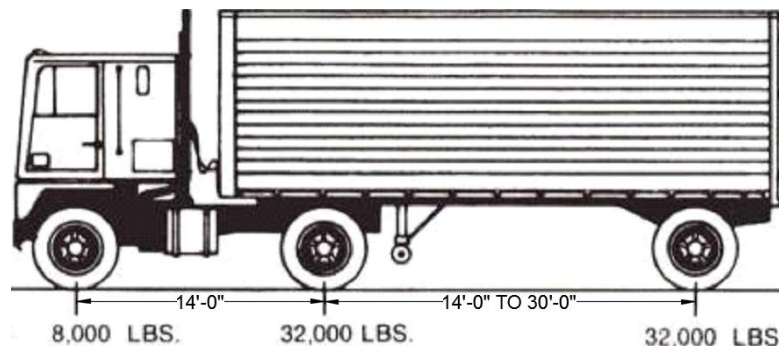


Figure 7-1: HL-93 Truck (AASHTO 2012)

Two 40 ft long full-scale bridge superstructure specimens, each consisting of two joined double tee girders, were designed, built, and tested under fatigue and ultimate loading conditions. The testing was performed at the Lohr Structures Laboratory. Each specimen represented two adjacent interior girders of a two-lane bridge. One specimen, labeled “Conventional”, incorporated the longitudinal joint detailing that has traditionally been used in South Dakota (grouted keyway with discrete welded steel connections). The other specimen, labeled “Proposed”, incorporated a redesigned continuous longitudinal joint with a grouted shear keyway that is 4 in. wider than the conventional shear keyway. The redesigned joint did not require welded connections, but was reinforced with overlapping wire mesh that was extended out from the decks. Shop drawings for the “Conventional” and the “Proposed” specimens are provided in Appendix D. The “Proposed” specimen was tested with and without precast concrete diaphragm placed between stems of adjacent girders to restrain transverse rotation of the joint. Details of the specimens are presented hereafter. The main objectives for the laboratory tests were to evaluate serviceability and strength of the conventional

and the proposed longitudinal joints when subjected to both fatigue (cyclic) and increasing monotonic loading until failure.

7.1.1 “Conventional” Specimen

The “Conventional” specimen represented two interior girders of a 40 ft span, 30.67 ft wide, two-lane hypothetical bridge. The hypothetical bridge, shown in Figure 7-2, consisted of eight standard 3 ft-10 in. wide by 23 in. deep precast/prestressed girder units. This bridge was representative of double tee girder bridges commonly used in South Dakota.

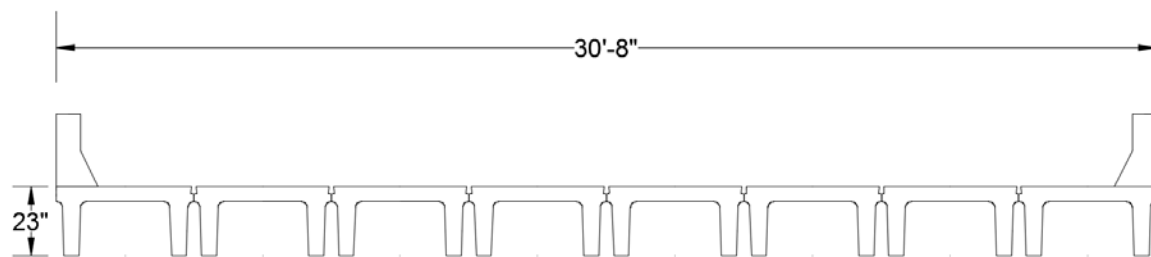


Figure 7-2: Cross Section of Hypothetical Bridge for Sizing the “Conventional” Specimen

A cross section of a typical precast/prestressed girder is shown in Figure 7-3. The flange was 5 in. thick and reinforced with two layers of $4 \times 8 - D8 \times D4$ wire mesh and four No. 4 bars. The stem was tapered from a width of 5 in. at the bottom to 6.25 in. at the top. The stem was reinforced with six 0.5 in. diameter 7-wire strands, each tensioned to 31 kips. The shear reinforcement in the stem consisted of a $4 \times 8 - D8 \times D4$ welded wire mesh.

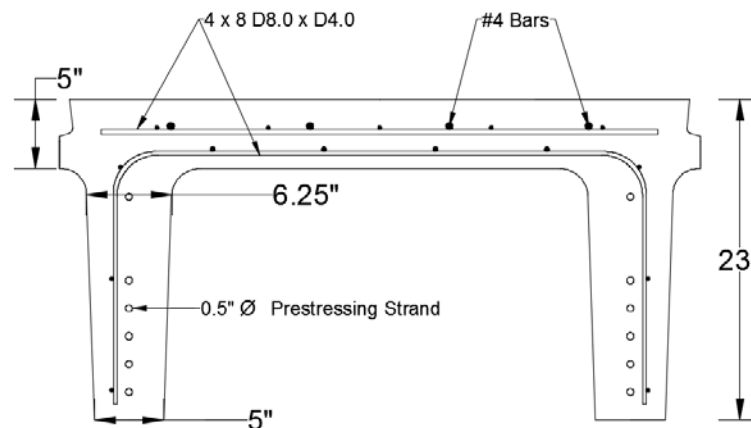


Figure 7-3: Standard 3 ft-10in Wide by 23 in. Deep Double Tee Section

Details of the “Conventional” specimen are shown in Figure 7-4. The longitudinal joint consisted of a grouted shear keyway that extended the length of the girder and incorporated welded steel connections at 5 ft center-to-center spacing along the girder length. The specified grout was a non-shrink, cement based grout with a minimum 28-day compressive strength of 4,500 psi, as required by South Dakota Department of Transportation (2004). The technical data sheet for the grout material is presented in Appendix E. The welded steel connection consisted of a 5 in. long by 0.25 in. thick A36 steel plate and a pair of 1.5 in. x 1.5 in. A36 steel angles that were embedded across each other in the deck concrete. The steel angle was 6 in. long and was fitted with two 3/8 in. diameter by 5 in.

long welded headed studs for anchorage into the concrete. The plate was field-welded to the two steel angles using 3/8 in. fillet weld.

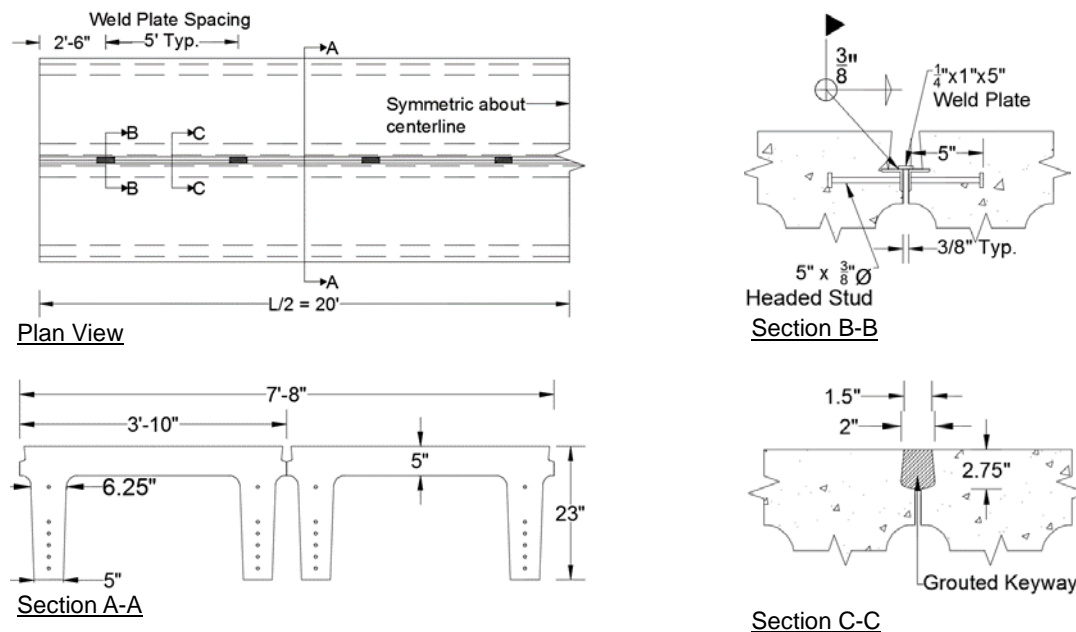


Figure 7-4: Details of the “Conventional” Specimen

7.1.2 “Proposed” Specimen

The “Proposed” specimen represented two interior girders of a 40 ft span, 33 ft wide, two-lane hypothetical bridge. The hypothetical bridge, shown in Figure 7-5, consisted of eight standard 3 ft-10 in. wide by 23 in. deep precast/prestressed girder units similar to those used for the “Conventional” specimen except that the deck’s top wire mesh would have to be extended a distance of 5 in. past the deck’s edge to allow for the construction of the “Proposed” joint. As a result of the wider joints, the deck for this bridge was 2 ft-4 in. wider than that for the “Conventional” hypothetical bridge.

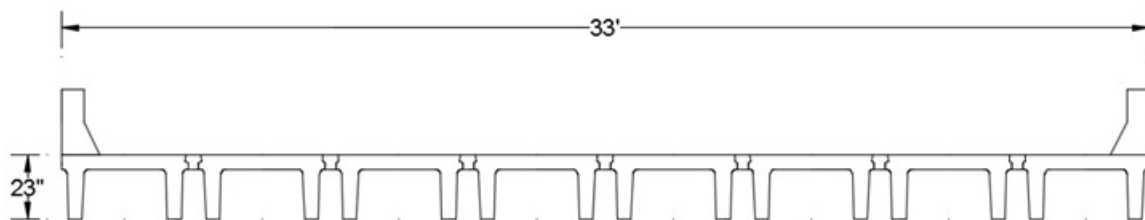


Figure 7-5: Cross Section of Hypothetical Bridge for Sizing the “Proposed” Specimen

The “Proposed” and the “Conventional” specimens were similar except for the connection between the two girders of each specimen. Figure 7-6 and Figure 7-7 show a cross section of the “Proposed” specimen and the corresponding joint details, respectively. For clarity, the second mesh in the deck which extends into the webs to form the shear reinforcement is not shown in Figures 7-6 and 7-7.

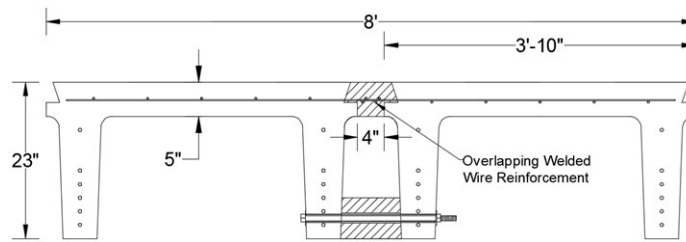


Figure 7-6: Cross Section of the “Proposed” Specimen (2nd Mesh Not Shown)

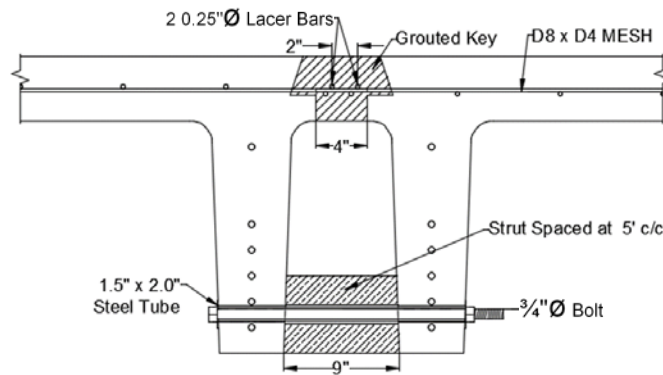


Figure 7-7: Joint Details of the “Proposed” Specimen (2nd Mesh Not Shown)

The longitudinal joint was 4 in. wider than that of the “Conventional” specimen and was reinforced with overlapping 4 x 8—D8.0 x D4.0 welded wire mesh that extended from the deck reinforcement for a distance of 5 in. The wire mesh extension was provided during the fabrication of the girders. Thus, the shear dowel reinforcement at the joint consisted of 0.319 in. diameter deformed wires spaced at 4 in. center-to-center for a total steel area of 0.24 in²/ft. Two 0.25 in. diameter longitudinal bars (lacer bars) were added between the overlapping mesh layers to develop the joint reinforcement; according to AASHTO (2012), two longitudinal wires spaced at least 2 in. apart are sufficient to develop the deformed wire in the transverse direction. The longitudinal joint was grouted the entire length of the girder using the non-shrink grout material described in Section 7.1.1. The construction of the longitudinal joint required temporary plywood to be placed at the bottom of the longitudinal joint while grout was being placed. The “Proposed” specimen was tested with and without an option to restrain the rotation of the girders relative to one another. The restraint was accomplished by means of a diaphragm assembly placed between interior stems of adjacent girders. The assembly consisted of a 6 in. x 12 in. concrete cylinder strut (to restrain the closing of the gap at the bottom of the stem) and A325 ¾ in. diameter tie bolt (to restrain widening of the gap between the stems). The cylinder ends were saw-cut to size and chamfered to allow for a snug fit between the stems. A 1 in. diameter polyvinyl chloride (PVC) sleeve at the center of the concrete cylinder allowed for placement of the tie bolt through the cylinder. Galvanized steel sleeves in the stems allowed for the passage of the steel bolts. The sleeves allowed for placement of the diaphragm assemblies at 5 ft on center along the length of the girder.

7.2 Fabrication and Assembly of the Test Specimens

The girders for the “Conventional” and the “Proposed” specimens were fabricated at the Cretex West Concrete Products facility in Mitchell, South Dakota. Members of the research team were present during the fabrication process to instrument the girders with strain gages, measure concrete fresh properties, cast concrete test cylinders, and oversee the construction process. This section covers the fabrication of the girders and assembly of the specimens in the laboratory.

7.2.1 “Conventional” Specimen

Fabrication of the girders for the “Conventional” specimen started on June 11, 2014 and was completed on June 13, 2014. The two girders were cast on the same bed. The prestressing strands were initially tensioned to 3,000 lbs to remove the slack and allow for the installation of surface-mounted strain gauges on the strands. The wire mesh reinforcement was then placed in position. Subsequently, embedded concrete strain gages in the deck were tied to the mesh using steel wire. Prior to tensioning, initial readings of the strands were taken for reference. The strands were then jacked to 75% of the ultimate strand stress ($0.75 f_{pu}$) which corresponded to a jacking force of 31,000 lbs per strand. Strain readings were then recorded after final tensioning.

During concrete casting, SDSU personnel tested the fresh concrete properties and prepared 15 standard 12 in. by 6 in. concrete cylinders. At release, the concrete strength was 6,300 psi which was greater than the specified minimum release strength of 5,000 psi. Before de-tensioning, strain gage readings were taken. The girders were then de-tensioned by torch cutting each strands simultaneously on the two girders. After de-tensioning, strain values were once again recorded. Figure 7-8 shows a sequence of pictures during fabrication.



Figure 7-8: Fabrication of the Girders for the “Conventional” Specimen

The girders were shipped to the Lohr Structures Laboratory on June 18, 2014. The two girders were unloaded and placed in position on concrete reaction blocks prior to joining along the longitudinal joint. Figure 7-9 shows a sequence of pictures detailing the unloading and positioning procedure in the Lohr Structures Laboratory.

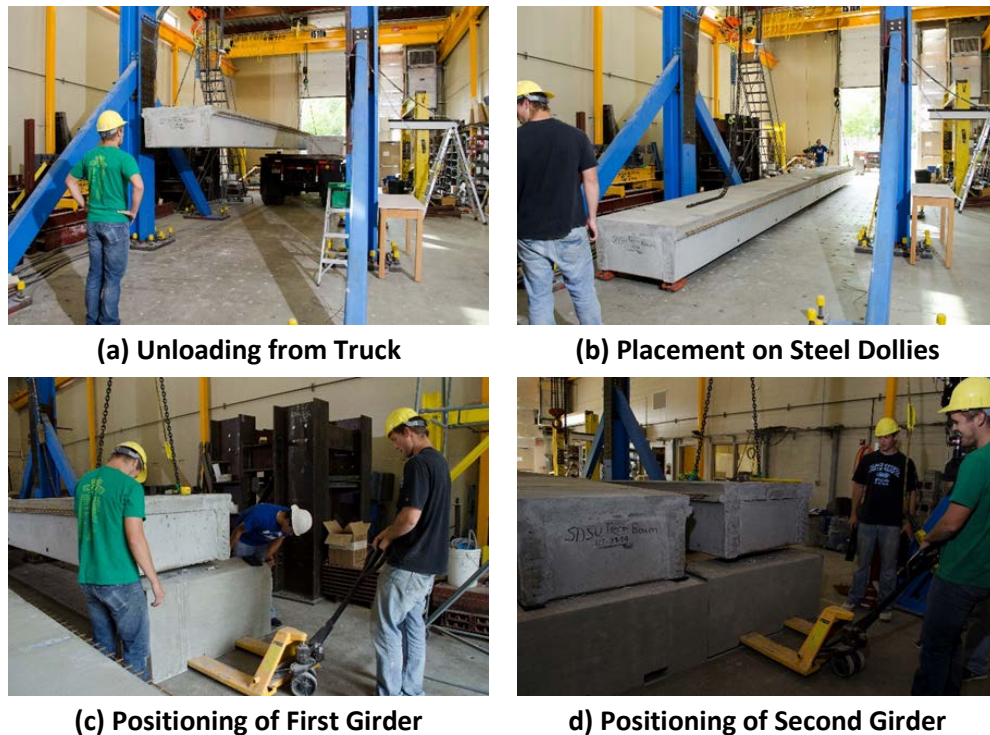


Figure 7-9: Unloading and Positioning of the Girders

After the girders were set in place, the difference in camber between the two girders did not exceed 0.25 in. The gap at the bottom of the longitudinal joint varied from 0 in. to 9/16 in. Figure 6-10 shows the gap between the welded connections in the longitudinal joint.

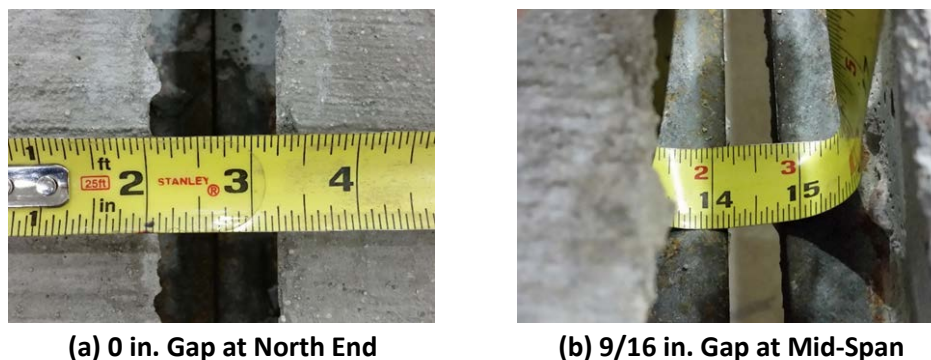


Figure 7-10: Varying Gap at Bottom of Longitudinal Joint of the "Conventional" Specimen

The girders were connected together by welding the $\frac{1}{4}$ in. \times 1 in. \times 5 in. steel plates to the steel angles that were anchored in the girders. The weld was a $\frac{3}{8}$ in. fillet weld that extended along the long sides of the steel plate. The welding was performed by a certified welder from a local steel fabricator in Brookings, South Dakota. Foam backer rod was placed at the bottom of the continuous shear key to prevent grout from leaking through the joint while grouting. The longitudinal joint was

then filled with the grout mix. Test cubes were cast and the slump was measured during grouting. In normal construction practices, the longitudinal joint would be grouted along the entire joint length. However, to allow for visual monitoring of the welded connections during the test, 6-in. gaps were left ungrouted at the locations of those connections. Figure 7-11 shows the welded plates and the grouted joint with block-outs for monitoring the welded connections.

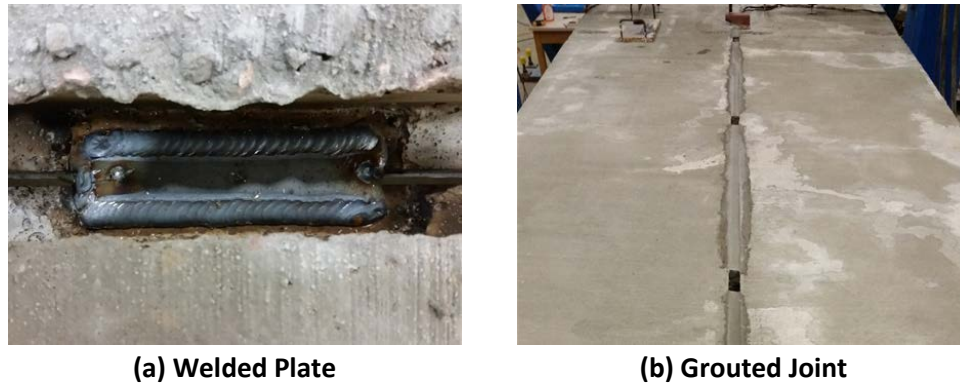


Figure 7-11: Connection at Longitudinal Joint of the “Conventional” Specimen

7.2.2 “Proposed” Specimen

Fabrication of the two girders for the “Proposed” specimen started on July 31, 2014 and was completed on August 1, 2014. The prestressing sequence and concrete sampling and testing were similar to those for the “Conventional” specimen; however, after the first strand was initially tensioned, 1.5 in. × 2 in. steel tubes were placed in position to form the sleeves needed for the diaphragm tie bolts. The steel forms used by the fabricator to cast the standard 23 in. deep double tee girders were not originally configured for extending the deck wire mesh beyond the deck width. Therefore, the shear key on the extended mesh side was molded using three 2 in. × 4 in. dimension lumber stacked on top of each other. The wire mesh was extended above the bottom board that was anchored to the prestressing bed, while the two upper boards were screwed to each other and beveled on the inside face to form the profile of the shear key. Foam backer rod was placed between the bottom and the middle boards to seal the gap and prevent concrete seepage during casting. Figure 7-12 shows the steel sleeve inside the form and the shear key timber formwork.

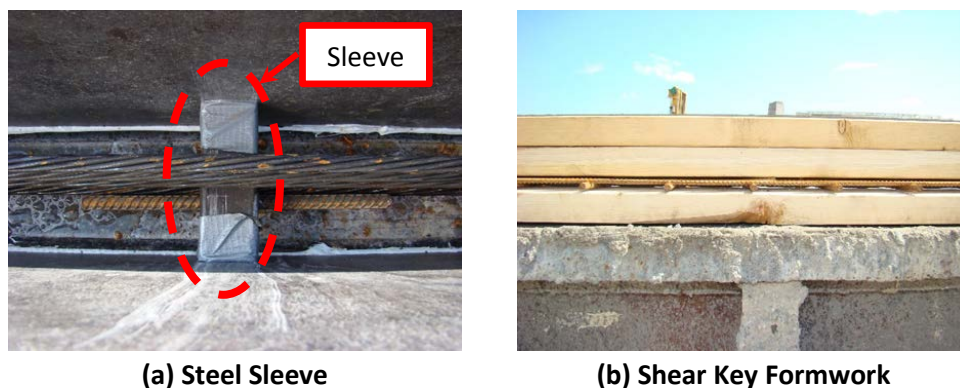


Figure 7-12: Steel Sleeve and Shear Key Timber Formwork – “Proposed” Specimen

The girders were shipped to the Lohr Structural Laboratory on August 5, 2014. The girders were unloaded and placed in position on top of the reaction blocks. Placing the second girder in position required some adjustment to be made at the overlapping wire mesh. The wire mesh from the second girder was bearing against the wire mesh from the first girder and preventing a full seating of the second girder. A crow bar was used to slightly separate the two layers of wire mesh and allow for the second girder to be fully seated on the supports. The adjustment process was simple and practical for field applications. The bottom of the longitudinal joint was formed with a 5 in. wide strip of plywood that was tied to the wire mesh. Steel wire ties were placed every two feet to hold the formwork in place. In field applications, the plywood form could be suspended from the first girder prior to placing the second girder then pulled up and tied into place. The longitudinal joint was then filled with the grout mix. Figure 7-13 shows the plywood form at the longitudinal joint.



(a) Bottom Side



(b) Top Side

Figure 7-13: Joint Formwork for the “Proposed” Specimen

The restraining diaphragms were installed at 5 ft spacing, starting at mid-span for a total of seven diaphragms. Figure 7-14 shows a diaphragms in place.



Figure 7-14: Restraining Diaphragm in Place

7.3 Test Setup

The test setup was identical for both test specimens. An isometric rendering of the test setup is shown in Figure 7-15. Each specimen was assembled under the loading frame and was simply supported on concrete reaction blocks. Elastomeric bearing pads were placed under the girder stems. The effective span length between the supports was 39.17 ft. The specimen was tested under three-point loading with the middle load being applied eccentrically relative to the joint at the specimen's mid-span.

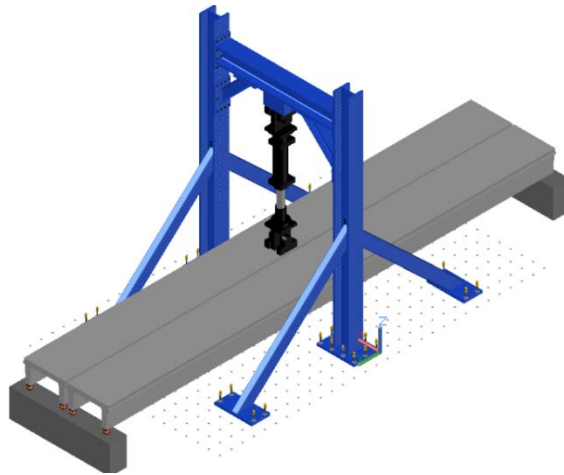


Figure 7-15: Isometric Rendering of the Test Setup

Details of the test setup are shown in Figure 7-16. The girders were labeled “A” and “B”, with girder “A” being the loaded girder and girder “B” being the trailing girder. Loading was applied at the mid-span of girder “A” by means of a 328 kip hydraulic actuator. The load was spread over a 10 in. x 20 in. loading steel plate, instead of the 16 in. x 16 in. plate proposed by the research team to the technical panel in a memorandum on May 15, 2014 (shown in Appendix C), to simulate the contact area specified by AASHTO (2012). The plate was placed at the edge of the longitudinal joint to maximize the shear stresses through the shear keyway. To investigate susceptibility of the joint to water seepage before and during loading, three 4 ft long wood dams were placed directly on top of the longitudinal joint and were filled with water prior to testing.

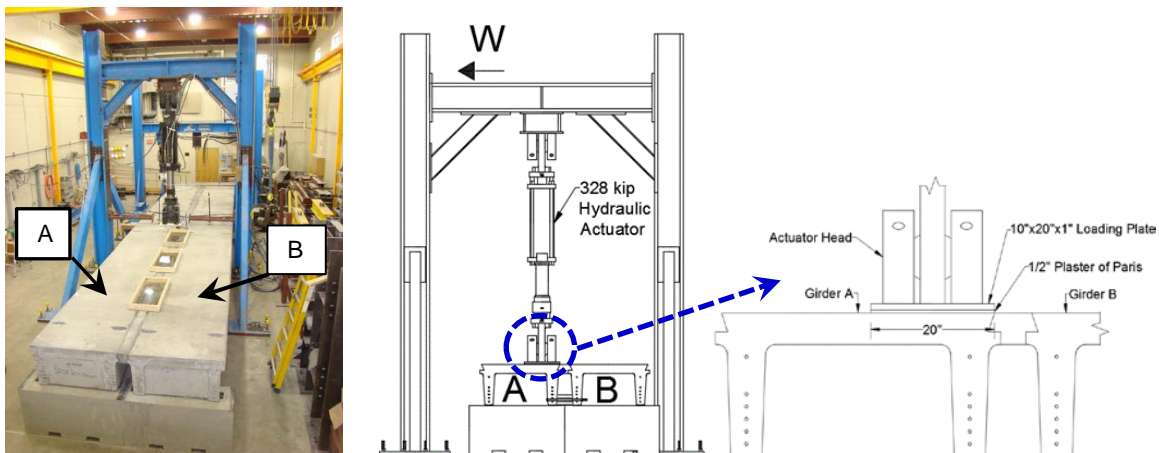


Figure 7-16: Details of the Test Setup

7.4 Instrumentation

Each specimen was instrumented with several electrical resistance strain gages, displacement transducers, and load cells. In addition, the hydraulic actuator used to load the specimens was equipped with a load cell and a position transducer.

7.4.1 Strain Gages

Each girder was instrumented at its mid-span with 12 surface-mounted strain gages to measure strain in the prestressing tendons and 7 embedded strain gages to measure strain in the concrete. Thus, 38 strain gages were placed in each specimen. Figure 7-17 shows typical surface-mounted and embedded gages.

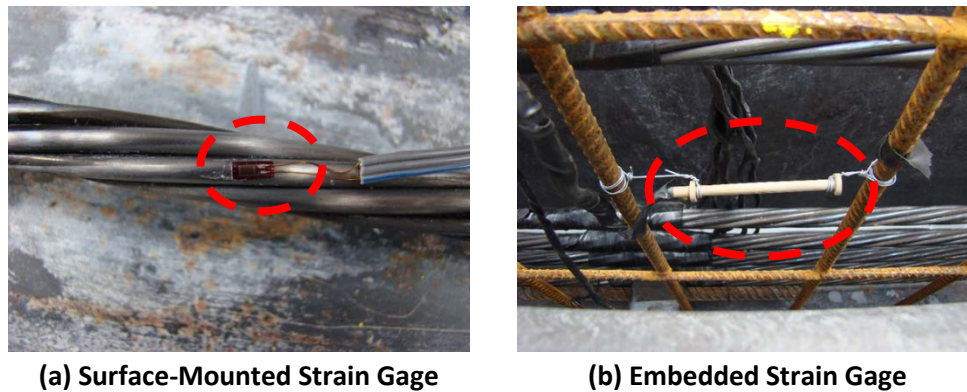


Figure 7-17: Surface-Mounted and Embedded Strain Gages

Figure 7-18 shows the distribution of the strain gages within the cross section. The West and East stem designations are in reference to the West direction shown in Figure 7-16. The embedded gages were placed at three levels: 1 in. from the bottom (stem), 15.25 in. from the bottom (neutral axis), and 2.5 in. from the top (deck).

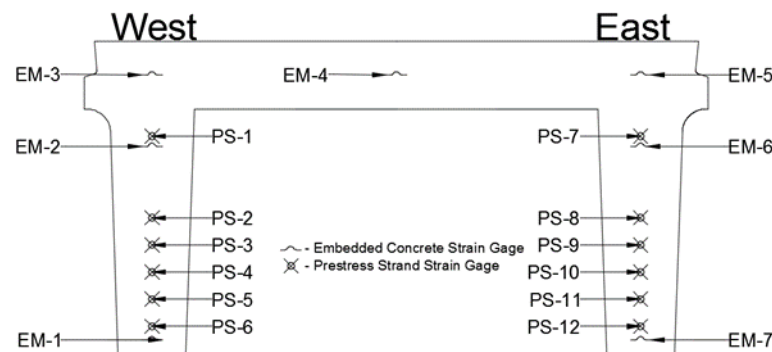


Figure 7-18: Strain Gage Placement

Additionally, four of the diaphragms placed over one-half of the span in the “Proposed” specimen were each fitted with a surface-mounted strain gage on the tie bolt to measure the restraining tension force in the bolt during the test.

7.4.2 Linear Variable Differential Transformers

A total of 7 linear variable differential transformers (LVDT) were mounted on each specimen to measure deflections and rotations during the test.

The measured absolute deflection at mid-span was determined by subtracting the deflection due to the compressibility of the elastomeric pads at the supports from the measured deflection at mid-span. The deflection of the specimen at mid-span was measured by means of two LVDTs; one LVDT was placed at the center of Girder A and the other LVDT was placed at the center of Girder B. A similar LVDT arrangement was placed over the specimen's end at the support. The LVDTs were attached to fixed steel frames and measured vertical deflection at the top of the deck. Figure 7-19 shows the system of LVDTs used for measuring mid-span deflection.

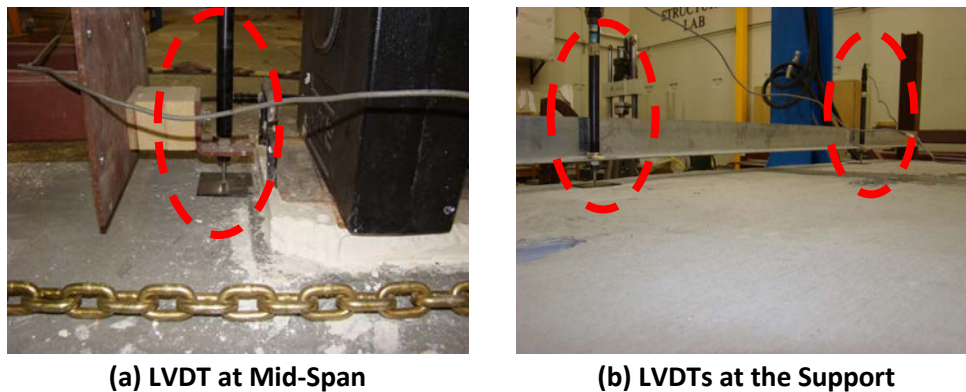


Figure 7-19: LVDT System for Measuring Vertical Deflection

The mid-span joint rotation in the transverse direction was measured with a pair of LVDTs. The LVDTs were placed transversely across the longitudinal joint at the top and the bottom of the specimens, as shown in Figure 7-20, to measure the movement of one girder relative to the other across the joint. The measurements from the top and bottom LVDTs were used to determine the angle of rotation between the two girders. The LVDTs had to be placed at 1.5 ft from mid-span to clear the actuator's head.

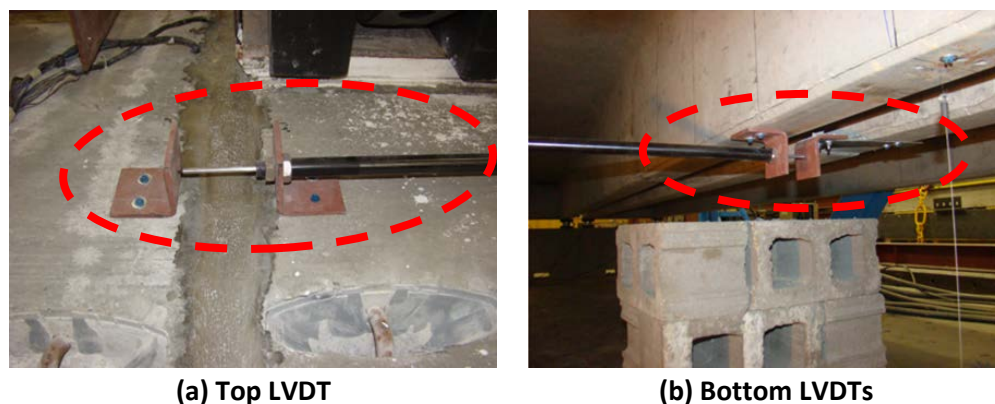


Figure 7-20: LVDT System for Measuring Joint Transverse Rotation

The vertical deflection of one girder relative to the other across the joint was measured by means of one LVDT as shown in Figure 7-21. The LVDT was mounted at 1.5 ft from mid-span to clear the actuator's head.

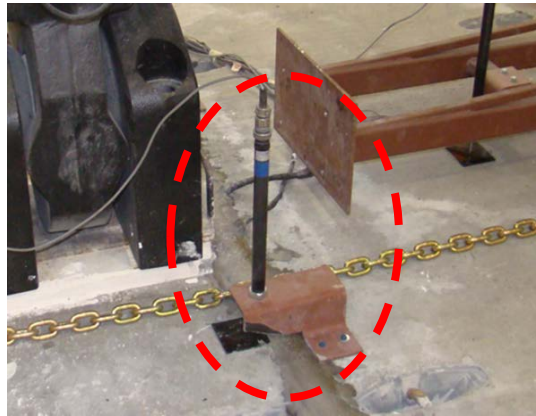


Figure 7-21: LVDT for Measuring Relative Vertical Displacement

7.4.3 Cable Extension Transducers

The LVDTs used for measuring vertical deflections had a maximum stroke of 4 in. A set of four cable extension transducers were used to capture deflections that would exceed the LVDT stroke as the specimen is tested for strength. Under each girder stem, a cable extension transducer was bolted to the floor and the cable was fastened to the bottom of the girder stem. Figure 7-22 shows the cable extension transducers in place.



Figure 7-22: Cable Extension Transducers

7.4.4 Load Cells

Reactions at each of the four girder stems were measured on one end using 100-kip load cells. Under each stem, a load cells was placed between 6 in. × 6 in. × 1 in. steel plates to ensure a flat bearing surface. An elastomeric pad was placed on top of the steel plate where the girder stem would be seated. Figure 7-23 shows one of the load cells in place under the girder stem.



Figure 7-23: Load Cell for Measuring Reactions

7.4.5 Data Acquisition System

The data acquisition system used had a capacity of scanning 128 channels at 10 to 2048 times per second. A scan rate of 10 readings per second was used for all of the testing.

7.5 Test Procedure

Each specimen was subjected to cyclic loading representative of Fatigue I and Fatigue II load combinations (AASHTO 2012), then tested to failure under increasing monotonic load. Fatigue I loading was included in this study to investigate the effects of maximum stress ranges that could result from potential overloads on agricultural routes. During fatigue testing, periodic quasi static load tests were performed to assess the effect of fatigue loading on stiffness, relative deflection at the joint, and joint rotation. The static load was equal in value to the cyclic load amplitude. The measured specimen stiffness was determined as the static load divided by the mid-span deflection at the center of girder A.

7.5.1 Fatigue Testing

The point load for the fatigue testing was determined by matching the maximum fatigue load moment on two interior girders of the two-lane hypothetical bridge described in Section 7.1.1. The fatigue load combination is based on the single AASHTO design truck described in Section 7.1 but with a 30 ft fixed spacing between the two 32-kip axles. The fatigue load incorporates a dynamic load allowance of 15%; however, the live load multiplier for Fatigue II load combination is 0.75 while that for Fatigue I load combination is 1.5.

Using a structural analysis software (CSI 2012) and Fatigue II live load, a moment envelope was developed for a 39.17 ft simply supported span. The span length was selected to match that of the test specimen. The corresponding maximum moment was 289.5 kip-ft. The AASHTO (2012) live load distribution factor for an interior girder of the two-lane hypothetical bridge was 0.35. Calculations of the maximum moment and the live load distribution factor are shown in Appendix F. Since the test specimen consisted of two girders, the fatigue load applied during the test was based on doubling the point load that would induce the maximum fatigue moment in one girder. Thus, the fatigue

loading consisted of a cyclic point load having amplitudes of 21 kips and 42 kips for Fatigue II and Fatigue I load combinations, respectively. The load application rate was governed by the actuator's hydraulic flow demand. The load was applied at a rate of one cycle per second for Fatigue II and 0.75 cycle per second for Fatigue I. Based upon expected average daily truck traffic (100 ADT with 15% truck traffic density), the number of load cycles corresponding to 75 year of service was determined to be 411,000.

7.5.2 Strength Testing

A strength test was performed for each specimen following the completion of the respective fatigue loading. The test setup for the strength tests was identical to that used for the fatigue tests. The strength test loading was quasi-static with displacement increments ranging between 0.02 in. during the initial elastic response and 0.05 in. after significant deflection had occurred. It should be noted that damage to the specimens during fatigue loading was repaired prior to the start of the subsequent testing regimen. The repair method is presented in Section 8.2.2.

8 EXPERIMENTAL RESULTS AND ANALYSIS

This chapter presents the results and analysis of the experimental data for the “Conventional” and the “Proposed” specimens. The results include the data gathered from the measured material properties and the fatigue and strength testing.

8.1 Material Properties

This section presents the measured material properties for the concrete and grout mixes and the mill certificate reported properties for the prestressing strands used in the specimens.

8.1.1 Fresh and Hardened Concrete Properties

The fresh and hardened concrete properties were tested according to ASTM standards (ASTM 2010a, 2010b, 2010c, and 2010d).

The fresh properties of the concrete used to construct the girders were measured at the fabrication facility. The concrete was tested for temperature, air content, unit weight, and slump. The average fresh properties of the concrete are summarized in Table 1.

Table 1: Fresh Concrete Properties

	Temperature (°F)	Air Content (%)	Unit Weight (lb/ft ³)	Slump (in.)
“Conventional” Specimen	77	5.5	144.8	4.00
“Proposed” Specimen	83	4.9	145.8	7.50

The specified minimum concrete strength was 5,000 psi at release and 6,000 psi at 28 days. During placement of concrete, concrete cylinders were cast and steam-cured with the girders until stress transfer the following morning. One cylinder was tested at release and the remaining cylinders were cured at room temperature at the Lohr Structures Laboratory. Three cylinders were tested at 7 days, 14 days, 28 days and the day of strength testing of the specimens. The average strength of the three cylinders was reported as the measured strength. The modulus of elasticity was determined experimentally for each concrete cylinder using an 8-in. extensometer. A summary of the measured compressive strength, f'_c , and modulus of elasticity, E_c , is presented in Table 2. The compressive strength gain is shown graphically in Figure 8-1.

Table 2: Fresh Concrete Properties

	“Conventional” Specimen		“Proposed” Specimen	
	f'_c (psi)	E_c (ksi)	f'_c (psi)	E_c (ksi)
@ Release	6,300	NA	5,000	NA
7 days	7,670	5,020	7,580	4,800
14 days	8,540	4,930	7,890	4,925
28 days	8,910	5,000	8,280	4,910
Day of Testing	9,140 [†]	5,140 [†]	8,570 [‡]	4,710 [‡]

[†]Tested 35 days after casting

[‡]Tested 49 days after casting

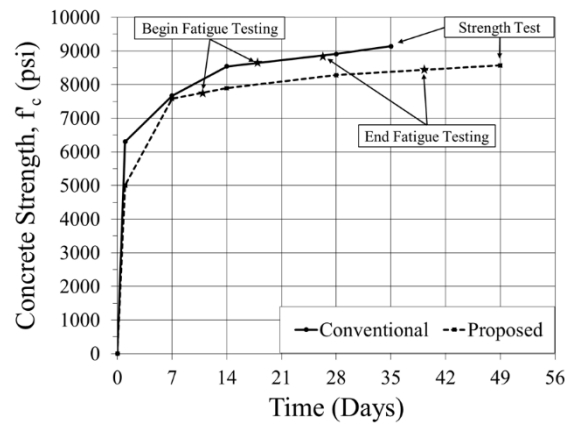


Figure 8-1: Concrete Strength Gain

8.1.2 Fresh and Hardened Properties of the Grout Mix

The fresh grout properties were measured at the time of placement at the Lohr Structures Laboratory. The fresh properties of the grout mix are summarized in Table 8.3. Three sets of data are shown for the “Conventional” specimen since new grouting was needed following each fatigue test.

Table 3: Fresh Properties of the Grout Mix

	Temperature (°F)	Slump (in.)
“Conventional” Specimen – Fatigue I Test	70	4.00
“Conventional” Specimen – Fatigue II Test	70	4.00
“Conventional” Specimen – Strength Test	74	4.25
“Proposed” Specimen	77	4.25

During placement of grout in the longitudinal joint, 2-in. cubes were cast for measuring the compressive strength of the grout. SDDOT requires the grout to have a minimum 28-day compressive strength of 4,500 psi. Two grout cubes were tested at 7 days and 28 days and the average strength of the two cubes was reported as the measured strength. Table 4 shows a summary of the compressive strength of the grout from the “Conventional” and “Proposed” specimens.

Table 4: Measured Compressive Strength of the Grout Mix

	Grout Compressive Strength (psi)			
	“Conventional” Specimen Fatigue I Test	“Conventional” Specimen Fatigue II Test	“Conventional” Specimen Strength Test	“Proposed” Specimen
7 Days	6,040	5,720	5,300	5,460
28 Days	6,650	6,210	5,630	5,610

8.1.3 Prestressing Strand Properties

The prestressing strands were 0.5-in. diameter, seven-wire, Grade 270, low-relaxation strands. The stress-strain properties were obtained from the mill certificate. According to the mill certificate, the strand had a cross-sectional area of 0.153 in², an average modulus of elasticity of 29,000 ksi, a yield stress of 256,870 psi at 1% extension, and ultimate stress of 283,740 psi at 5.2% extension.

8.2 Test Results – “Conventional” Specimen

The “Conventional” specimen was first subjected to Fatigue I cyclic loading, followed by Fatigue II cyclic loading, and was finally loaded monotonically until failure. The original testing plan called for Fatigue II testing to be performed prior to Fatigue I testing. However, the testing order for the “Conventional” specimen was inadvertently switched. After realizing that Fatigue I testing had already been started prior to fatigue II testing, the research team decided to complete Fatigue I testing since approximately 10,000 Fatigue I load cycles had already been applied at the time.

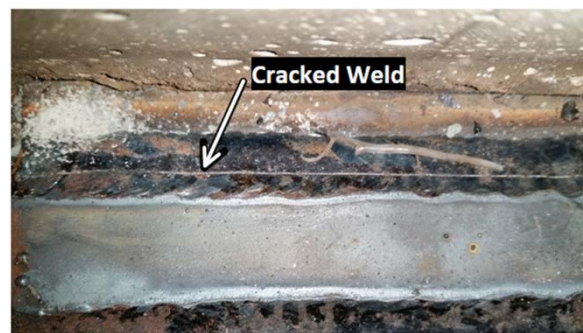
8.2.1 Fatigue I Loading

A 42-kip load amplitude was applied at a rate of 0.75 cycle per second for a total of 56,000 cycles. Load tests to measure the stiffness of the specimen were originally planned to be administered every 50,000 cycles over an anticipated 500,000 load cycles. However, after the longitudinal joint began to fail earlier than expected, stiffness readings were taken as deemed necessary based on visual inspection of the joint.

The first sign of joint deterioration appeared at approximately 15,000 cycles when water from the water dam closest to mid-span started to seep through the longitudinal joint. At 31,500 cycles, the welded connection located at 2.5 ft south of mid-span failed when the weld connecting the welded plate and the angles cracked longitudinally along the length of the connection. The same type of connection failure occurred at 2.5 ft north of mid-span at 37,500 cycles. The welded connection at 7.5 ft south of mid-span failed at 44,000 cycles. At 56,000 cycles, connection failure occurred at 7.5 ft north of mid-span. The test was stopped at 56,000 cycles because the specimen was no longer capable of transferring shear adequately across the longitudinal joint. As the connections failed, the resulting moment in Girder A increased and a ½-in. long flexural crack was noticed at the bottom of the east stem on Girder A at 56,000 cycles. The flexural crack may have resulted from a spike in the applied load between 38,000 and 44,000 cycles. Figure 8-2 shows signs of joint deterioration.



(a) Water Seepage through the Joint



(b) Failure of Welded Connection

Figure 8-2: Deterioration of the Joint in the “Conventional” Specimen

Stiffness measurements were taken at 0 cycles, 33,500 cycles, 37,500 cycles, 44,000 cycles, and 56,000 cycles. During each stiffness test, a monotonic load of approximately 42 kips was applied at a rate of 10 kips per minute. The stiffness of the specimen was determined by dividing the peak load from the load test by the corresponding net mid-span deflection at the center of Girder A. The net mid-span deflection is the deflection measured with the mid-span LVDT at the center of Girder A minus the deflection resulting from the compression of the elastomeric pads at the reactions. The

load-deflection graphs from the load tests are presented in Figure 8-3. The load tests show the reduction in stiffness as the welded connections failed. The first three measurements have an approximately linear load-deflection; however, the load test data at 44,000 cycles and 56,000 cycles are slightly non-linear, suggesting a flexural crack may have occurred between 38,000 and 44,000 cycles.

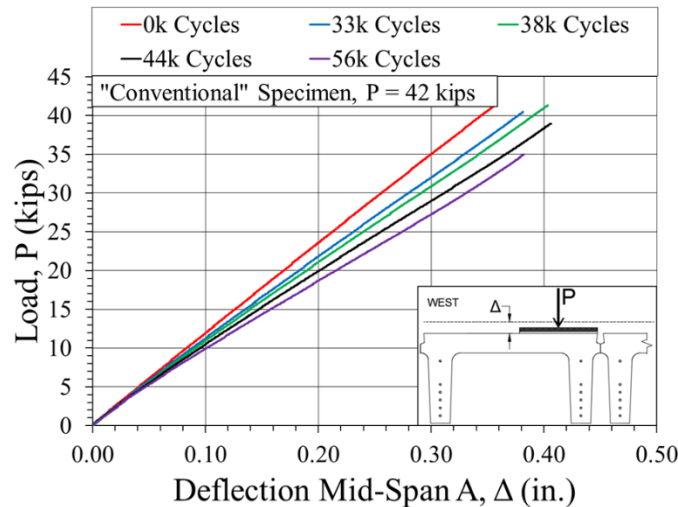


Figure 8-3: Measured Stiffness during Fatigue I – “Conventional” Specimen

The measured stiffness values are plotted in Figure 8-4 against the number of load cycles. A “best fit” line was added to show the effective rate of stiffness degradation during the Fatigue I test. The stiffness reduced from an initial value of 116 kip/in to a final value of 92 kip/in with a stiffness degradation effective rate of 0.406 kip/in/1000 load cycles.

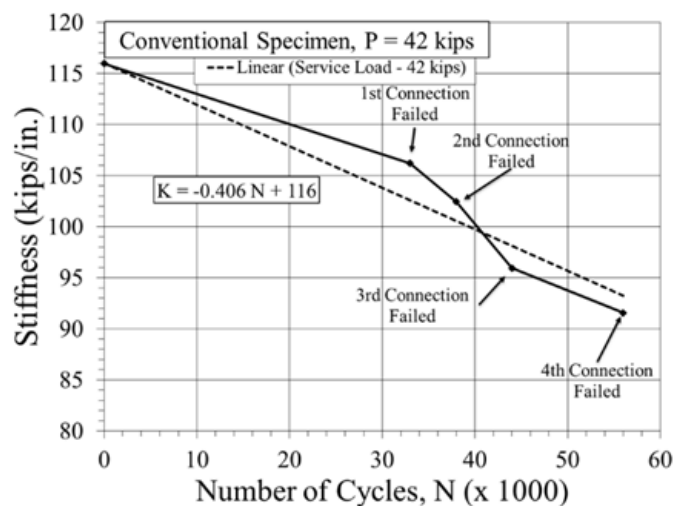


Figure 8-4: Stiffness Degradation during Fatigue I – “Conventional” Specimen

Figure 8-5 shows the measured relative deflection and joint rotation versus the number of load cycles. The values plotted in Figure 8-5 corresponded to an applied monotonic load of 35 kips. The relative deflection and joint rotation increased by 0.14 in. and 0.21 degrees, respectively when the number of load cycles increased from 0 to 55,000. Figure 8-6 shows the relative deflection between Girder A and Girder B during the Fatigue I test.

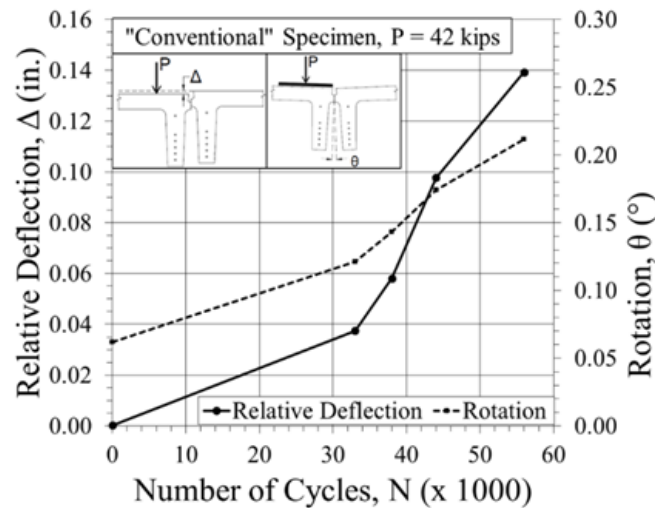


Figure 8-5: Relative Deflection and Joint Rotation during Fatigue I – “Conventional” Specimen



Figure 8-6: Relative Deflection at the Joint – “Conventional” Specimen

8.2.2 Fatigue II Loading

The longitudinal joint of the “Conventional” specimen was repaired to its original condition before the start of the Fatigue II test. To repair the joint, the grout was chipped out of the joint and the welded connections were cut at the weld joining the steel plate and the embedded steel angles. The girders were then moved apart to allow access to the embedded steel angles. The original weld was completely removed by grinding off the weld material on top of the angle to a smooth surface. The girders were moved back to their original position and the connections were welded together by a certified welder. Subsequently, the joint was grouted. Prior to applying the 21 kip fatigue loading, the stiffness of the specimen was measured to verify that the stiffness was not affected by the previous fatigue loading or the longitudinal joint repair. The measured stiffness was found to be identical to the original stiffness of 116 kip/in.

At 19,500 load cycles water began to seep through the longitudinal joint close to mid-span. Similar to the Fatigue I test, the leak spread farther away from mid-span with increasing number of load cycles. At 62,000 cycles, the first welded connection failed at 2.5 ft north of mid-span when the weld between the angle and the connection plate cracked. The connections at 2.5 ft south of mid-span and 7.5 ft north of mid-span broke at 67,000 and 80,000 cycles, respectively. The test was stopped at 80,000 cycles as the specimen was no longer capable of adequately transferring shear between the

two girders. The load-deflection results from the monotonic load tests are presented in Figure 8-7. The load-deflection plots were approximately linear suggesting that the girders were acting as uncracked. Although Girder A was cracked in the previous test, the prestressing force prevented the development of tensile stresses at the bottom of the section under the 21 kip load.

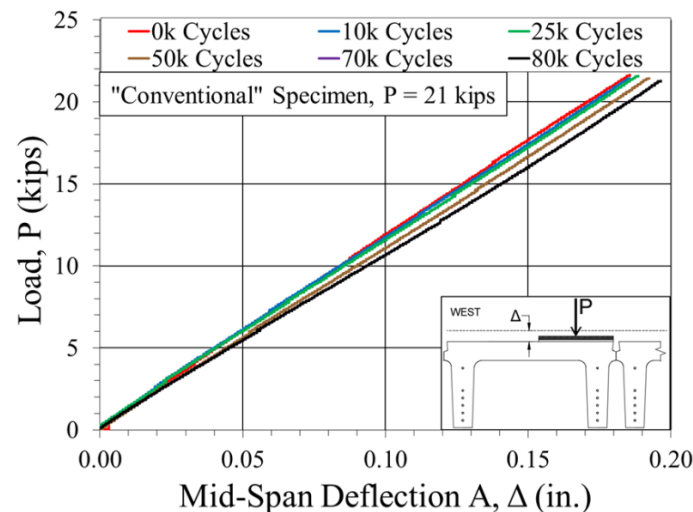


Figure 8-7: Measured Stiffness during Fatigue II – “Conventional” Specimen

The measured stiffness values are plotted in Figure 8-8 against the number of load cycles. The stiffness reduced from an initial value of 116.5 kip/in to a final value of 104 kip/in with an effective stiffness degradation rate of 0.130 kip/in/1000 load cycles. Doubling the fatigue load level to 42 kips resulted in more than three times the stiffness degradation rate.

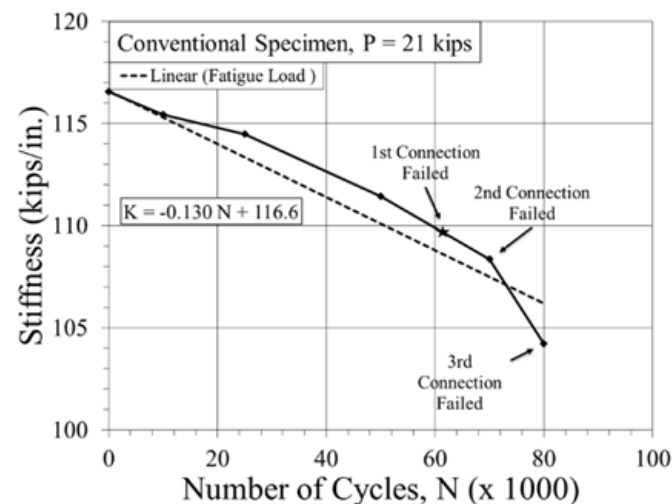


Figure 8-8: Stiffness Degradation during Fatigue II – “Conventional” Specimen

Figure 8-9 shows the measured relative deflection and joint rotation. For the Fatigue II load, the relative deflection and the joint rotation increased by 0.05 in. and 0.13 degrees, respectively when the number of load cycles increased from 0 to 80,000.

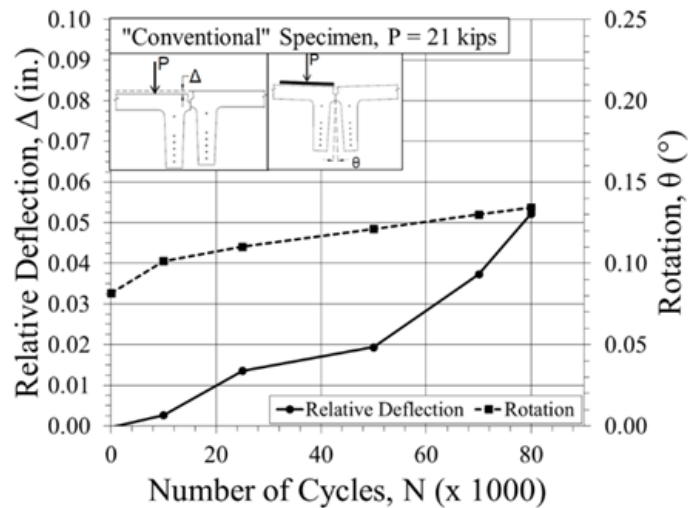


Figure 8-9: Relative Deflection and Joint Rotation during Fatigue II – “Conventional” Specimen

8.2.3 Strength Test

The longitudinal joint was repaired to its original condition prior to performing the strength test. The repair was done following the procedure presented in Section 8.2.2. Figure 8-10 shows the load-deflection plot. The deflection of Girder A at the equivalent service load of 42 kips was 0.4 in. At a load of 69.4 kips the welded connection at 2.5 ft north of mid-span failed when the connecting plate underwent significant double curvature bending as the two girders started to separate vertically. This was followed by complete separation between the angle and its embedded headed stud. The peak load reached during the test was 73.8 kips at a displacement of 1.12 in. measured at girder A. The peak load occurred immediately before the second connection failed at 2.5 ft south of mid-span. After the second connection failed, the deflection of girder B started to decrease with an increase in the actuator’s head displacement, indicating decreased shear transfer across the joint. The first prestressing strand yielded at the bottom of girder A when the load dropped to 66.1 kips at a displacement of 1.9 in. Plots of the measured strains are presented in Appendix G. The test was stopped after the longitudinal joint had completely separated. Figure 8-11 shows the “Conventional” specimen at failure.

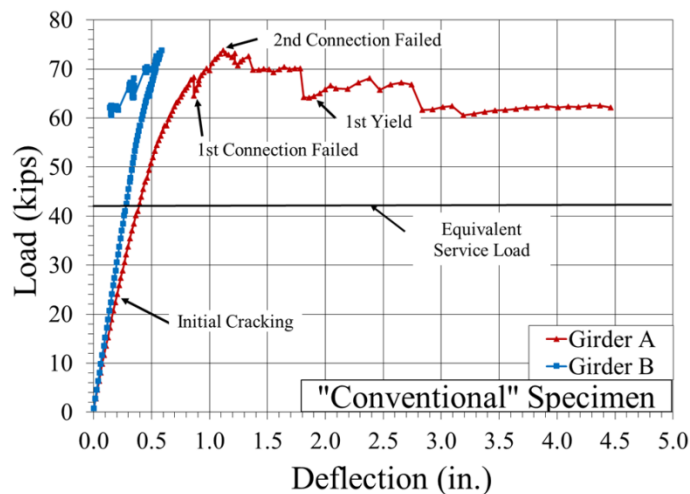


Figure 8-10: Measured Load-Deflection during Strength Test – “Conventional” Specimen



Figure 8-11: “Conventional” Specimen at Failure

The relative deflection and joint rotation of the “Conventional” specimen during the strength test is presented in Figure 8-12. The relative deflection and joint rotation at the equivalent service load of 42 kips were 0.036 in. and 0.27 degrees, respectively. The LVDTs used to monitor the relative deflection and the joint rotation were removed before the strength test was completed to prevent damage to the LVDTs. The ultimate relative deflection was in excess of 4 in. due to joint failure.

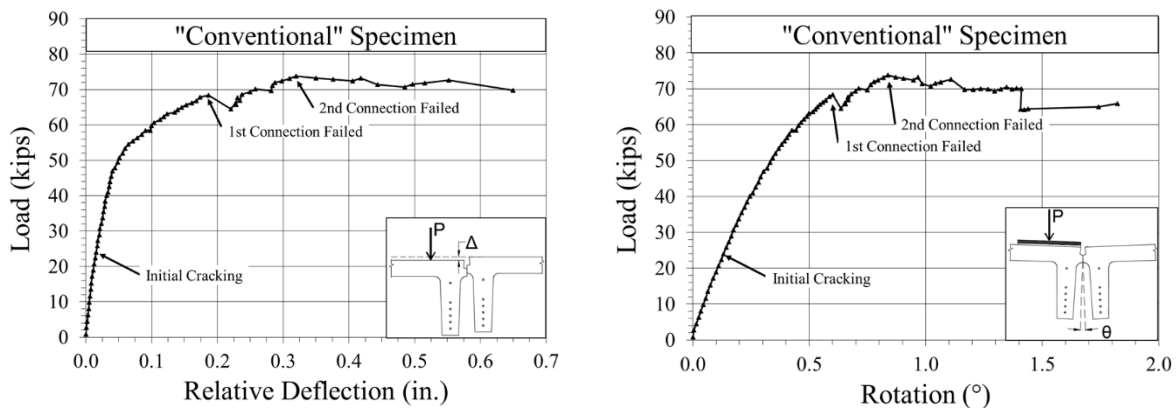


Figure 8-12: Measured Relative Deflection and Joint Rotation – “Conventional” Specimen

The north end reactions at the stems of Girder A and Girder B were measured under an applied load of 42 kips. The stems were labeled AW (Girder A, West stem), AE (Girder A, East stem), BW (Girder B, West Stem), and BE (Girder B, East Stem). Figure 8-13 shows the distribution of the total end reaction to the stems of the two girders. The reaction at the exterior stem BE of Girder B (trailing girder) was a negative force of 1.1 kips. This negative reaction was counteracted by the girder self-weight which prevented uplift at stem BE. The reaction at the interior stem BW of Girder B accounted for 49% of the entire reaction at the north end. These results indicate that the joint behaved as a hinge and the shear force that was transferred across the hinge acted as an eccentric force on Girder B, thus inducing an overturning moment that increased the reaction at BW and reduced the reaction at BE. The reactions at the interior stem AE and exterior stem AW of Girder A accounted for 31% and 25% of the entire reaction at the north end of the specimen.

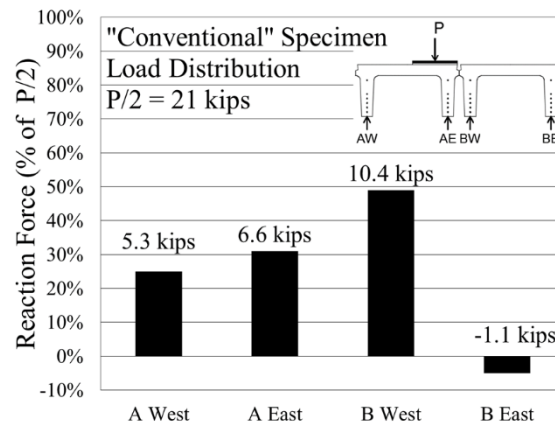


Figure 8-13: Measured End Reactions – “Conventional” Specimen

8.3 Test Results – “Proposed” Specimen

The “Proposed” specimen was first subjected to Fatigue II cyclic loading, followed by Fatigue I cyclic loading, and was finally loaded monotonically until failure. To study the effect of the diaphragms (joint rotation restraints) on improving the joint performance, the Fatigue II loading was performed with 7, 5, 3, and no diaphragms in place.

8.3.1 Fatigue II Loading

The “Proposed” specimen was first fatigue tested while all seven diaphragms between the stems were in place. A 21-kip load was applied at 1 cycle per second for a total of 500,000 cycles. No signs of joint deterioration or leakage were observed. Stiffness measurements were made periodically. The stiffness of the specimen was determined in a fashion similar to that of the “Conventional” specimen described in Section 8.2.1. The load-deflection graphs from the stiffness tests are presented in Figure 8-14. The measured stiffness values are plotted against the number of load cycles in Figure 8-15. The stiffness reduced from an initial value of 114.3 kip/in to a final value of 113.3 kip/in with negligible effective stiffness degradation rate of 0.0023 kip/in/1000 load cycles.

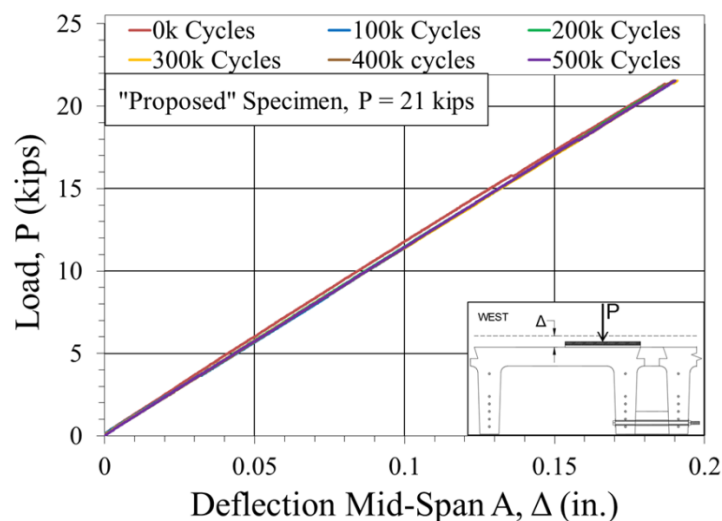


Figure 8-14: Measured Stiffness during Fatigue II with 7 Diaphragms – “Proposed” Specimen

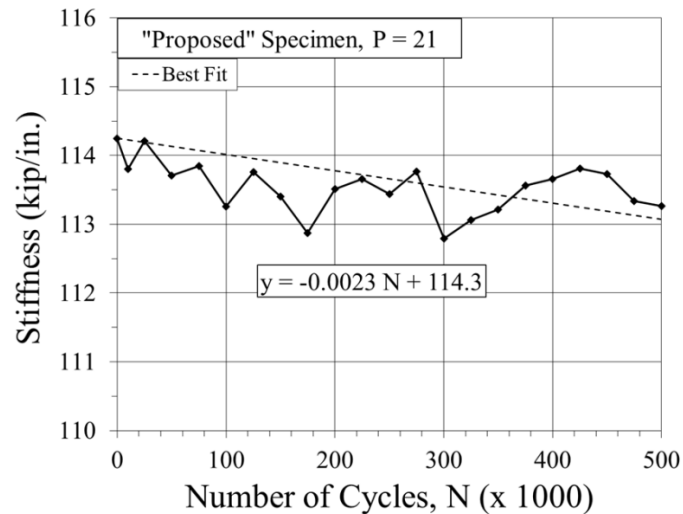


Figure 8-15: Stiffness Degradation during Fatigue II with 7 Diaphragms – “Proposed” Specimen

Figure 8-16 shows the measured relative deflection and joint rotation versus the number of load cycles. The values plotted in Figure 8-6 corresponded to an applied monotonic load of 21 kips. The changes in the relative deflection and joint rotation with increased loading cycles were negligible.

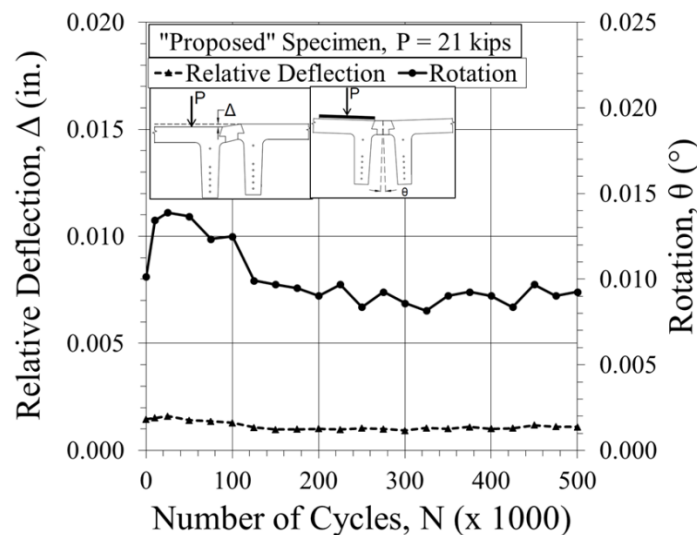


Figure 8-16: Relative Deflection and Joint Rotation during Fatigue II with 7 Diaphragms – “Proposed” Specimen

The diaphragms were removed and an additional 200,000 fatigue cycles were applied. No joint deterioration or leakage was observed. The load-deflection graphs from the stiffness tests are presented in Figure 8-17 and the measured stiffness values are plotted in Figure 8-18. The stiffness reduced from an initial value of 115 kip/in to a final value of 113.5 kip/in. Although the effective stiffness degradation rate was 0.0046 kip/in/1000 load cycles, twice that for the case with seven diaphragms, it was considered negligible when compared to the stiffness degradation rate for the “Conventional” specimen. Figure 8-19 shows a plot of the relative deflection and joint rotation. The relative deflection and joint rotation remained essentially unchanged during the 200,000 load cycles. Therefore, the diaphragms were redundant and did not provide tangible benefits to the performance

of the proposed joint. The construction time and cost would be reduced if the diaphragms were not included in the longitudinal joint detail.

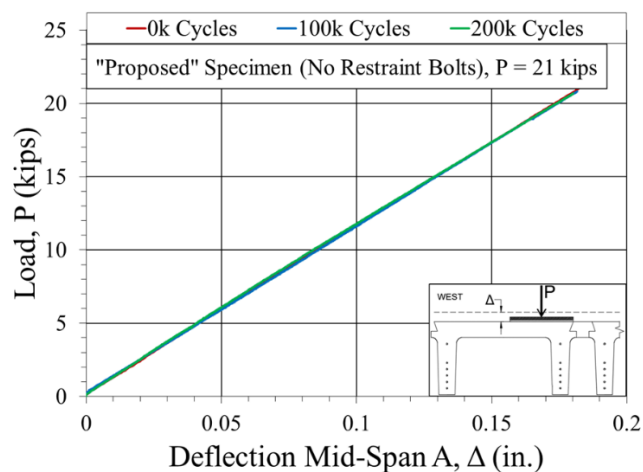


Figure 8-17: Measured Stiffness during Fatigue II without Diaphragms – “Proposed” Specimen

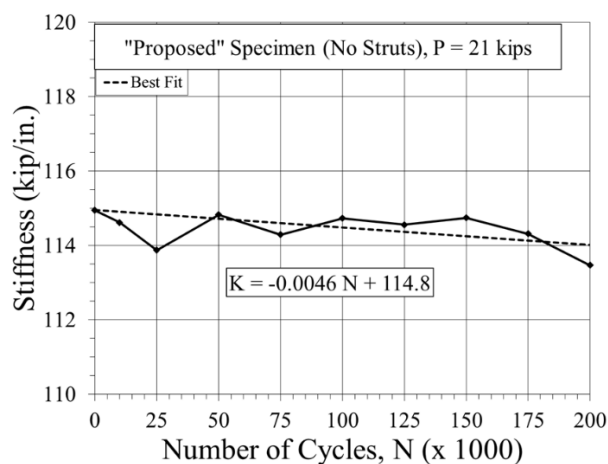


Figure 8-18: Stiffness Degradation during Fatigue II without Diaphragms – “Proposed” Specimen

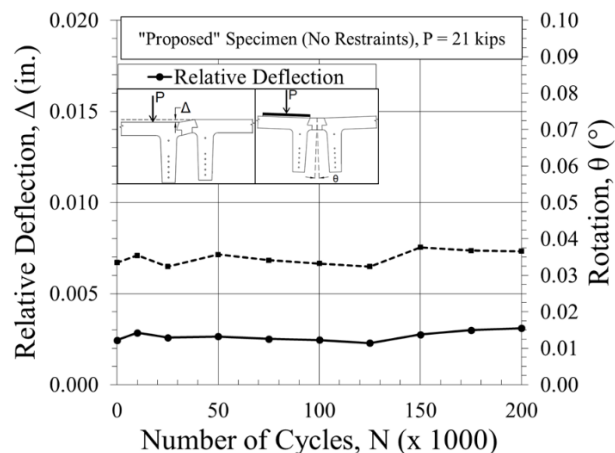


Figure 8-19: Relative Deflection and Joint Rotation during Fatigue II without Diaphragms – “Proposed” Specimen

8.3.2 Fatigue I Loading

Following the Fatigue II tests, the “Proposed” specimen was subjected to Fatigue I loading (42 kips) without any diaphragms for an additional 100,000 cycles. The specimen did not exhibit any noticeable signs of joint deterioration or loss of stiffness. The load-deflection graphs from the stiffness tests are presented in Figure 8-20 and the corresponding stiffness values are plotted in Figure 8-21. Figure 8-22 shows a plot of the relative deflection and joint rotation. The stiffness, relative deflection, and joint rotation remained essentially unchanged with added number of load cycles.

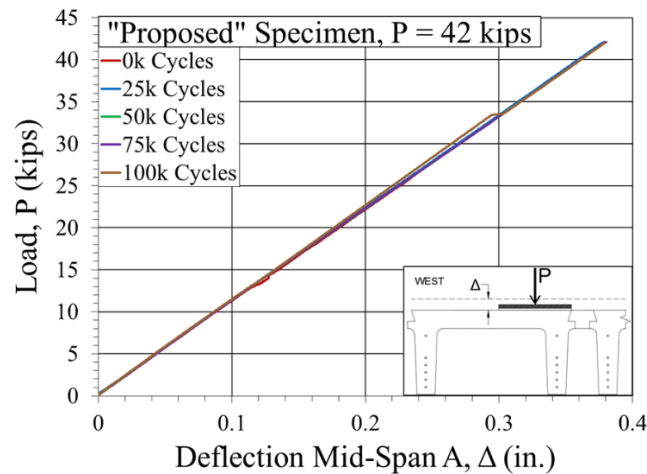


Figure 8-20: Measured Stiffness during Fatigue I – “Proposed” Specimen

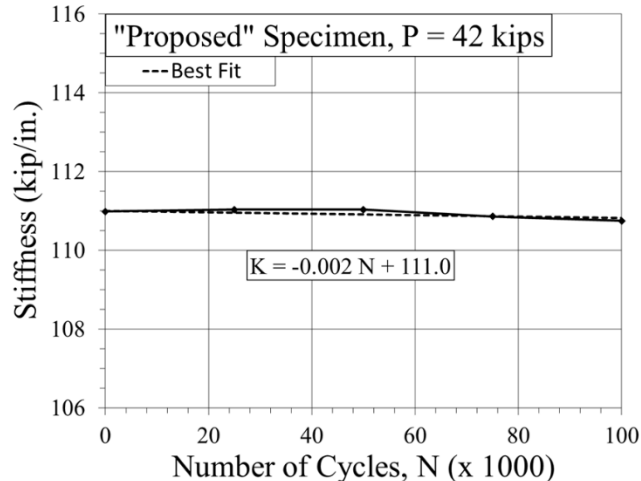


Figure 8-21: Stiffness Degradation during Fatigue I – “Proposed” Specimen

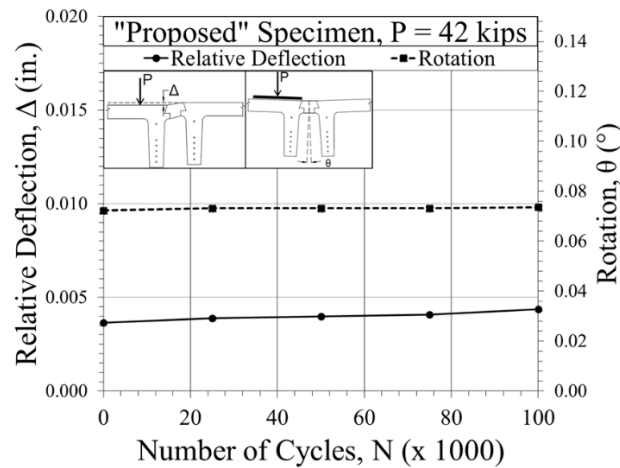


Figure 8-22: Relative Deflection and Joint Rotation during Fatigue I – “Proposed” Specimen

8.3.3 Strength Test

The “Proposed” specimen was tested for strength without the diaphragms. The load-deflection plot for the strength test is shown in Figure 8-23. The first flexural cracks appeared on the interior stem of girder A (Stem AE) at a load of 28 kips. Although this flexural crack was not noticed during fatigue testing, visual inspection during the static test revealed that the east stem was cracked prior to the test. Girder B initially cracked at the interior stem (Stem BW) at an applied load of 46.3 kips. The deflection of Girder A at the equivalent service load of 42 kips was 0.31in. The first strand yield occurred at a load of 96.5 kips and a corresponding displacement at the center of Girder A of 2.6 in. Plots of the measured strains are presented in Appendix G. The maximum load reached during the strength test was 113.1 kips at a displacement of 7.2 in. measured at the center of girder A. The longitudinal joint remained intact and girder B trailed closely the deflection of girder A during the entire test until flexural failure of the specimen was initiated by crushing of concrete at mid-span in girder A. The failed specimen is shown in Figure 8-24.

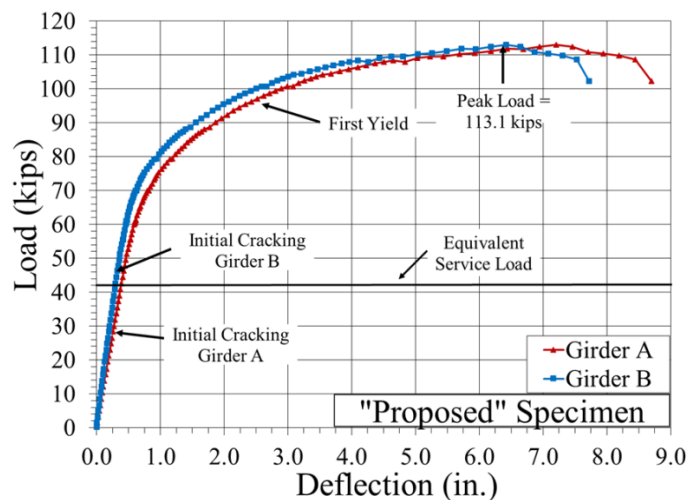


Figure 8-23: Measured Load-Deflection during Strength Test – “Proposed” Specimen



Figure 8-24: “Proposed” Specimen at Failure

The relative deflection and joint rotation of the “Proposed” specimen during the strength test is presented in Figure 8-25. The relative deflection and joint rotation at the equivalent service load of 42 kips were 0.008 in. and 0.09 degrees, respectively.

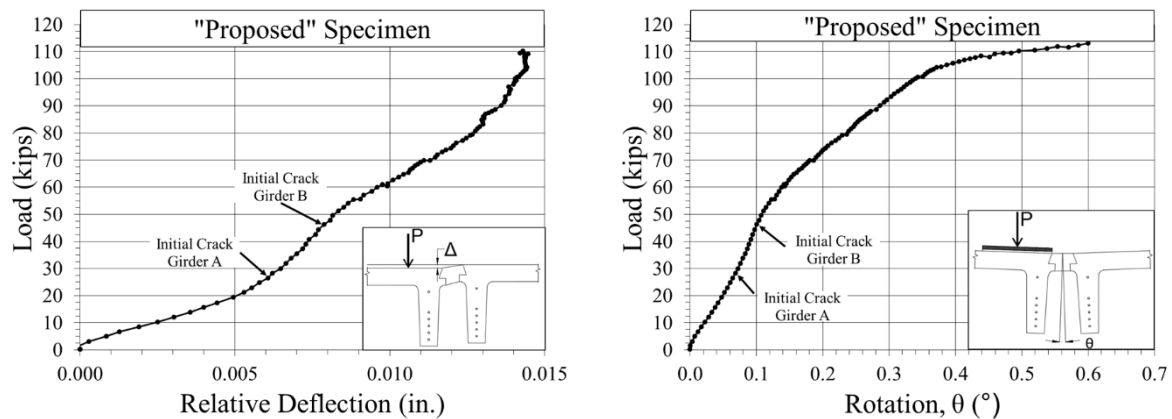


Figure 8-25: Measured Relative Deflection and Joint Rotation – “Proposed” Specimen

The north end reactions at the stems of Girder A and Girder B were measured under an applied load of 42 kips. Figure 8-26 shows the distribution of the total end reaction to the stems of the two girders. The results indicate that the joint provided continuity and enabled the two girders to act as one unit. The eccentric force P on the unit created a counterclockwise overturning moment that increased the reaction in the exterior stem of Girder A (AW) and reduced the reaction in the exterior stem of Girder B (BE). The combined reactions at the interior stems (AE and BW) constituted approximately 60% of the total reaction at the support.

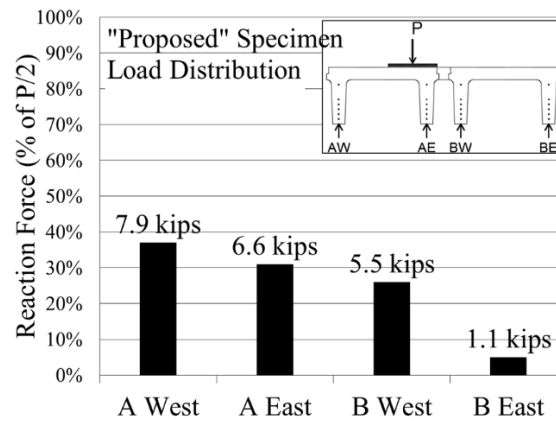


Figure 8-26: Measured End Reactions – “Proposed” Specimen

8.4 Analysis of Experimental Results

This section presents analysis of the experimental results and comparative evaluation of the effect of joint detailing on the serviceability and strength of the test specimens.

8.4.1 Fatigue Life

Based upon expected average daily truck traffic on typical local roads in South Dakota (see Section 7.5.1), the number of load cycles corresponding to 75 years of service was determined to be 411,000.

The joint of the “Conventional” specimen exhibited rapid deterioration under fatigue loading. Table 5 and Table 6 summarize the deterioration stages and the equivalent service years.

Table 5: Stages of Joint Deterioration during Fatigue I – “Conventional” Specimen

Joint Degradation	Number of Load Cycles	Equivalent Service Years
Water Seepage	15,000	2.7
Failure of 1 st Welded Connection	31,500	5.7
Failure of 2 nd Welded Connection	37,500	6.8
Failure of 3 rd Welded Connection	44,000	8.0
Failure of 4 th Welded Connection (Complete Joint Failure)	56,000	10.2

Table 6: Stages of Joint Deterioration during Fatigue II – “Conventional” Specimen

Joint Degradation	Number of Load Cycles	Equivalent Service Years
Water Seepage	19,500	3.6
Failure of 1 st Welded Connection	62,000	11.3
Failure of 2 nd and 3 rd Welded Connections	67,000	12.2
Failure of 4 th Welded Connection (Complete Joint Failure)	80,000	14.6

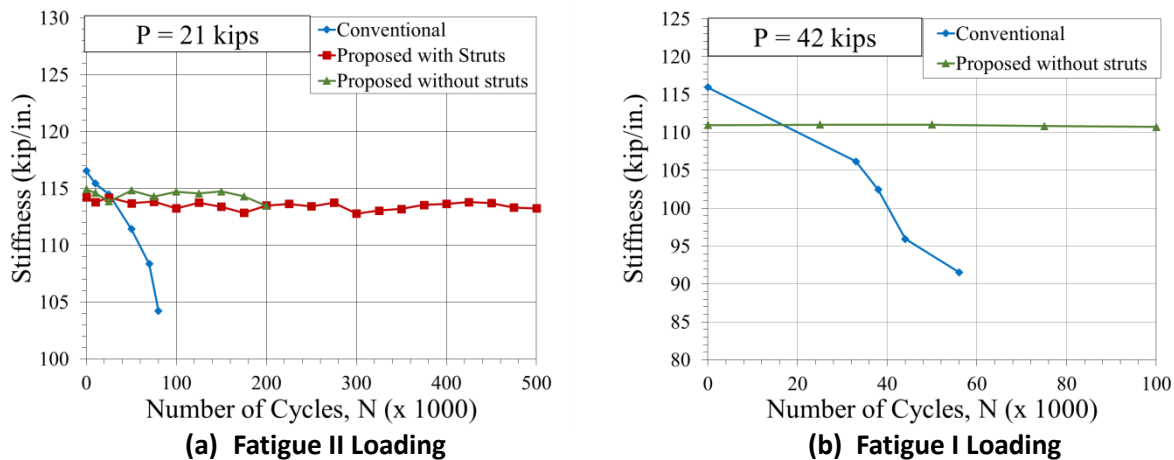
The joint of the “Proposed” Specimen remained intact throughout the fatigue testing program. Table 7 summarizes the loading conditions and the corresponding service life. The total equivalent service years was 145.9 years with no signs of fatigue deterioration.

Table 7: Stages of Joint Fatigue – “Proposed” Specimen

Joint Degradation	Number of Load Cycles	Equivalent Service Years
No Damage	500,000 (Fatigue II with 7 Diaphragms in Place)	91.2
No Damage	200,000 (Fatigue II with no Diaphragms)	36.5
No Damage	100,000 (Fatigue I with no Diaphragms)	18.2

8.4.2 Stiffness Degradation

Under fatigue loading, the “Conventional” specimen experienced significant stiffness degradation while the stiffness of the “Proposed” specimen was practically unchanged. Figure 8-27 shows a graphical comparison of the stiffness degradation for the “Conventional” and the “Proposed” specimens. Table 8 presents a summary of the stiffness degradation rates.

**Figure 8-27: Comparison of Stiffness Degradation****Table 8: Stiffness Degradation Effective Rates**

	Degradation Effective Rate (kip/in/1000 cycles)	
	“Conventional” Specimen	“Proposed” Specimen with no Diaphragms
Fatigue II Test	0.130	0.0046
Fatigue I Test	0.406	0.0023

The stiffness degradation effective rate for the conventional specimen was 0.130 and 0.406 kip/in/1000 cycles for Fatigue II and Fatigue I loading, respectively. Thus, doubling the fatigue load intensity resulted in three times the stiffness degradation rate. On the other hand, the stiffness degradation rates for the “Proposed” specimen were practically negligible.

8.4.3 Flexural Strength

The nominal flexural strength of one girder was calculated using the method prescribed in AASHTO (2012) and was found to be equal to 580 kip-ft. The calculation details are shown in Appendix F.

The maximum bending moment attained during the strength test of the “Conventional” specimen was 722.6 kip-ft. Thus, the conventional joint was capable of developing only 61.9% of the combined theoretical flexural capacity for the two girders before joint failure.

The maximum bending moment attained by the “Proposed” specimen was 1107 kip-ft. Thus, the proposed joint was capable of engaging the trailing girder and developing 95.4% of the combined theoretical flexural strength for the two girders, indicating an excellent ability for load transfer to adjacent girders.

Under the loading condition considered in this study, the load carrying capacity of the “Proposed” specimen was more than 1.5 times that of the “Conventional” specimen.

8.4.4 Reactions at the Support

The measured reactions at the girder stems to the applied load were heavily dependent upon the joint detailing. The measured support reactions at the stems under an applied 42-kip load are presented graphically in Figure 8-13 and 8-26 for the “Conventional” and “Proposed” specimens, respectively, and are summarized in Table 9. For the “Conventional” specimen, the measured reaction at the interior stem of the trailing girder (BW) constituted close to 50% of the system’s total reaction, while the reaction at the interior stem of the loaded girder (AE) was only 31% of the total reaction despite the fact that the load was applied almost on top of the stem. On the other hand, the “Proposed” specimen results indicate that the joint enabled more uniform load distribution to the interior stems and better engagement of the exterior stems. The combined reaction at the interior stems (AE and BW) was approximately 60% of the total reaction for the “Proposed” specimen as compared to 80% for the “Conventional” specimen.

Table 9: Measured Reactions at the Stems of the North End Support (P = 42 kips)

	Reaction (kips)				Total (kips)
	AW	AE	BW	BE	
“Conventional” Specimen	5.3	6.6	10.4	-1.1	21.2
“Proposed” Specimen	7.9	6.6	5.5	1.1	21.1

The reaction distribution is indicative of a joint that resembles a hinge in the case of the “Conventional” specimen and a relatively rigid connection in the case of the “Proposed” specimen. To illustrate this, a simplified structural analysis approach was considered. The girders were assumed to be infinitely stiff. Thus, the specimens were modelled as two dimensional elements. The free body diagrams for the two dimensional representation of the “Conventional” and the “Proposed” specimens are shown in Figure 8-28 and Figure 8-29, respectively. The simplified analysis was performed to determine the stem reactions at one end of the specimen.

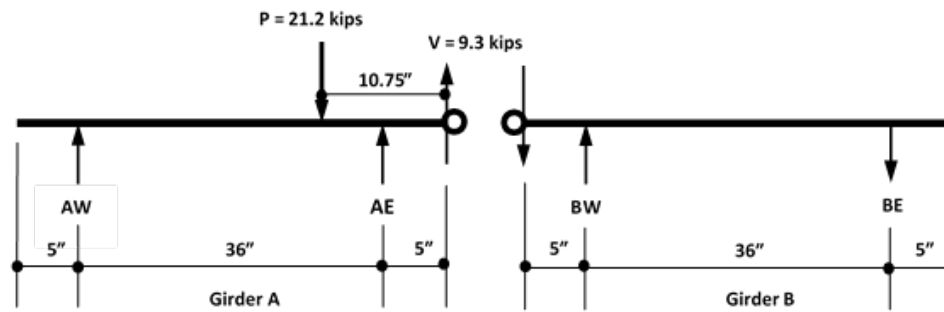


Figure 8-28: Free Body Diagram – “Conventional” Specimen

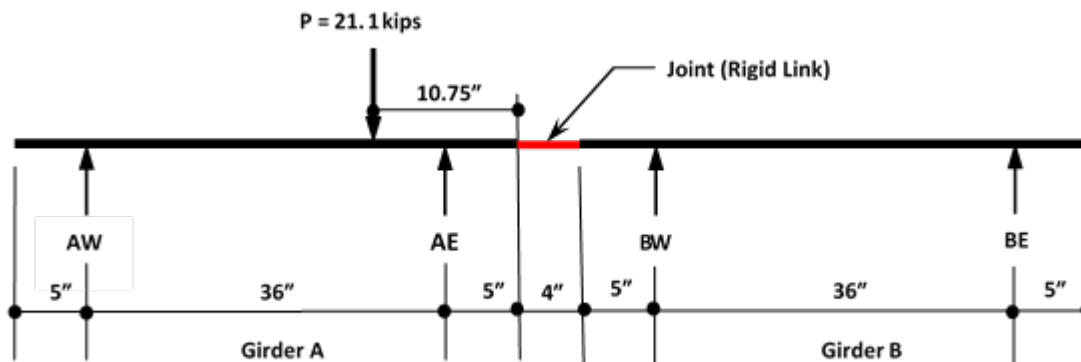


Figure 8-29: Free Body Diagram – “Proposed” Specimen

For the “Conventional” specimen, a hinged joint was assumed. Thus, the joint could transfer shear but not moment. The shear force that is applied at the hinge in Figure 8-28 was determined from the measured reactions. For the “Proposed” specimen, the joint was assumed to be a rigid connection. The calculated reactions in Figure 8-28 and Figure 8-29 are summarized in Table 10. The results of the simplified structural analysis approach show reactions and reaction distributions that closely resemble the measured distributions. Therefore, the joint behavior was close to that of a hinge in the “Conventional” specimen and to that of a rigid connection in the “Proposed” specimen.

Table 10: Reactions Based on Simplified Structural Analysis (P = 42 kips)

	Reaction (kips)				Total (kips)
	AW	AE	BW	BE	
“Conventional” Specimen	4.7	7.2	10.6	-1.3	21.2
“Proposed” Specimen	8.3	5.8	4.8	2.2	21.1

The measured reactions were verified analytically using a structural analysis software (CSI 2012). A finite element model was developed for each specimen and analyzed under a 21-kip applied load. The finite element model is described in Appendix H. The experimental and analytical stem reactions for the “Conventional” specimen and the “Proposed” specimen without diaphragms are presented in Table 11 and Table 12, respectively. A graphical presentation of those results is shown in Figure 8-30. The results indicate good agreement between the experimental and analytical results. The difference between the experimental and the analytical results ranged between 3% and 13% for the

“Conventional” specimen and between 2% and 18% for the “Proposed” specimen. Therefore, the reaction measurement at the girder stems was considered reliable.

Table 11: Experimental and Analytical Reactions (P = 21 kips) – “Conventional” Specimen

	North End Reaction (kips)		
	Experimental	Analytical	% Difference
AW	2.63	2.30	12%
AE	3.26	3.61	11%
BW	5.15	5.04	2%
BE	-0.53	-0.46	13%

Table 12: Experimental and Analytical Reactions (P = 21 kips) – “Proposed” Specimen with No Diaphragms

	North End Reaction (kips)		
	Experimental	Analytical	% Difference
AW	3.89	3.44	12%
AE	3.26	3.32	2%
BW	2.73	3.22	18%
BE	0.53	0.52	2%

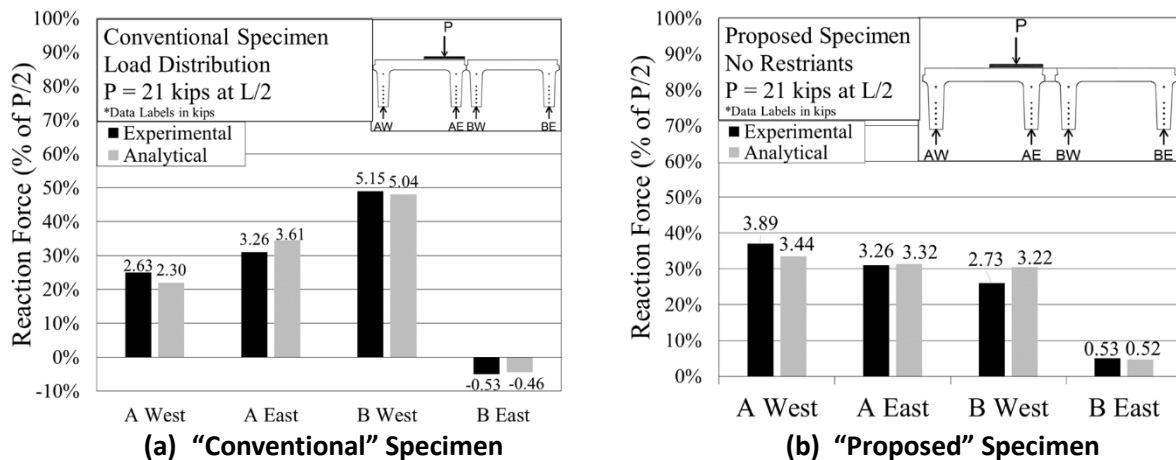


Figure 8-30: Reaction Force Distribution to the Girder Stems (P = 21 kips)

8.4.5 Effect of Shear Span on Reaction Force Distribution to the Girder Stems

Using the finite element model, the effect of the shear span on the reaction force distribution was analyzed. In addition to $L/2$, where L is the span length, two additional shear spans were considered; $L/3$ (13.33 ft from support) and $L/6$ (6.67 ft from support). Figure 8-31 shows the reaction force distribution for an applied load of 21 kips. The reactions are shown as a percentage of the applied load P rather than $P/2$ because the end reactions deviate from $P/2$ when the load position is not at mid-span.

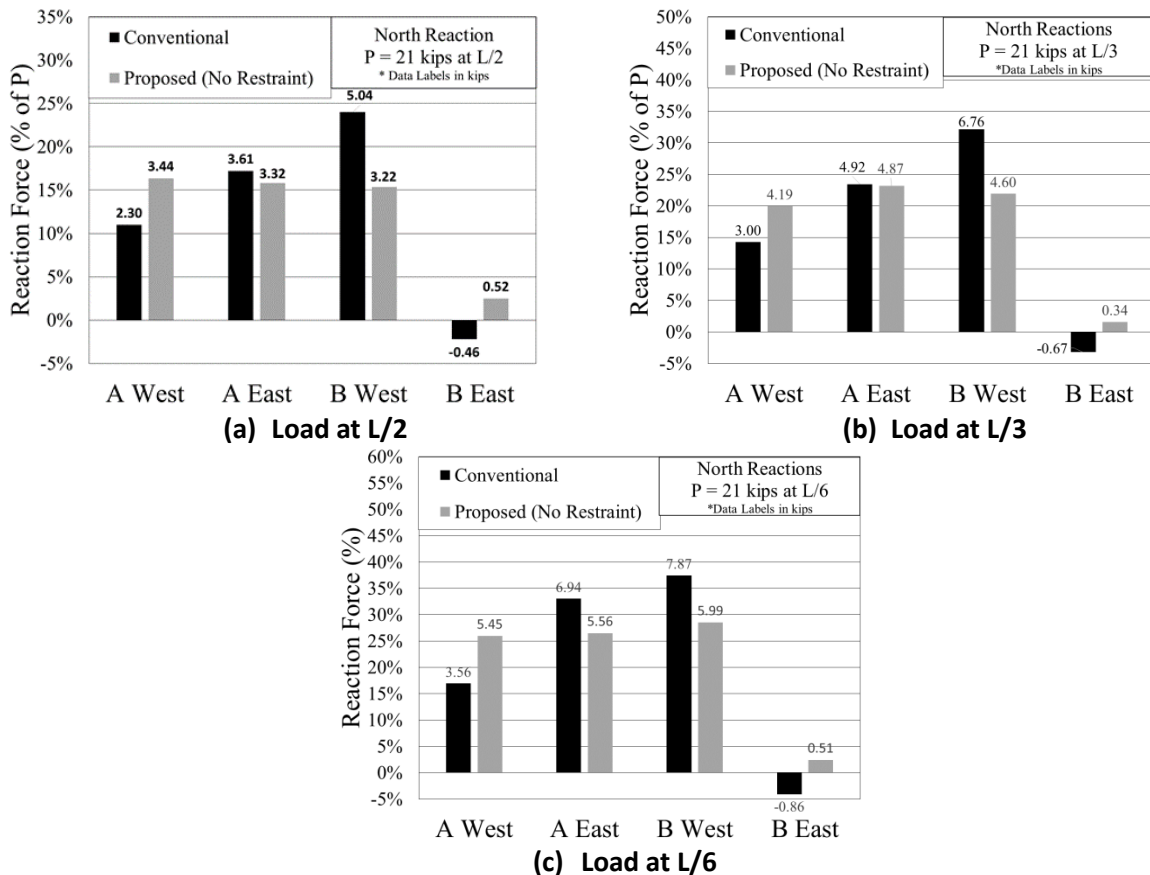


Figure 8-31: Analytical Reaction Force Distribution for Shear Spans of L/2, L/3, and L/6

Table 13 presents a summary of the reaction values as a percentage of the total reaction for the three shear span cases considered above. The analytical results indicate that the shear span had only a marginal effect on the load distribution to the stems. For the “Proposed” specimen, approximately one-third of the applied loads was carried by each of the stems of the loaded girder (AW and AE) and the first interior stem of the trailing girder (BW). For the “Conventional” specimen, close to one-half of the applied load was carried by the first interior stem of the trailing girder (BW).

Table 13: Summary of Analytical Reaction Force Distribution for Different Shear Spans

		Reaction (% of Support Reaction)			
	Shear Span	AW	AE	BW	BE
“Conventional” Specimen	L/2	21.9	34.4	48.1	-4.4
	L/3	21.4	35.1	48.3	-4.8
	L/6	20.3	39.7	45.0	-4.9
“Proposed” Specimen	L/2	32.8	31.6	30.7	5.0
	L/3	29.9	34.8	32.9	2.4
	L/6	31.1	31.8	34.2	2.9

8.4.6 Joint Shear

The joint shear for the test specimens was calculated using the measured reactions of Girder A and Girder B. For a 21-kip load, the joint shear was 9.24 kips (44% of applied load) for the “Conventional”

specimen and 6.52 kips (31% of applied load) for the “Proposed” specimen. Therefore, for the cases considered in this study, the “Proposed” specimen resulted in approximately 30% decrease in the joint shear demand.

The joint shear force in the “Conventional” specimen was carried mainly by the welded connections as verified by the finite element analysis. The highest shear force was developed in the middle two welded connections closest to the applied load. For a 21-kip load, the shear force in a middle connection was 3.9 kips, or 18.6% of the applied load. Analysis was also performed for load placements at $L/3$ and $L/6$ to examine the potential for development of higher shear forces in the welded connections. The shear forces in the connections for $L/2$, $L/3$, and $L/6$ load placements are shown in Figure 8-32. The results indicate that the shear force may reach 4.6 kips in the connections located at 7.5 ft and 12.5 ft from the end of the specimen.

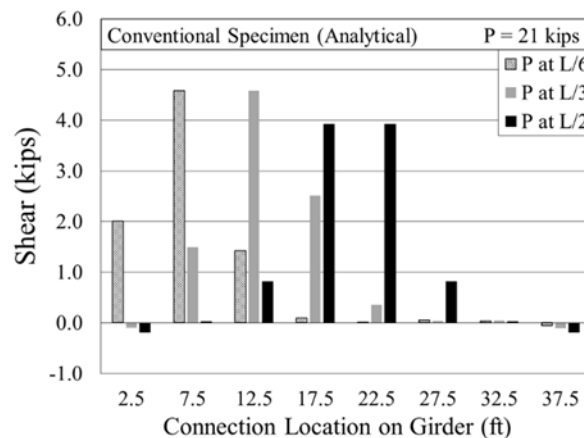


Figure 8-32: Shear Force in the Welded Connections of the “Conventional” Specimen

On the other hand, the joint shear in the “Proposed” specimen was carried by shear stress along the joint length. As expected, the finite element analysis showed that the highest joint shear stresses developed in the vicinity of the applied load and reduced gradually as the distance to the applied load increased. The joint shear stress in the vicinity of the applied load was approximately 11.5 psi. For a shear force of 6.52 kips and joint thickness of 5 in., a joint length of 114 in. would be required to carry the shear force.

For practical applications, a rational procedure for shear design of the “Proposed” joint is suggested. The procedure requires determination of an effective joint length for resisting the shear force and a shear strength model that lends itself to the joint cross sectional geometry which represents a deep beam condition. A deep beam is defined as a member with a span length less than four times its depth (ACI 2014). A conservative estimate for the effective joint length can be based on the assumption that the applied load spreads out from the corners of the 20 in. by 10 in. contact area at 45° angles as shown in Figure 8-33. Thus, the effective joint length would be equal to 50 in. This value is approximately 44% of the 114-in. length determined by using the shear stress value from the finite element analysis.

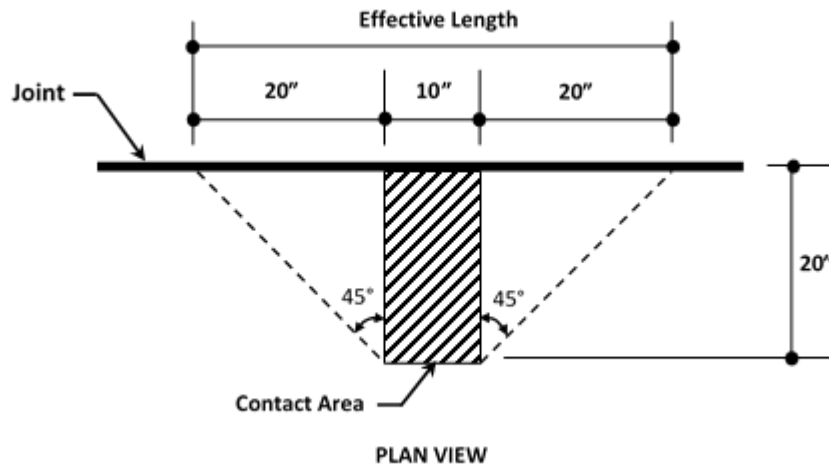


Figure 8-33: Suggested Effective Joint Length for Shear Strength Design

For shear design, the factored shear force (required strength) must not exceed the design shear force as expressed in Equation 8.1:

$$V_u \leq \phi V_n \quad (\text{Eq. 8.1})$$

Where

V_u = factored shear force

V_n = nominal shear strength

ϕ = strength reduction factor

ϕV_n = design shear strength

The shear-friction method (ACI 2014) is suitable for determining the nominal shear strength of proposed joint. In this method, the nominal shear strength is determined using the following equation:

$$V_n = A_{vf} f_y (\mu \sin \alpha + \cos \alpha) \quad (\text{Eq. 8.2})$$

Where

V_n = nominal shear strength

A_{vf} = shear-friction reinforcement

f_y = yield strength of the shear-friction reinforcement

μ = coefficient of friction

α = angle between shear-friction reinforcement and shear plane

The shear-friction coefficient for concrete placed against hardened concrete not intentionally roughened is 0.6 (ACI 2014). The shear plane in the joint is assumed to occur along the interface of the girder deck and the grout. Therefore, the angle α is 90°. For the “Proposed” specimen, the shear-friction reinforcement is 0.24 in²/ft, or 1.0 in² per 50 in. of effective length. Assuming the yield strength of the mesh reinforcement is 40 ksi, then the nominal shear strength would be 24 kips.

8.5 Cost Estimate for the Proposed Joint

This section presents an estimate of the cost to implement the proposed longitudinal joint in double tee bridges in South Dakota. A preliminary estimate was performed by a bridge construction company in Mitchell, South Dakota. The estimate reflects the prevailing prices in 2014.

The cost estimate was based on a two-lane 65-ft bridge with eight 30-in. deep double tee girders. The additional fabrication and construction cost for the double tee girders with the proposed joint without diaphragms would be \$9,350. If the diaphragms were included in the longitudinal joint system, the cost would be \$13,720. Bids for previous double-tee bridge projects with 65-ft spans have ranged from \$250,000 to \$300,000. Implementing the proposed joint without diaphragms could increase the initial project cost by 3% to 4%.

9 FINDINGS AND CONCLUSIONS

The research study presented in this report was conducted at South Dakota State University (SDSU) to develop new longitudinal joint detailing for use with precast/prestressed double tee bridge girders and to assess the structural performance of the proposed new joint and the conventional joint that has been used in South Dakota. The study included experimental and analytical work. The experimental work included fatigue and strength testing of two full-scale bridge deck sub-assemblages.

The proposed joint exhibited substantially improved serviceability and strength performance characteristics over the conventional joint at no significant increase in initial construction cost.

9.1 Findings

Based on the experimental and analytical results, the following findings were identified.

- The proposed joint construction process was relatively simple and did not require special expertise or tools. The conventional joint required a certified welder to attach the welded connections.
- The proposed joint survived 800,000 of combined Fatigue II and Fatigue I load cycles (146 service years) without exhibiting any signs of failure. The conventional joint experienced structural failure at 62,000 load cycles (11.3 service years) under normal service loading conditions (Fatigue II).
- Water seepage through the conventional joint started at 19,500 load cycles (3.6 service years) and 15,000 load cycles (2.7 service years) for Fatigue II and Fatigue I loads, respectively. The proposed joint remained water tight under 800,000 cycles of combined Fatigue I and Fatigue II loading. It should be noted that non-shrink grout material specified by South Dakota DOT (described in this report) is adequate for the proposed joint. However, the joint must be cast in one continuous pour to eliminate cold joints that might allow for the passage of water.
- Under fatigue loading, the conventional joint deteriorated rapidly resulting in significant stiffness degradation, while the proposed joint remained essentially intact and had negligible effect on stiffness degradation. For Fatigue II loading, the stiffness degradation rate of the “Conventional” specimen was 26 times that of the “Proposed” specimen.
- The addition of rotation-restraining diaphragms to the proposed joint detail reduced the stiffness degradation rate by a factor of 2 (from 0.0046 kip/in/1000 load cycles to 0.0023 kip/in/1000 load cycles). However, even without diaphragms, the stiffness degradation rate was negligible and had no negative effects on the joint performance.
- The behavior of the conventional joint was close to that of a hinged connection while the behavior of the proposed joint was close to that of a rigid connection. The difference in behavior had significant implications on flexural strength, distribution of the support reactions to the girder stems, and joint shear.

- The conventional joint allowed for the development of only 61.9% of the loaded and trailing girders combined flexural strength. The proposed joint was capable of engaging the trailing girder and developing 95.4% of the combined flexural strength.
- For the “Conventional” specimen, the measured reaction at the interior stem of the trailing girder constituted close to 50% of the system’s total support reaction, while the reaction at the interior stem of the loaded girder was only 31% of the total support reaction despite the fact that the load was applied almost on top of the stem. The combined reaction at the interior stems was approximately 60% of the total reaction for the “Proposed” specimen as compared to 80% for the “Conventional” specimen.
- The analytical results indicated that the shear span had a minor effect on the load distribution to the stems. For each of the three shear spans considered in this study, approximately one-third of the applied load was carried by each of the stems of the loaded girder and the first interior stem of the trailing girder of the “Proposed” specimen, while close to one-half of the applied load was carried by the first interior stem of the trailing girder of the “Conventional” specimen.
- The joint shear force, as calculated using the measured reactions, was 44% of the applied load for the “Conventional” specimen and 31% of the applied load for the “Proposed” specimen.
- The joint shear force was carried mainly by the welded connections in the conventional joint and by shear stresses in the proposed joint. A rational procedure based on an effective joint length and the ACI shear-friction equation was developed for the design of the proposed joint for shear.
- Implementing the proposed joint without diaphragms could increase the initial project cost by 3% to 4%.

9.2 Conclusions

Following are the conclusions of this study.

- The proposed joint is feasible for field construction and does not require special skills.
- The proposed joint service life exceeds the desired bridge design life of 75 years while the conventional joint would fail during the early service years of a bridge.
- The proposed joint is successful in mitigating water seepage while the conventional joint is susceptible to water seepage at an early age.
- The proposed joint virtually eliminates stiffness degradation due to fatigue while the conventional joint would result in rapid stiffness degradation.
- The rotation-restraining diaphragms are redundant and do not provide tangible benefits to the performance of the proposed joint. Eliminating the diaphragms would reduce construction cost and time.

- The conventional joint behaves as a hinge which allows for shear transfer only. The proposed joint behavior is similar to a stiff link between the girders.
- Under the loading conditions considered in this study, the flexural strength of specimen with the proposed joint was more than 1.5 times that of the specimen with the conventional joint.
- The proposed joint allowed for a better spread of the support reactions over the girder stems.
- The analytical results indicate that the shear span had only a marginal effect on the load distribution to the stems.
- For the cases considered in this study, the proposed joint results in approximately 30% decrease in the joint shear demand.
- A rational procedure may be used for the shear design of stiff joints with shear-friction reinforcement similar to the proposed joint.
- The added initial construction cost for implementing the proposed joint is approximately 3% to 4% of the total bridge construction cost. The added cost is inconsequential when compared to potential savings obtained extending the joint service life to more than 75 years.

10 RECOMMENDATIONS

Based on the findings of this study, the research team offers the following recommendations.

10.1 Terminology

Future reference to the conventional joint and the proposed joint in double tee girder bridges should be “discrete welded joint” and “monolithic joint”, respectively.

The proposed terminology provides concise description of the anatomy and performance of the two joint types considered in this study.

10.2 Discrete Welded Joint

The discrete welded joint detailing should not be used for the construction of new double tee girder bridges.

The discrete welded joint is severely inadequate at both the serviceability and the strength limit states. Water seepage through the joints could occur within the first three years of service life, leading to moisture ingress and concrete deterioration. Failure of the welded connections could start at less than 15 years in service. Loss of the welded connections will compromise the structural integrity of the bridge and reduce its design load carrying capacity.

10.3 Monolithic Joint

The monolithic joint detailing concept should be adopted for the construction of new double tee girder bridges.

The monolithic joint provides substantially improved serviceability and strength performance characteristics over the discrete welded joint at no significant increase in initial construction cost. The rotation-restraining diaphragms are redundant and unnecessary for improving the performance of monolithic joints. The joint service life may well exceed the bridge design life of 75 years. The joint is water-tight, exhibits negligible stiffness degradation, leads to better distribution of the support reaction to the girder stems, and engages adjacent girders at the strength limit state.

10.4 Future Research

A future study is needed to calibrate AASHTO’s wheel load distribution factors, provide a simple method for determining the distribution of support reaction to the girder stems, and evaluate the joint shear demand in full bridge systems.

AASHTO LRFD Bridge Design Specifications provide live load distribution factors for determining the moment and shear demands in girders of double tee girder bridges. The AASHTO distribution factors are limited to joints that are “connected only enough to prevent relative vertical displacement at the interface.” Moreover, AASHTO does not provide methods for determining the live load shear force (reaction) at each stem or the critical shear force transferred at longitudinal joints.

The results of the current study clearly show that the joint behavior has significant influence on the support reaction at the girder ends, the distribution of the support reaction to the stems, and the value of the shear force transmitted through the joint. However, this study was limited to testing and analyzing a two-girder sub-assembly system using one of the standard double tee girder cross

sections. The basic finite element models developed in this study can be expanded in a follow up parametric study to analyze full bridges with different spans and girder cross sections. The main objective of the future study would be to develop empirical equations that will enable the designer to determine load demands in different double tee bridge configurations.

11 RESEARCH BENEFITS

The number of structurally deficient bridges on the local road system in South Dakota continues to grow due to the unexpected early deterioration of a large number of the existing bridges. The expected design life of these bridges was 50 to 70 years, but some built less than 40 years ago already need replacement. Due to its rapid and ease of construction, the double tee precast girder bridge is the standard bridge system used for the majority of bridges on local roads. The most common problem in double tee bridges is that longitudinal joints become damaged over time, most likely due to inadequate shear transfer between the girders, allowing water and debris to enter the joints. It is only a matter of time before the joint begins to spall, creating a path for moisture to reach the prestressing steel, initiate corrosion, and degrade the structural capacity of the bridge.


Facing limited budgets, local governments in South Dakota are in need of a robust, inexpensive, and easy to construct bridge system that will last for at least 75 years. The double tee bridge system provides a viable option only if longitudinal joints are made to provide more than 75 years of service without deterioration or losing structural integrity. The new joint detailing that was developed in this study is easy to construct, lasts longer than the equivalent of 100 years of truck traffic, and incurs minor additional initial cost. By adopting the proposed joint detail for the construction of new bridges, local governments in South Dakota are expected to realize significant bridge repair and replacement cost savings.

12 REFERENCES

- American Association of State Highway and Transportation Officials (AASHTO) (2012). "AASHTO-LRFD Bridge Design Specifications, Sixth Edition." Washington, DC.
- American Concrete Institute (ACI) (2014). "Building Code Requirements for Structural Concrete and Commentary." Farmington Hill, MI.
- American Society for Testing Materials (ASTM) (2010a). "Standard Test Method for Air Content of Freshly Mixed Concrete by the Pressure Method." ASTM International, West Conshohocken, PA.
- American Society for Testing Materials (ASTM) Standard C39 (2010b). "Standard Test Method for Compressive Strength of Cylindrical Concrete Specimens." ASTM International, West Conshohocken, PA.
- American Society for Testing Materials (ASTM) Standard C109 (2010c). "Standard Test Method for Compressive Strength of Hydraulic Cement Mortars (Using 2-in. Cube Specimens)." ASTM International, West Conshohocken, PA.
- American Society for Testing Materials (ASTM) Standard C143 (2010d). "Standard Test Method for Slump of Hydraulic-Cement Concrete." ASTM International, West Conshohocken, PA.
- Computers and Structures, Inc. (2012). "SAP2000, Version 14." Berkeley, CA.
- Culmo, M. and Seraderian, R. (2010). "Development of the Northeast Extreme Tee (NEXT) Beam for Accelerated Bridge Construction (ABC)." PCI Journal, Summer 2010, Chicago, IL.
- Eriksson Technologies, Inc. (2011). "PSBEAM, Version 4.27." Temple Terrace, FL.
- French, C.E, Shield, C.K., Klaseus, D., Smith, M., Eriksson, W., Ma, Z. J., Zhu, P., Lewis, S., Chapman, C.E. (2011). "Cast-in-Place Concrete Connections for Precast Deck Systems." NCHRP Project 10-71 Report No. 173, Transportation Research Board, Washington, DC.
- Jones, Harry (2001). "Lateral Connections for Double Tee Bridges." Report No. FHWA/TX-01/1856-2, US DOT, Federal Highway Administration
- Li L., Ma Z., and Oesterle R.G. (2010). "Improved Longitudinal Joint Details in Decked Bulb Tees for Accelerated Bridge Construction: Fatigue evaluation." Journal of Bridge Engineering, Vol. 15, No. 5, pp 511-522
- Ma, Z., Chaudhury, and S., Millam, J.L., and Hulsey, J.L. (2007). "Field Test and 3D FE Modeling of Decked Bulb-Tee Bridges." Journal of Bridge Engineering, Vol. 12, No. 3, pp 306-314
- Maguire, M., Morcos, G. and Tadros, M. (2013). "Structural Performance of Precast/Prestressed Bridge Double-Tee Girders Made of High-Strength Concrete, Welded Wire Reinforcement, and 18-mm-Diameter." Journal of Bridge Engineering, Vol. 18, No. 10, pp 1053-1061.
- Rouse, J., Wipf, T., Phares, B., Fanous, F., Berg, O. (2011). "Design, Construction, and Field Testing of an Ultra-High Performance Concrete Pi-Girder Bridge." Iowa State University, Ames, IA.
- South Dakota Department of Transportation (SDDOT) (2004). "Standard Specifications for Roads and Bridges." SDDOT, Pierre, SD.

Zhu, P., Ma, Z., and French, C. (2012). "Fatigue Evaluation of Transverse U-Bar Joint Details for Accelerated Bridge Construction." *Journal of Bridge Engineering*, Vol. 17, No. 2, pp 201-210.


APPENDIX A: KICKOFF MEETING



Kickoff Meeting
Pierre – December 19, 2013

Precast Bridge Girder Details for Improved Performance

Nadim Wehbe
Junwon Seo
Michael Konrad



Background

- Many bridges on highways across the State of South Dakota need replacement due to deterioration associated with increased traffic and environmental conditions
- The current bridge type used for bridge replacement is the double tee precast girder
- Design life of double tee bridge was expected to be 50 to 70 years, but is closer to 40 years
- Most common problem is reflective cracking of longitudinal joints, leading to acute deterioration


December 19, 2013 Precast Bridge Girder Details for Improved Performance



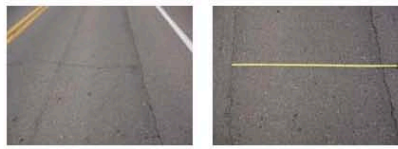
Double Tee Girder Joints



December 19, 2013 Precast Bridge Girder Details for Improved Performance




Reflective Cracks



December 19, 2013

Precast Bridge Girder Detail for Improved Performance




Objectives

- Determine from literature review whether alternatives to the double tee girder exist with improved details for shear transfer between longitudinal joints
- Perform load testing on alternative girder and conventional double tee girder, and compare the results
 - Fatigue Testing
 - Ultimate Capacity Destructive Testing
 - Provide recommended girder system with improved longitudinal joint details based upon the testing results

December 19, 2013

Precast Bridge Girder Detail for Improved Performance



Research Plan

- **Task 1:** Meet with technical panel to review scope and work plan
- **Task 2:** Perform literature review for improved details
- **Task 3:** Create and administer survey to other DOTs to identify other viable precast girder designs
- **Task 4:** Contact precast companies to inquire about possible improved details
- **Task 5:** Tech memo to panel on suggested improved girder details
- **Task 6:** Tech memo describing testing and instrumentation plan

December 19, 2013

Precast Bridge Girder Detail for Improved Performance

Research Plan

- **Task 7:** Construction and instrumentation of test girders
 - Current double tee and alternative girder
- **Task 8:** Provide tech panel opportunity to observe testing of girders
- **Task 9:** Compare test results of double tee and alternative girder
- **Task 10:** Recommendation based on cost and performance of alternative girder
- **Task 11:** Prepare final report for research findings and recommendations
- **Task 12:** Executive presentation to SDDOT Research Review Board at conclusion of project

December 19, 2013

Precast Bridge Girder Detail for Improved Performance

Time Schedule (Month)

Task	FY 14												FY 15												FY 16											
	1	2	3	4	5	6	7	8	9	10	11	12	1	2	3	4	5	6	7	8	9	10	1	2	3	4	5	6	7	8	9	10				
1*																																				
2																																				
3																																				
4																																				
5*																																				
6																																				
7*																																				
8																																				
9																																				
10*																																				
11																																				
12																																				

*Tasks that involve input from tech panel

December 19, 2013

Precast Bridge Girder Detail for Improved Performance

List of Literature Review

- **Jones et al 2001 (TxDOT)**
 - Lateral Connections for Double Tee Bridges
- **Li et al 2010 (University of Tennessee)**
 - Longitudinal Joint Detail in Decked Bulb Tee
- **Zhu P. et al 2012 (University of Tennessee)**
 - Evaluation of U-Bar Joint Detail
- **Culmo M. and Seraderian R. (PCI)**
 - Northeast EXtreme Tee (NEXT) Beam

December 19, 2013

Precast Bridge Girder Detail for Improved Performance

3

Precast Bridge Girder Detail for Improved Performance

65

May 2017

U-Bar Longitudinal Detail

- Detail
 - #5 U-Bar
 - Spaced 4.5" c/c
 - Overlap 6"
 - 8" wide longitudinal joint
- Testing
 - Used slab specimens with U-bar detail
 - Fatigue test did not reduce joint strength

December 19, 2013

Precast Bridge Girder Detail for Improved Performance

NEXT Beam

- Northeast Extreme Tee (NEXT)
- Developed by PCI
- F Beam
- D Beam
- Depth
 - 24" to 36"
- Width
 - 8' to 12'
- Span
 - 30' to 90'

December 19, 2013

Precast Bridge Girder Detail for Improved Performance

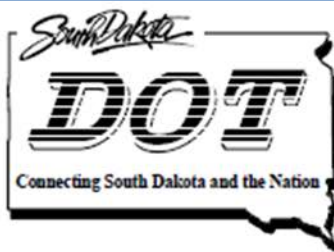
Needed from Tech Panel

- Cross-sectional details for current SDDOT double tee girder

December 19, 2013

Precast Bridge Girder Detail for Improved Performance

APPENDIX B: SURVEY TOOL



Department of Transportation

Division of Planning & Engineering

Office of Research

700 E Broadway Avenue

Pierre, South Dakota 57501-2586

605.773.3292 FAX: 605.773.4713

Greetings,

We, at South Dakota State University, are researching improved bridge girder cross sections for short to medium span bridges without cast-in-place decks on behalf of the South Dakota Department of Transportation. Our goal in utilizing this survey is to gather design and performance information about decked concrete girder bridges. The survey will inquire about the design and construction of decked girder bridges and the performance of these bridges. The objective of the study is to minimize cracking along the longitudinal joints (reflective cracking). With this information, we hope to produce an improved cross section with improved longitudinal joint performance.

In this survey a "decked" concrete girder is defined as a precast, prestressed concrete I, bulb-tee, double-tee, single-tee, etc., with an integral deck that is cast and prestressed with the girder.

BRIDGE SYSTEMS

Q1: WHAT IS THE MOST COMMONLY USED DECKED CONCRETE BRIDGE SYSTEM BY YOUR AGENCY?

1. Section shape (bulb-tee, double-tee, single-tee, etc.) _____
 - a. % decked girder bridges with this section shape _____
 - b. Typical span lengths _____ to _____ (ft)
 - c. What is the typical center to center spacing of the girders? _____ (ft)
 - d. What types of connections between the adjacent units are used? (shear key, weld plates, etc.)

 - e. Please provide details of the girder and longitudinal connection if possible.

Q2: WHAT IS THE SECOND MOST COMMONLY USED DECKED CONCRETE BRIDGE SYSTEM BY YOUR AGENCY?

1. Section shape (bulb-tee, double-tee, single-tee, etc.) _____
 - a. % decked girder bridges with this section shape _____
 - b. Typical span lengths _____ to _____ (ft)
 - c. What is the typical center to center spacing of the girders? _____ (ft)
 - d. What types of connections between adjacent units are used? (shear key, weld plates, etc.)

e. Please provide details of the girder and longitudinal connection if possible.

Q3: WHAT TYPE OF INTERMEDIATE DIAPHRAGM DO YOU USE (IF ANY)?

Q4: DO YOU USE AN OVERLAY ON DECKED BRIDGE GIRDERS? (IF YES, PLEASE PROVIDE INFORMATION BELOW)

Asphalt	%bridges _____	Thickness _____
Concrete	%bridges _____	Thickness _____
Other _____	%bridges _____	Thickness _____

GROUTING:

Q5: HAVE YOU DEVELOPED SPECIFICATIONS FOR THE GROUT IN THE LONGITUDINAL CONNECTION? YES/NO

If yes, please provide information below

Compressive strength _____ (psi)

Type of grout (Non-shrink, Epoxy, Cast-in-place concrete, other) _____

Other Information _____

Q6: IS ANY AGGREGATE USED IN THE GROUT FOR THE LONGITUDINAL CONNECTION? YES/NO

If yes, what percent? _____ % (by weight)

REFLECTIVE CRACKING:

Q7: ABOUT WHAT PERCENTAGE OF DECKED GIRDER BRIDGES EXPERIENCE LONGITUDINAL REFLECTIVE CRACKING ALONG THE LONGITUDINAL JOINT?

- 0 to 20%
- 21 to 40%
- 41 to 60%
- 61 to 80%
- 81 to 100%
- Unknown

Q8: IS CORROSION OR SPALLING OF CONCRETE AN ISSUE ON BRIDGES WITH SIGNS OF LONGITUDINAL REFLECTIVE CRACKING? YES/NO

- If yes, please answer the question below
 - Identify on the scale below how concerned you are with the corrosion or spalling of concrete due to reflective cracking?
 - ♦ (Not Concerned) 1 2 3 4 5 6 7 8 9 10 (Concerned)
- If no, please explain why

Q9: IN YOUR OPINION, IS REFLECTIVE CRACKING MORE COMMON IN BRIDGES WITH CONCRETE OR ASPHALT OVERLAYS?

OTHER COMMENTS REGARDING THE MITIGATION OF REFLECTIVE CRACKING ALONG THE LONGITUDINAL JOINTS IN DECKED GIRDER BRIDGES?

ARE THERE OTHER BRIDGE SYSTEMS YOUR AGENCY IS USING IN PLACE OF “DECKED” GIRDER BRIDGES?

Follow up information

Name

State

County

Position

Phone

E-mail

Is it OK to call you for a follow-up conversation? Yes/No

Please return surveys via mail or email listed below.

Contact Information

Michael Konrad

Civil and Environmental Engineering

South Dakota State University

Crothers Engineering Hall

Box 2219, CEH 138

Brookings, SD 57007

E-mail: michael.konrad@sdstate.edu

Phone: (605) 359-6326

APPENDIX C: TECHNICAL MEMORANDA (TASKS 5 AND 6)

SD 2013-01 Research Project Precast Bridge Girder Details for Improved Performance

MEMORANDUM

To: Technical Panel
From: Michael Konrad, Nadim Wehbe, Junwon Seo
Date: 3/25/14
Subject: Proposed details and systems for improved precast girder performance

Introduction

To gain a better understanding of the structural performance of longitudinal joints between precast double tee bridge girders, relevant literature was reviewed, surveys were sent to Departments of Transportation and Local Transportation Assistance Program (LTAP) contacts, and meetings were held between the research team and local precast companies, (Gage Brothers and Cretex West Inc.). After the results were compiled, the following major conclusions were drawn:

1. Current methods of connecting decks of adjacent girders with a grouted shear key and weld plates along longitudinal joints are effective in transferring shear across the joint, but do not offer resistance to transverse rotation of the joint.
2. Transverse rotation of the joints is the primary cause of joint movement, leading to reflective cracking between girders.
3. The most common method to reduce joint rotation without post-tensioning is to extend reinforcement out of the deck flange and develop the reinforcement in a grouted longitudinal joint.
4. Precast alternatives to decked girders capable of transferring shear and providing resistance to transverse rotation between adjacent girders may exist.

The following potential prototypes were selected on the basis that the construction of the precast bridge system superstructure should not require any fresh concrete and that reflective cracking between girders under service load conditions should be eliminated.

Option 1

The research team met with Cory Header, Brian Jenner, and Dan Bjerke of Cretex on March 4, 2014 to discuss potential improvements to double tee bridge girders. Cretex remarked that issues causing reflective cracking may include placing thick asphalt overlays that had not been accounted for in the design and lack of sufficient air entrainment in the double tee bridge girders. Cretex was also in agreement that one of the major causes of reflective cracking is the relative transverse rotation between adjacent bridge girders because the current connection cannot sufficiently resist rotation. They also suspected that the steel plates may not be fully welded together in the field and this could lead to more joint rotation. Cretex had inspected double tee bridges in the past where the grout in the longitudinal joint was deteriorating and spalling from the longitudinal joint.

The proposed joints for the double tee girder from literature review consisted of headed studs, U-bars, or deck reinforcement extending out of the deck flange into a grouted joint. After reviewing the

proposed longitudinal joints, Cretex believed that the proposed joints may be difficult to construct using existing formwork and considering the tight tolerances of placement and alignment needed for successful construction. Cretex suggested a similar joint that would make use of the welded wire fabric (WWF) in the deck. A larger mat of WWF would be extended out of the flanges into a grouted joint and use the current shear key detail from the double tee girder.

Cretex also suggested placing struts between adjacent girders towards the bottom of the stem to decrease the rotation of the girder relative to one another. The strut could be constructed out of a 6 in. diameter concrete cylinder and bolted between adjacent girder stems. The proposed can be seen in Fig. 1.

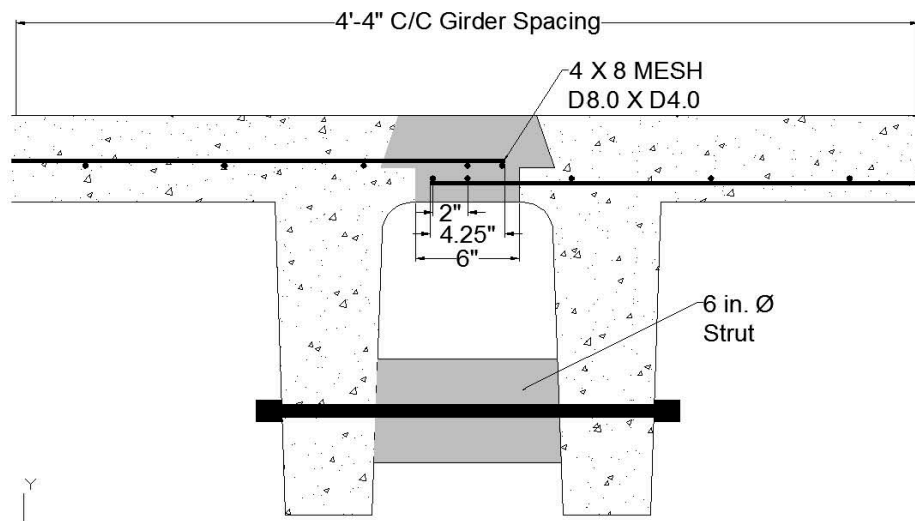


Figure 1 Option #1 Improved Longitudinal Joint

The WWF can be developed in very short distances in the joint, because each bar of the mesh in the transverse direction is anchored by 2 longitudinal bars of the mesh in the joint. American Association of State Highway and Transportation Officials (AASHTO) section 5.11.2.6.3. specifies that two longitudinal bars spaced at least 2 in. apart can develop the reinforcement in the transverse direction. Similar joints using mild steel in a longitudinal moment connection generally specify a 5000 psi grout. The strut between the girder stems can be precast and bolted in place and can be spaced along the length of the girder based on its performance in reducing rotation of the girders. Slab specimens with headed studs and U-bars extending into the longitudinal joint have been fatigue tested 2 million cycles under service loads successfully in other research studies.

Option 2

Gage Brothers in Sioux Falls proposed an inverted tee girder with precast full-depth precast panel system. Many bridges built with precast panels have been in service for more than 10 years and the performance has been noted as excellent in Culmo (2009). The connections between deck panels and the supporting girders have been researched to develop composite action. Most of the research has been done on the connections between precast panels and steel girders but some universities have researched the connection between precast girders and precast deck panels. The Precast/Prestressed Concrete Institute (PCI) Northeast Committee has already published design and detailing standards for these types of systems.

The research team met with Collin Moriarty from Gage Brothers on March 13, 2014 to discuss the proposed inverted tee system. The proposed system would be a single span system using prestressed precast inverted tee girders and full-depth (8 in.) prestressed precast deck panels.

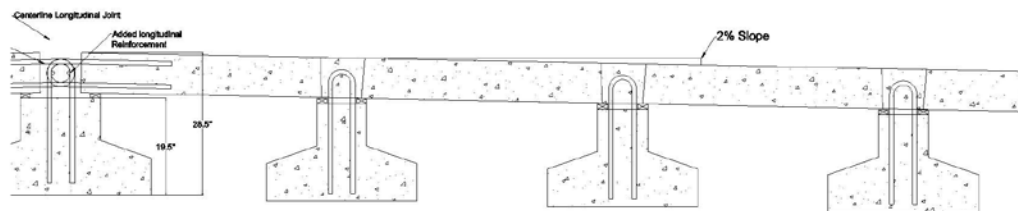


Figure 2 Option #2 Inverted Tee with Precast Deck Panels

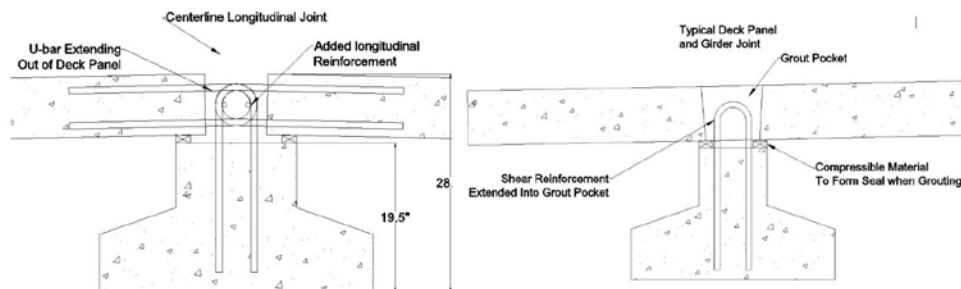


Figure 3 Typical Joints between Precast Panel and Girder

To develop composite action between the deck panels and girder, the shear reinforcement is extended into pockets in the precast panels that are later grouted. This type of detail has been researched and found to be effective in developing composite action (Menkulasi and Roberts-Wollmann 2005). The spacing of the pockets can be varied based on the shear value, but a maximum spacing of 24 in. was suggested by the PCI Northeast Committee. To accommodate the crown of the road, two panels are

joined with a grouted longitudinal joint that has U-bar reinforcement extending out of the deck panels. This U-bar joint is one of the joints previously mentioned that has been successively fatigue tested 2 million cycles. A compressible material such as polystyrene is glued to the top of the girder to accommodate differential camber between the girders and precast panels and also to form a seal between the girder and precast panel for when the joints and pockets are grouted. The transverse joints of the deck panels are joined with a grouted female to female shear key. The performance of this joint is expected to be good because the joint will be in compression and not have a tendency to rotate. The placement of precast deck panels is shown below in Fig. 4.

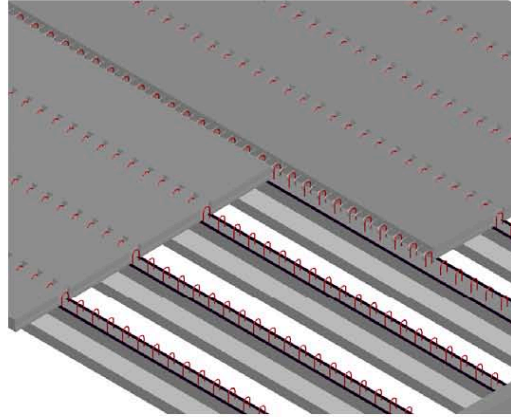


Figure 4 Precast Panels Placed on Girders before Grouting

Testing

The conventional double tee girder will first be tested as the control case at the Lohr Structures Laboratory at South Dakota State University (SDSU). The test setup will consist of two double tee girders joined with weld plates and a grouted longitudinal joint to replicate current construction practices in South Dakota. The 23 in. double tee section is used for spans of 45 ft and shorter, and the 30 in. section is typically used for spans longer than 45 ft with HL93 live loading. The control specimen section size and span can be determined at the next meeting with the technical panel. The specimen will be placed on concrete reaction blocks that will set the testing height accordingly to allow for easy inspection of the specimens during testing. A 3D model of the proposed test setup up with a 23 in deep double tee section and 40 ft span length is shown below in Fig. 5.

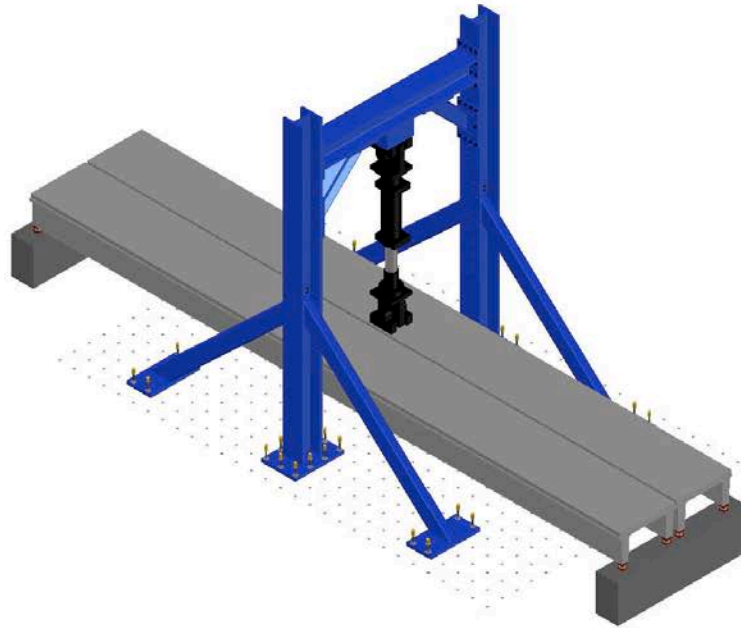


Figure 5 Proposed Test Setup

The test specimen will be instrumented to measure the following:

1. Reaction force at support
 - a. Load cells placed under the stem of each girder will measure the reaction force and help determine an equivalent joint stiffness and live load distribution factors.

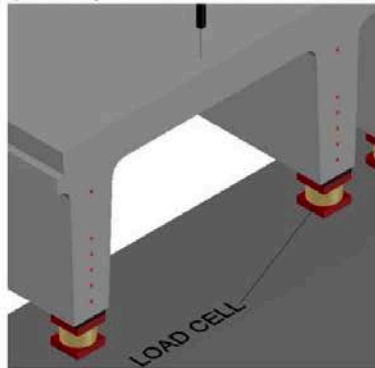


Figure 6 Load Cell Placement

2. Deflection of girders
 - a. Displacement gages will be positioned at the end of the girders to measure deflection from the compressible material the girders rest on and at mid-span to measure relative displacement of the adjacent girder units and the total deflection of the girders.
3. Rotation of the girders
 - a. Because rotation of the girders is a primary cause of reflective cracking, the rotation of the control specimen and prototype specimen will be monitored at mid-span or where deemed necessary for joint rotation.
4. Prestressing strand stress
 - a. Strain gages will be placed on the prestress strands at mid-span before placement of concrete to measure the effective prestress at the time of testing.
5. Concrete stress
 - a. Strain gages will be embedded in the concrete to monitor strains in the concrete during fatigue and ultimate loading.

The instrumentation of the alternative section will match that of the control specimen. The specimens will be tested under ultimate and fatigue loads, where the fatigue load will be based on the fatigue load prescribed by AASHTO. Based upon the expected average daily truck traffic (100 vehicles per day with a 15% truck density) over a 75 year design life, the number of fatigue cycles was determined to be 400,000 cycles. Therefore a total of 500,000 cycles is proposed for testing. An ultimate load of approximately 140 kips at mid-span is expected to fail the specimen.

References

American Association of State and Highway Transportation Officials (AASHTO). (2012). AASHTO LRFD Bridge Design Specifications, 6th Edition, Washington D.C.

Culmo, Michael P. 2009. "Connection Details for Prefabricated Bridge Elements and Systems."

French, C. E., C. K. Shield, D. Klaseus, M. Smith, W. Eriksson, Z. J. Ma, Peng Zhu, Samuel Lewis, and Cheryl E. Chapman. 2011. *Cast-in-Place Concrete Connections for Precast Deck Systems*. National Cooperative Highway Research Program.

Menkulasi, F., and C. L. Roberts-Wollmann. 2005. "Behavior of Horizontal Shear Connections for Full-Depth Precast Concrete Bridge Decks on Prestressed I-Girders." *PCI Journal* 50: 60-73.

SD 2013-01 Research Project
Precast Bridge Girder Details for Improved Performance

MEMORANDUM

To: Technical Panel

From: Michael Konrad, Nadim Wehbe, Junwon Seo

Date: 5/15/14

Subject: Testing and Instrumentation Plan for conventional and proposed double tee girders

Specimens

Conventional Double Tee

Two double tee girders joined using the conventional longitudinal joint will be used for the conventional specimen. Each double tee girder will have the cross section shown in Fig. 1 with a 23 in. section height and a 40 ft simply supported span length.

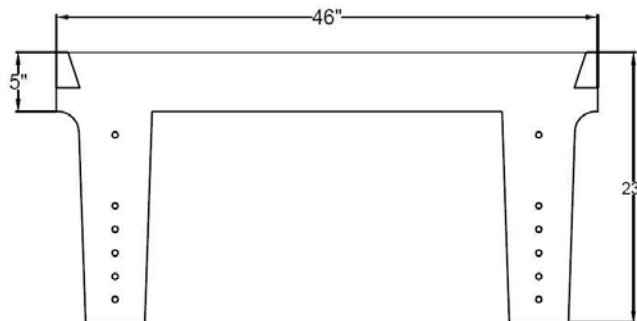


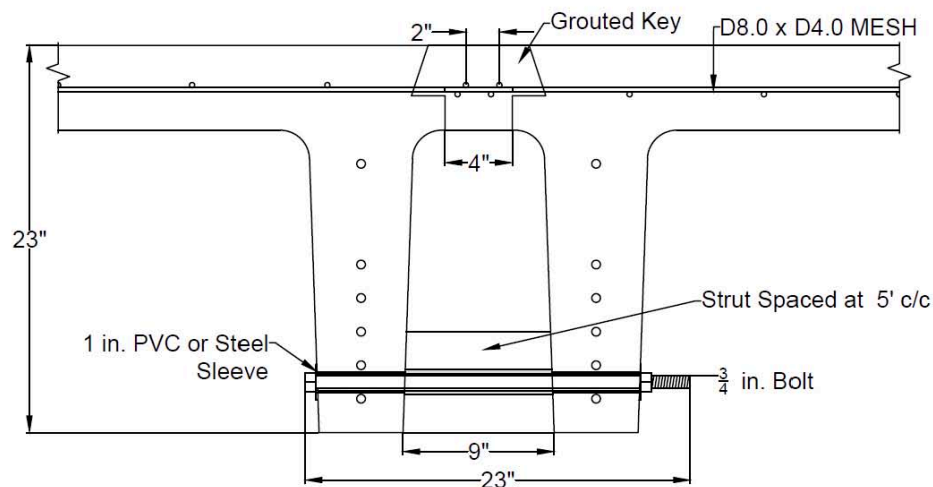
Figure 1 Conventional Double Tee Detail

Steel embedded plates spaced 5 ft center to center in the longitudinal joint will be welded together and the continuous shear key will be grouted to join the girders. The grout used in the longitudinal shear key will be a non-shrink, non-metallic grout with a minimum compressive strength of 4,500 psi.

The girders will be supported by concrete reaction blocks with sufficient height to allow for inspection of the underside of the specimens during testing.

Proposed Double Tee

The proposed double tee specimen will consist of two double tee girders with a 23 in. section height and 40 ft simply supported span length joined with an alternate longitudinal joint. The alternate longitudinal joint is formed by widening the conventional longitudinal joint by 4 inches and extending the deck reinforcement into the longitudinal joint which is then grouted. The proposed section also has compression struts placed between the stems of adjacent girders at 5 ft spacing along the girders. The struts consist of precast 6 in. diameter concrete cylinder with beveled ends to fit between the stems. The strut is held in place by means of A307 $\frac{3}{4}$ in. diameter bolt. The proposed joint is shown below in Fig. 2. Note that the steel mesh layer that extends from the deck into the stems is not shown for clarity.



The longitudinal joint of the proposed double tee will be constructed using the same grout used for the conventional double tee. The ends of the compression strut will be lightly coated with epoxy and then bolted into place. Preliminary tests measuring rotation and deflection of the system with varying number and spacing of struts will be used to determine the configuration of the struts during the fatigue and ultimate loading.

The proposed and conventional double tee specimens will be supported with the same concrete reaction blocks.

Instrumentation

Instrumentation of the conventional specimen and the improved specimen will be the same in order to have accurate comparisons.

Load Cells

Load cells will be placed under each stem on one side of the specimen to measure the reaction force at the supports. A total of four load cells will be used. The applied force will be measured with the load cell on the hydraulic actuator.

Deflection Monitoring

Deflections will be monitored using Linear Variable Differential Transformers (LVDT). Total deflection at mid span will be measured at the centerline of each girder using two LVDTs. Relative deflection across the longitudinal joint will be monitored at mid-span using one LVDT. Deflection at the end span of the specimen will be measured using two LVDTs. The deflection at end-span is measured so that deflection from the compression of the elastomeric pad that the girders bear on can be subtracted from the measured total deflection to calculate an accurate total deflection at mid-span.

Rotation Monitoring

Rotation of the girders at mid-span will be monitored by placing horizontal LVDTs across the longitudinal joints at the top and bottom of the specimen. Two LVDTs will be used to monitor rotations at mid-span.

Strain Gages

Electric Resistance type strain gages will be placed on all the prestressing strands at mid-span to determine the effective prestress. Embedded concrete strain gages will also be placed in the stems and deck of the girders at span to measure concrete strain to form a strain profile. The location of the instrumentation is shown in Fig. 3 below.

Mid-span Instrumentation

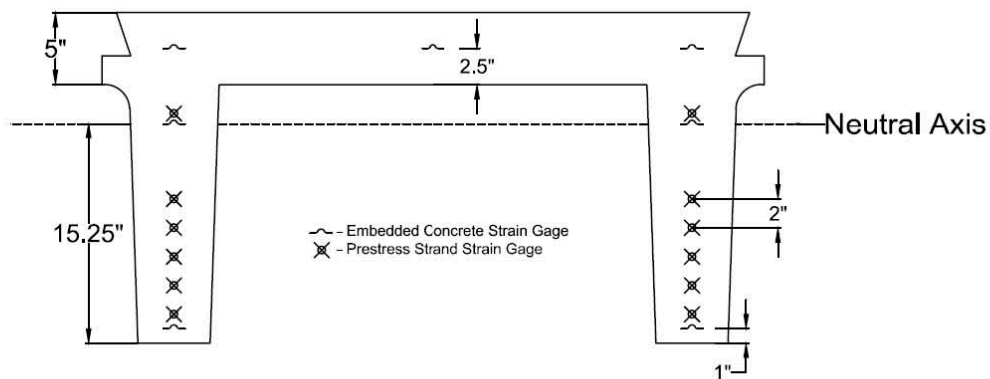


Figure 3 Instrumentation at Mid-span

Specimen Material Properties

Fresh Concrete Properties

Prior to casting the test specimens at the Cretex West facility, fresh concrete properties will be tested. The following properties will be measured:

1. Concrete Temperature (ASTM C 1064)
2. Air Content (ASTM C 231)
3. Slump (ASTM C 143)

Hardened Concrete Properties

Concrete cylinders will be cast for each girder to measure the hardened properties of the concrete. Twelve 6 in. x 12 in. concrete cylinders will be cast for each girder. The cylinders will be tested as needed during de-tensioning and also at 7 days, 28 days, and the day of flexural testing. The compressive strength of the grout in the longitudinal joint will also be tested.

Construction and Delivery

The girders will be constructed at the Cretex West facility in Mitchell, South Dakota under the supervision of a graduate student. The technical panel will be notified before the date of casting so that they may observe the construction of the specimens. The specimens will be delivered to the Lohr Structures Laboratory in Brookings, South Dakota by Cretex.

Testing

Both the conventional and improved double tee specimen will be tested in the same manner. The technical panel will be notified in advance when testing of the specimens will take place so that they have an opportunity to observe testing.

Ponding Test

After the grout in the longitudinal joint has met its minimum compressive strength the joint will be ponded with water for 24 hours to determine if any seepage of water through the joint is observed. The same procedure will be performed after the 500,000 cycle fatigue test.

Fatigue Test

Each specimen will undergo a 500,000 cycle fatigue test to determine if the strength of the joint is affected with increasing fatigue cycles. The load applied during the fatigue test for HL-93 loading is based on the prescribed fatigue limit state loads by the American Association of State Highway and Transportation Officials (AASHTO) LRFD Bridge Design Manual. The fatigue load is based on a design truck with two 32 kip axles and one 8 kip axle. No lane load is considered for the fatigue load, however, a dynamic factor of 1.15 is applied to the load for the fatigue limit state. The live load distribution factor for each girder is 0.41 based on the lever rule in AASHTO LRFD Bridge Design Manual, therefore the total load for the fatigue test will be given by:

$$\text{Fatigue Load} = \# \text{ girders} * \text{LL Dist. Factor} * \text{Load} = 2 * 0.41 * 70 \text{ kips} = 57.4 \text{ kips}$$

The load will be placed on a 16 in. by 16 in. steel plate to simulate a truck tire. The steel plate will be seated over a layer of plaster of paris to ensure a uniform contact area. The load will be placed such that the edge of the steel plate is on the precast girder/longitudinal joint interface at mid-span to produce the critical loading situation for the longitudinal joint. Placement of the load is shown in Fig. 4 below.

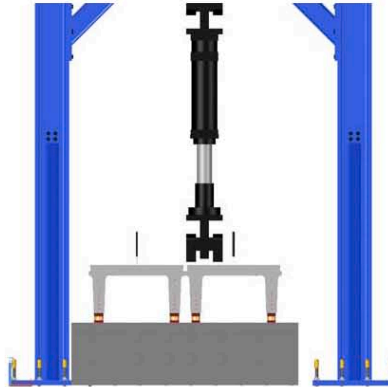


Figure 4 Placement of Load

The number of fatigue cycles was determined to be 410,625 cycles, based upon the expected average daily truck traffic (100 vehicles per day with a 15% truck density) over a 75 year design life. The total was increased to 500,000 cycles for the fatigue test.

The stiffness of the system will be measured every 50,000 cycles by a monotonic load to determine if the stiffness of the system is reduced with increasing fatigue cycles.

Ultimate Capacity Test

The ultimate capacity of the system will be determined by loading the system until failure. The load will be applied at the same location as in the fatigue test. A load of approximately 150 kips is expected to fail the specimen.

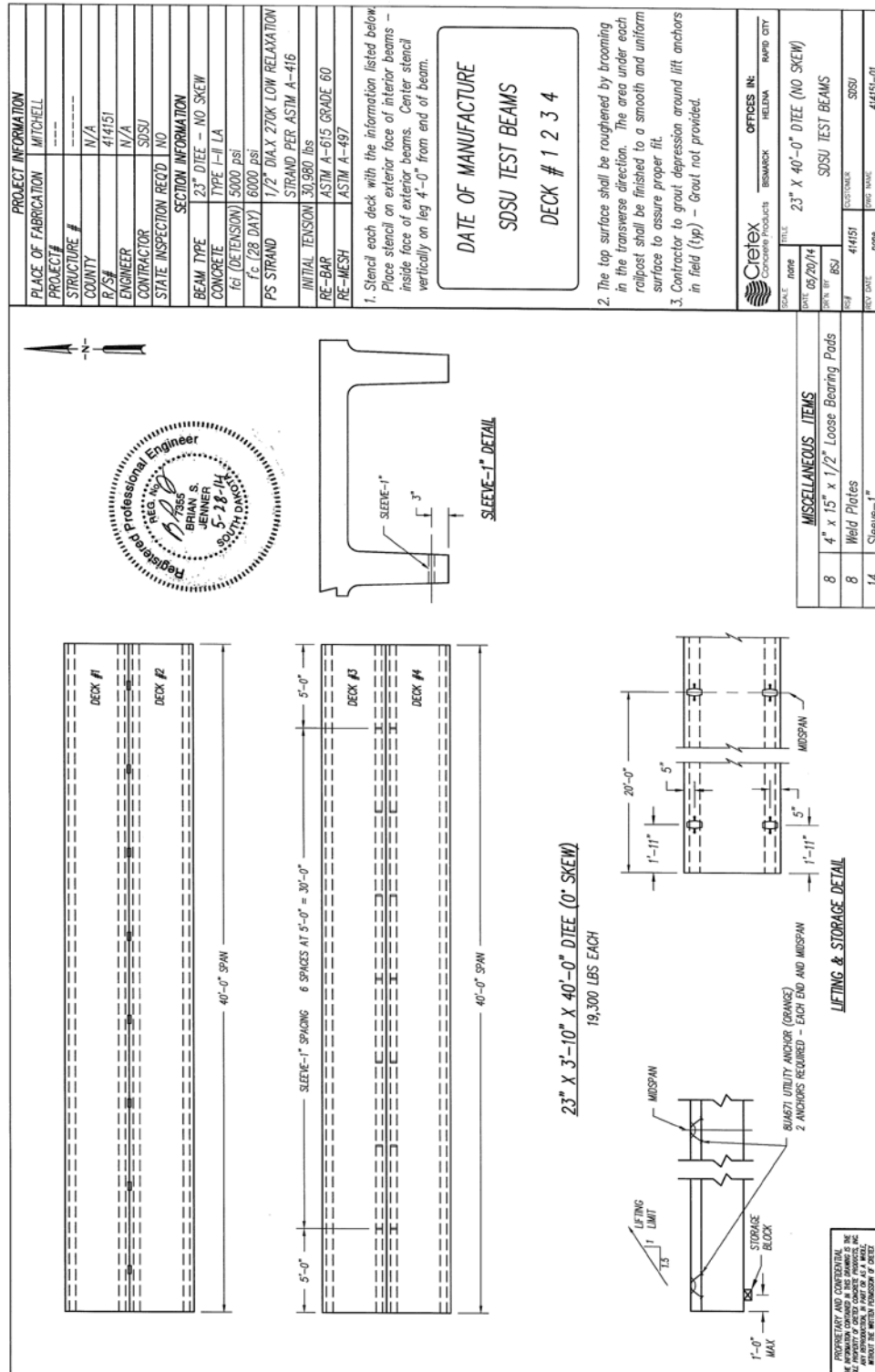
Test Schedule

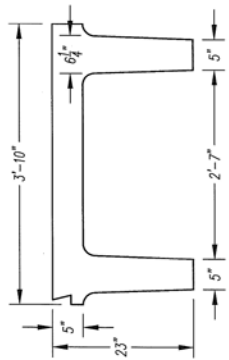
Table 1 Anticipated Testing Schedule

Week 1	June 8-14	Construction and instrumentation of both specimens
Week 2	June 15-21	Delivery and set up of conventional specimen
Week 3	June 22-28	Ponding test and begin fatigue on conventional
Week 4	June 29-July 5	Fatigue test on conventional
Week 5	July 6-12	Fatigue test on conventional specimen/Ponding test
Week 6	July 13-19	Ultimate test on conventional specimen/ Delivery of Improved specimen
Week 7	July 20-26	Delivery and set up of improved specimen/Ponding test
Week 8	July 27-Aug 2	Preliminary tests and begin fatigue test
Week 9	Aug 3- Aug 9	Fatigue test on improved specimen
Week 10	Aug 10-16	Fatigue test on improved specimen
Week 11	Aug 17-23	Ultimate test on improved specimen

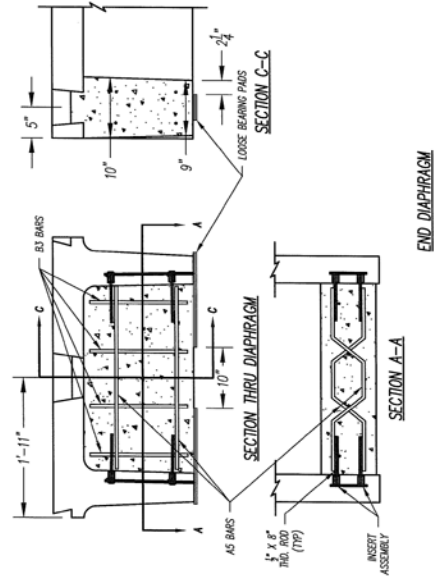
The technical panel will be notified a week in advance of construction or testing so that they may have an opportunity to observe.

APPENDIX D: PLANS AND DETAILS OF TEST SPECIMENS



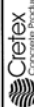


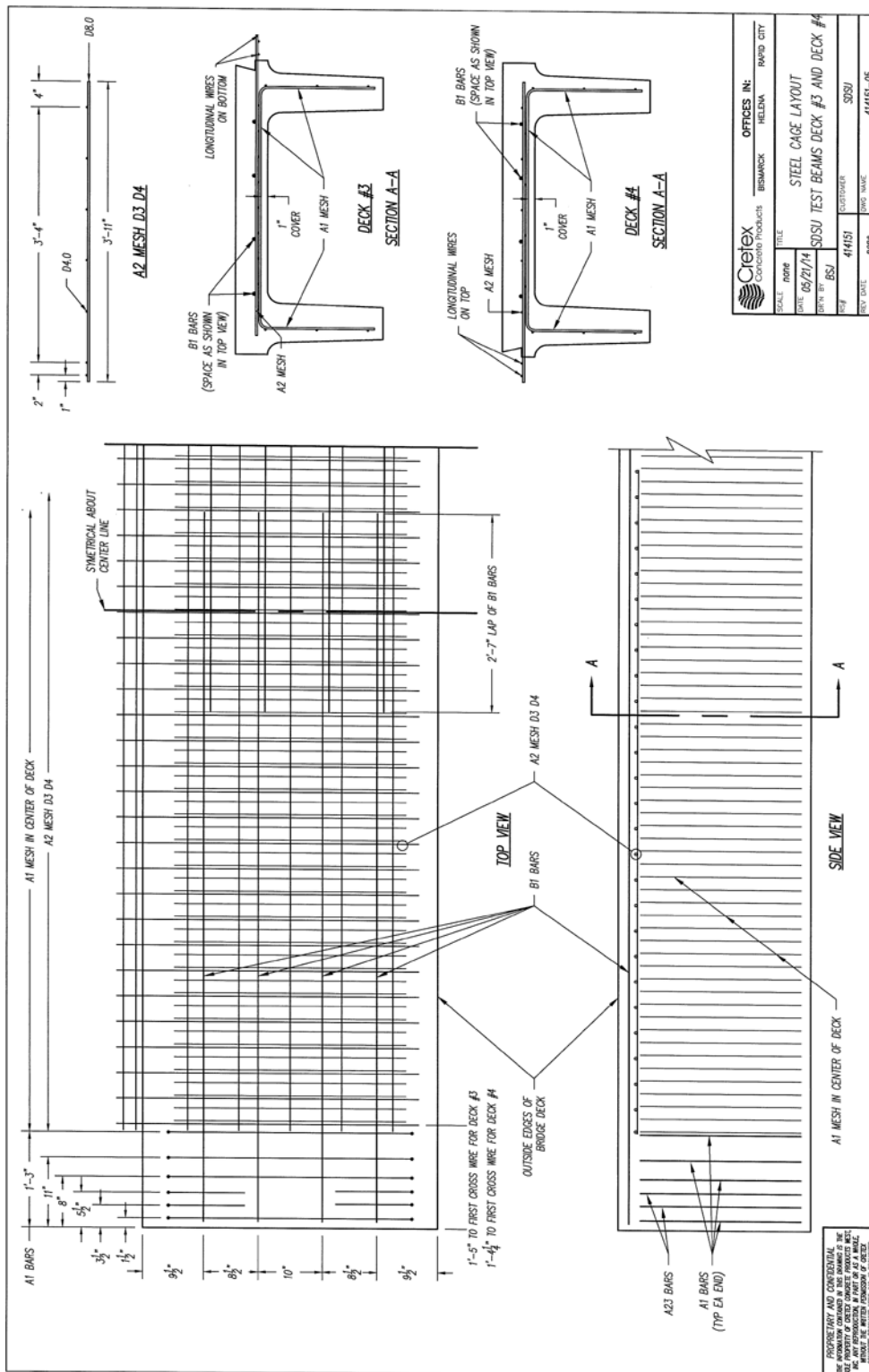
TYPICAL SECTION VIEW
23" DEEP PRESTRESSED CONCRETE CHANNEL

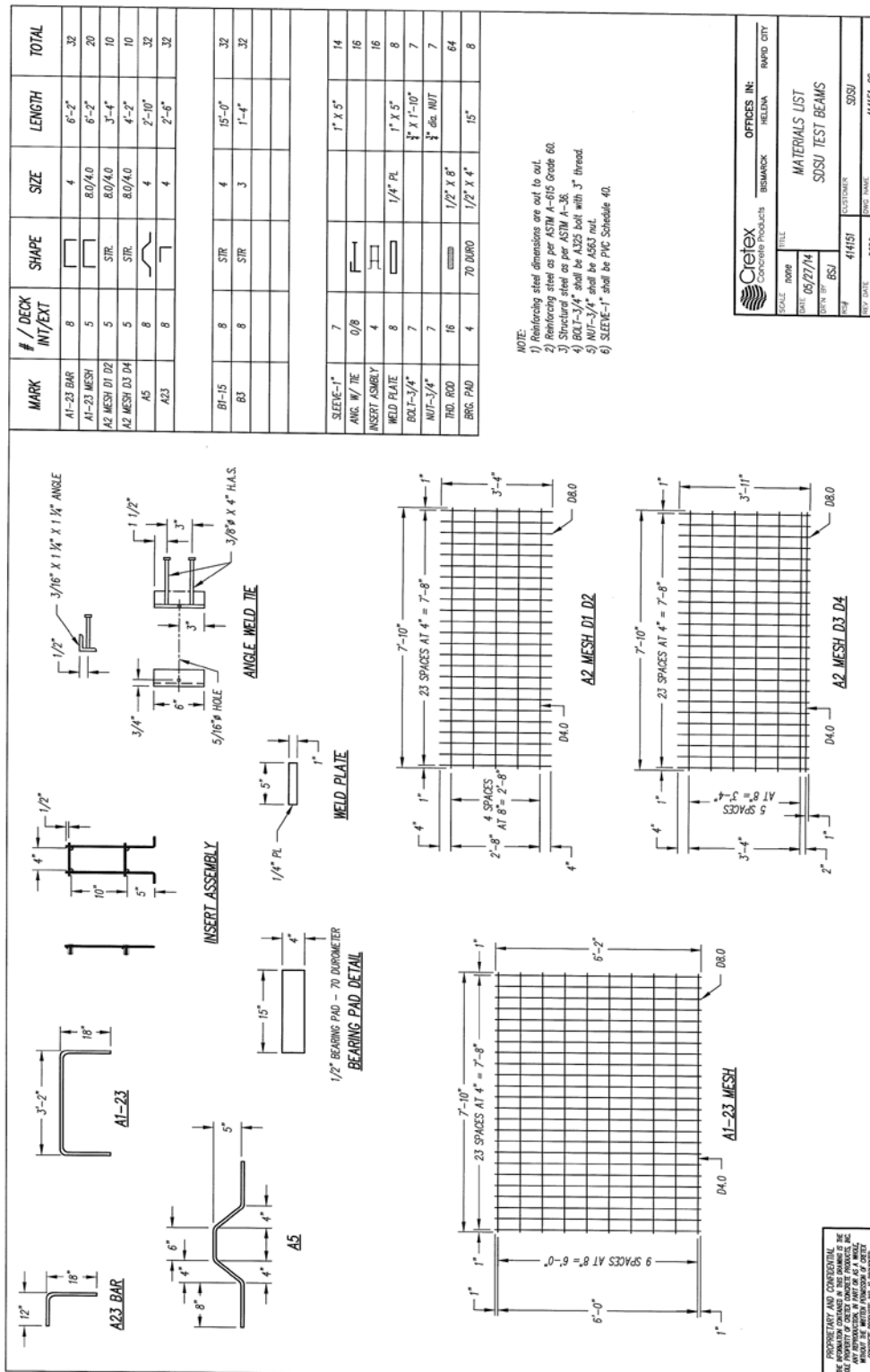


END DIAPHRAGM

PROPRIETARY AND CONFIDENTIAL
THE INFORMATION CONTAINED IN THIS DRAWING IS THE
SOLE PROPERTY OF CREX CONCRETE PRODUCTS, INC. AND IS
TO BE USED ONLY FOR THE PROJECT AND SITE SPECIFICALLY
IDENTIFIED HEREIN. WITHOUT THE WRITTEN PERMISSION OF CREX
CONCRETE PRODUCTS, INC. IT IS FORWARDED

		OFFICES IN:			
CONCRETE PRODUCTS		BISMARCK			
		HELENA			
		RAPID CITY			
TITLE					
RAIL POST & DIAPHRAGM DETAILS					
SDSU TEST BEAMS					
SCALE					
none					
DATE					
05/27/14					
DRAWN BY					
BSJ					
REV#					
44151					
REV DATE					
none					
CUSTOMER					
SDSU					
DRAW NAME					
44151-03					





APPENDIX E: TECHNICAL DATA SHEET FOR THE GROUT MATERIAL



1107 Advantage™ Grout Cement Based Grout

TECHNICAL DATA SHEET

DESCRIPTION

1107 Advantage™ Grout is a non-shrink, non-corrosive, non-metallic cementitious grout. 1107 Advantage™ Grout is designed to provide a controlled, positive expansion to ensure an excellent bearing area. 1107 Advantage™ Grout can be mixed from a fluid to a stiff plastic consistency.

USE

1107 Advantage™ Grout is designed for interior and exterior grouting of structural column base plates, pump and machinery bases, anchoring bolts, dowels, bearing pads and keyway joints. It finds applications in paper mills, oil refineries, food plants, chemical plants, sewage and water treatment plants etc.

FEATURES

- Controlled, net positive expansion
- Non shrink
- Non metallic/non corrosive
- Pourable, pumpable or dry pack consistency
- Interior/exterior applications

PROPERTIES

Corps of Engineers Specification for non-shrink grout: CRD-C 621 – Grades A, B, C

ASTM C-1107 – Grades A, B, C Specification for non-shrink grout
ASTM C-827 – 1107 Advantage™ Grout yielded a controlled positive expansion

Expansion - ASTM C-1090

1 day	≥ 0, ≤ 0.3
3 days	≥ 0, ≤ 0.3
14 days	≥ 0, ≤ 0.3
28 days	≥ 0, ≤ 0.3

Test Results – ASTM C-1107

Compressive Strength

	@ 1 Day		@ 3 Days		@ 7 Days		@ 28 Days	
Fluidity	PSI	MPa	PSI	MPa	PSI	MPa	PSI	MPa
Dry-Pack	5000	34.5	7000	48.2	9000	62.0	10000	68.9
Flowable	2500	17.2	5000	34.5	6000	41.4	8000	55.1
Fluid	2000	13.8	4000	27.6	5000	34.5	7500	51.7

Note: The data shown is typical for controlled laboratory conditions. Reasonable variation from these results can be expected due to interlaboratory precision and bias. When testing the field mixed material, other factors such as variations in mixing, water content, temperature and curing conditions should be considered.

Estimating Guide

Yield: (Flowable Consistency)

0.43 cu. ft. /50 lbs. (0.0122 cu m/22.67 kg) bag

0.59 cu. ft. /50 lbs. (0.017 cu m/22.67 kg) bag extended with 25 lbs. (11.34 kg) of washed 3/8 in. (1cm) pea gravel

PACKAGING

ITEM #	PACKAGE	SIZE	
		lbs	kg
67435	Bag	50	22.67
67437	Supersack	3,000	1,360.78

STORAGE

Store in a cool, dry area free from direct sunlight. Shelf life of unopened bags, when stored in a dry facility is 12 months. Excessive temperature differential and /or high humidity can shorten the shelf life expectancy.

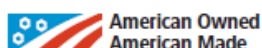
APPLICATION

Surface Preparation: Thoroughly clean all contact surfaces. Existing concrete should be strong and sound. Surface should be roughened to insure bond. Metal base plates should be clean and free of oil and other contaminants. Maintain contact areas between 45°F (7°C) and 90°F (32°C) before grouting and during curing period. Thoroughly wet concrete contact area 24 hours prior to grouting, keep wet and remove all surface water just prior to placement. If 24 hours is not possible, then saturate with water for at least 4 hours. Seal forms to prevent water or grout loss. On the placement side, provide an angle in the form high enough to assist in grouting and to maintain head pressure on the grout during the entire grouting process. Forms should be at least 1 in. (2.5 cm) higher than the bottom of the base plate.

Mixing: A mechanical mixer with rotating blades like a mortar mixer is best. Small quantities can be mixed with a drill and paddle. When mixing less than a full bag, always first agitate the bag thoroughly so that a representative sample is obtained. Place approximately 3/4 of the anticipated mix water into the mixer and add the grout mix, adding the minimum additional water necessary to achieve desired consistency. For hot weather conditions, greater than 85°F (29°C), mix with cold water approximately 40°F (4°C). For cold weather conditions, less than 50°F (10°C), mix with warm water, approximately 90°F (29°C). For additional hot and cold weather applications, contact Dayton Superior.

Sec
16

Grouts



1107 Advantage™ Grout

Cement Based Grout

TECHNICAL DATA SHEET CONTINUED

Mix for a total of five minutes ensuring uniform consistency. For placements greater in depth than 3 in. (7.6 cm), up to 25 lbs. (11.34 kg) of washed 3/8 in. (1 cm) pea gravel must be added to each 50 lbs. (22.67 kg) bag of grout. The approximate working time (pot life) is 30 minutes. This will vary somewhat with ambient conditions.

Water Requirements:

Desired Mix	Water / 50 lbs. (22.67 kg) Bag
Dry Pack	5 pints (2.4 L)
Flowable	8 pints (3.8 L)
Fluid	9 pints (4.2 L)

Placement: Grout should be placed preferably from one side using a grout box to avoid entrapping air. Grout should not be over-worked or over-watered causing segregation or bleeding. Vent holes should be provided where necessary. When possible, grout bolt holes first. Placement and consolidation should be continuous for any one section of the grout. When nearby equipment causes vibration of the grout, such equipment should be shut down for a period of 24 hours. Forms may be removed when grout is completely self-supporting. For best results, grout should extend downward at a 45 degree angle from the lower edge of the steel base plates or similar structures.

CURING

Exposed grout surfaces must be cured. Dayton Superior recommends using a Dayton Superior curing compound, cure & seal or a wet cure for 3 days. Maintain the temperature of the grout and contact area at 45°F (7°C) to 90°F (32°C) for a minimum of 24 hours.

CLEAN UP

Use clean water. Hardened material will require mechanical removal methods.

LIMITATIONS

FOR PROFESSIONAL USE ONLY

Do not re-temper after initial mixing.

Do not add other cements or additives.

Setting time for the 1107 Advantage™ Grout will slow during cooler weather, less than 50°F (10°C) and speed up during hot weather, greater than 80°F (27°C).

Prepackaged material segregates while in the bag, thus when mixing less than a full bag it is recommended to first agitate the bag to assure it is blended prior to sampling.

PRECAUTIONS

READ MSDS PRIOR TO USING PRODUCT

- Product contains Crystalline Silica and Portland Cement, Avoid breathing dust – Silica may cause serious lung problems
- Use with adequate ventilation
- Wear protective clothing, gloves and eye protection (Goggles, Safety Glasses and/or Face Shield)
- Keep out of the reach of children
- Do not take internally
- In case of ingestion, seek medical help immediately
- May cause skin irritation upon contact, especially prolonged or repeated. If skin contact occurs, wash immediately with soap and water and seek medical help as needed
- If eye contact occurs, flush immediately with clean water and seek medical help as needed
- Dispose of waste material in accordance with federal, state and local requirements

MANUFACTURER

Dayton Superior Corporation
1125 Byers Road
Miamisburg, OH 45342
Customer Service: 888-977-9600
Technical Services: 866-329-8724
Website: www.daytonsuperior.com

WARRANTY

Dayton Superior Corporation ("Dayton") warrants for 12 months from the date of manufacture or for the duration of the published product shelf life, whichever is less, that at the time of shipment by Dayton, the product is free of manufacturing defects and conforms to Dayton's product properties in force on the date of acceptance by Dayton of the order. Dayton shall only be liable under this warranty if the product has been applied, used, and stored in accordance with Dayton's instructions, especially surface preparation and installation, in force on the date of acceptance by Dayton of the order. The purchaser must examine the product when received and promptly notify Dayton in writing of any non-conformity before the product is used and no later than 30 days after such non-conformity is first discovered. If Dayton, in its sole discretion, determines that the product breached the above warranty, it will, in its sole discretion, replace the non-conforming product, refund the purchase price or issue a credit in the amount of the purchase price. This is the sole and exclusive remedy for breach of this warranty. Only a Dayton officer is authorized to modify this warranty. The information in this data sheet supersedes all other sales information received by the customer during the sales process. THE FOREGOING WARRANTY SHALL BE EXCLUSIVE AND IN LIEU OF ANY OTHER WARRANTIES, EXPRESS OR IMPLIED, INCLUDING WARRANTIES OF MERCHANTABILITY AND FITNESS FOR A PARTICULAR PURPOSE, AND ALL OTHER WARRANTIES OTHERWISE ARISING BY OPERATION OF LAW, COURSE OF DEALING, CUSTOM, TRADE OR OTHERWISE.

Dayton shall not be liable in contract or in tort (including, without limitation, negligence, strict liability or otherwise) for loss of sales, revenues or profits; cost of capital or funds; business interruption or cost of downtime, loss of use, damage to or loss of use of other property (real or personal); failure to realize expected savings; frustration of economic or business expectations; claims by third parties (other than for bodily injury), or economic losses of any kind; or for any special, incidental, indirect, consequential, punitive or exemplary damages arising in any way out of the performance of, or failure to perform, its obligations under any contract for sale of product, even if Dayton could foresee or has been advised of the possibility of such damages. The Parties expressly agree that these limitations on damages are allocations of risk constituting, in part, the consideration for this contract, and also that such limitations shall survive the determination of any court of competent jurisdiction that any remedy provided in these terms or available at law fails of its essential purpose.

Sec 16 Grouts



APPENDIX F: CALCULATIONS

F.1: Fatigue II Moment Envelope Using SAP 2000

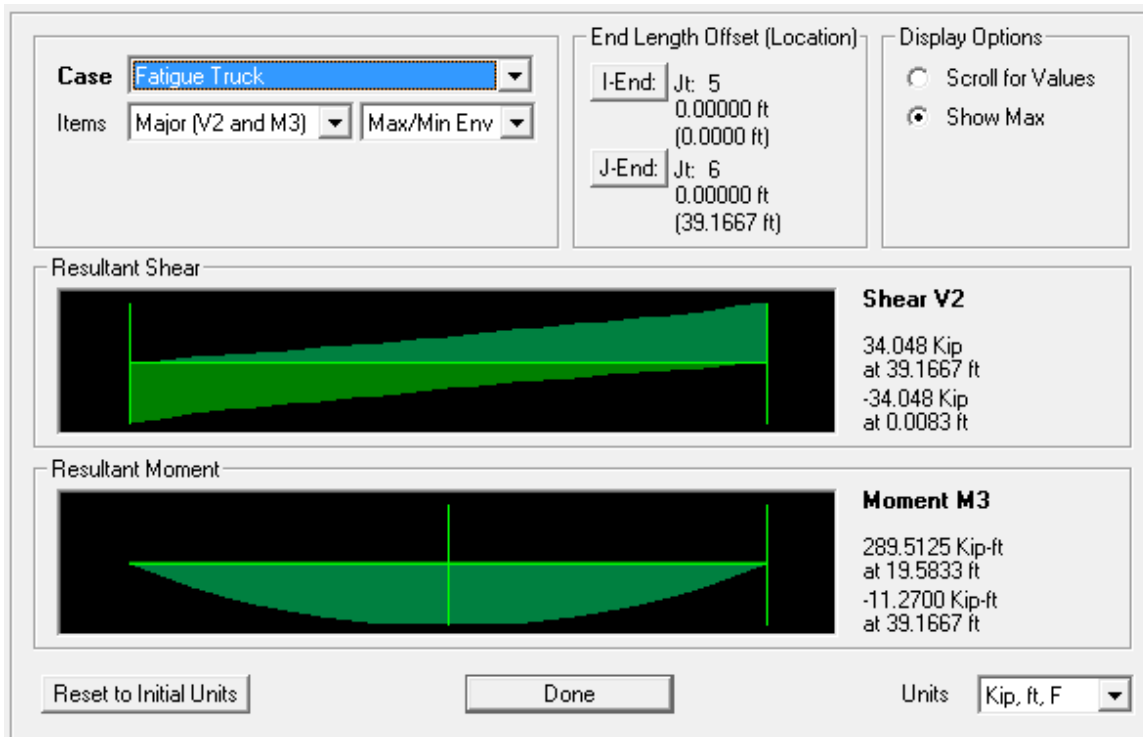
$$\text{Scale Factor} = \gamma * \left(1 + \frac{IM}{100}\right)$$

where:

γ = load factor for Fatigue II Limit State= 0.75

IM = dynamic load allowance factor for Fatigue II Limit State = 15%

$$\text{Scale Factor} = 0.75 * (1 + 0.15) = 0.8625$$



$$M_{max} = 289.5 \text{ kip} - \text{ft}$$

F.2: Live Load Distribution Factor to Interior Girders of Double Tee Bridge Deck

$$g = \frac{S}{D}$$

where:

g = live load distribution factor

S = spacing of beams (ft) = 3.86 ft

D = width of distribution per lane (ft)

$$D = 11.5 - N_L + 1.4N_L(1 - 0.2C)^2 \text{ when } C \leq 5, \text{ or}$$

$$D = 11.5 - N_L \text{ when } C > 5$$

$$C = K \left(\frac{W}{L} \right) \leq K$$

$$K = \sqrt{\frac{(1 + \mu)I}{J}}$$

where:

C = stiffness parameter

K = constant for different types of construction

W = edge-to-edge width of bridge (ft) = 30.67 ft

L = span of beam (ft) = 40 ft

N_L = number of design lanes = 2

μ = Poisson's ratio of concrete = 0.2

J = St. Venant's torsional inertia of girder cross-section (in^4) = 4,351 in^4

I = moment of inertia of beam (in^4) = 19,498 in^4

$$K = \sqrt{\frac{(1 + 0.2) \cdot 19,498 \text{ in}^4}{4,351 \text{ in}^4}} = 2.32$$

$$C = 2.32 \left(\frac{30.67'}{40'} \right) = 1.81 < 5$$

$$\therefore D = 11.5 - 2 + 1.4 \cdot 2(1 - 0.2 \cdot 1.81)^2 = 10.64 \text{ ft}$$

$$g = \frac{3.86'}{10.64'} = 0.35$$

F.3: Flexural Strength

$$M_n = A_{ps} f_{ps} \left(d_p - \frac{a}{2} \right)$$

in which:

$$f_{ps} = f_{pu} \left(1 - k \frac{c}{d_p} \right)$$

$$k = 2 \left(1.04 - \frac{f_{py}}{f_{pu}} \right)$$

$$c = \left(\frac{A_{ps} f_{pu}}{0.85 f'_c \beta_1 b + k A_{ps} \frac{f_{pu}}{d_p}} \right)$$

$$a = c \beta_1$$

where:

M_n = nominal flexural resistance (kip-in.)

A_{ps} = area of prestressing steel (in²)

f_{ps} = average stress in prestressing steel at nominal bending resistance (ksi)

f_{pu} = specified tensile strength of prestressing steel (ksi)

f_{py} = yield strength of prestressing steel (ksi)

d_p = distance from extreme compression fiber to the centroid of prestressing tendons (in.)

c = depth of neutral axis (in.)

a = depth of equivalent stress block (in.)

f'_c = specified compressive strength of concrete (ksi)

β_1 = stress block factor

k = factor depending on type of prestressing steel

b = width of the compression face of the member; for a flange section in compression, the effective width of the flange (in.)

$$f_{pu} = 270 \text{ ksi for Grade 270 low lax strand}$$

$$f_{py} = 0.9 \cdot f_{pu} = 0.9 \cdot 270 \text{ ksi} = 243 \text{ ksi}$$

$$k = 2 \left(1.04 - \frac{243 \text{ ksi}}{270 \text{ ksi}} \right) = 0.28$$

$$\beta_1 = 0.65 \text{ for } f'_c \geq 8 \text{ ksi}$$

$$A_{ps} = 12 \cdot 0.153 \text{ in}^2 = 1.836 \text{ in}^2$$

$$c = \left(\frac{1.836 \text{ in}^2 \cdot 270 \text{ ksi}}{0.85 \cdot 8.5 \text{ ksi} \cdot 0.65 \cdot 46 \text{ in} + 0.28 \cdot 1.836 \text{ in}^2 \frac{270 \text{ ksi}}{15.34 \text{ in}}} \right) = 2.20 \text{ in}$$

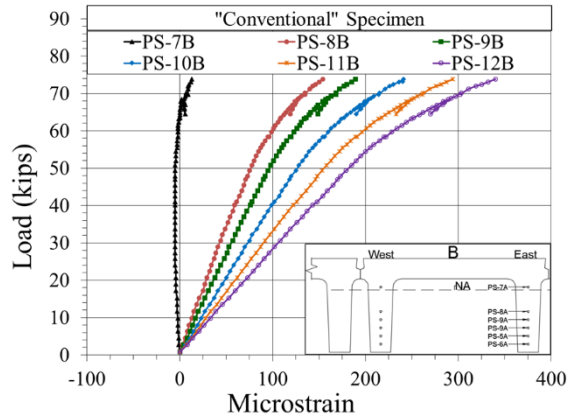
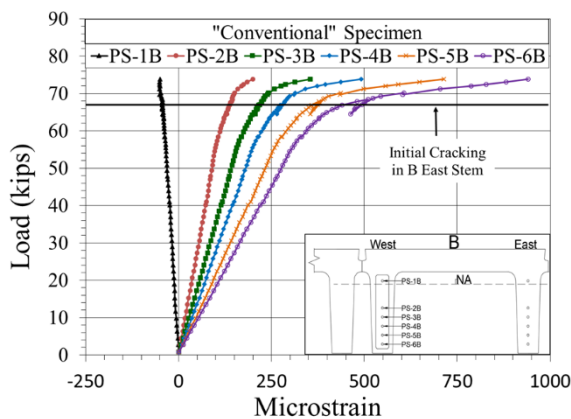
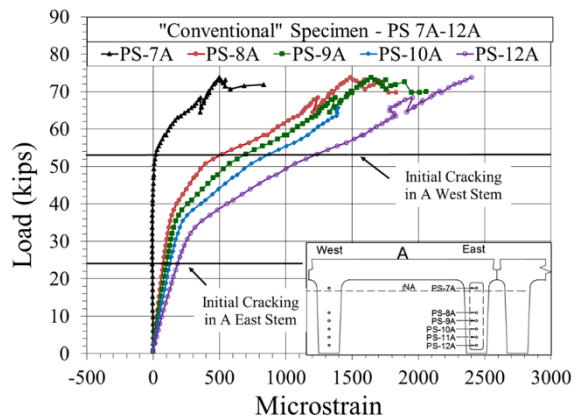
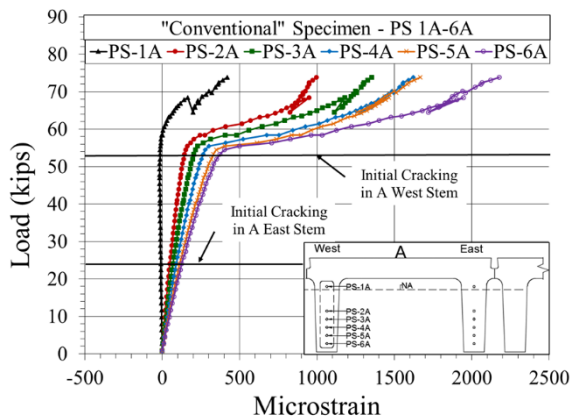
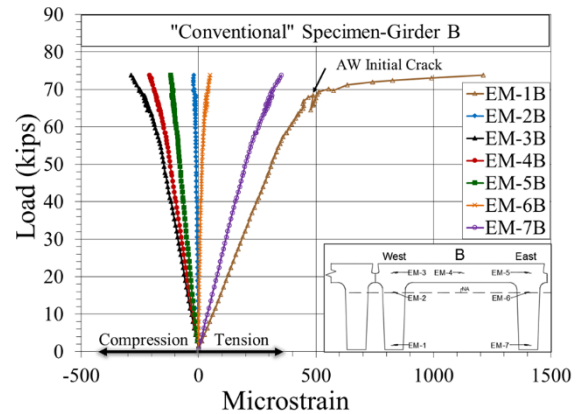
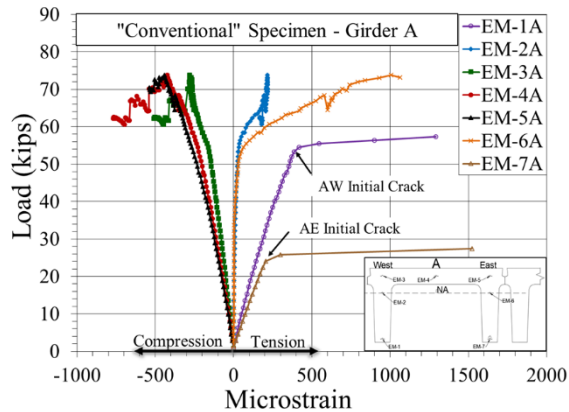
$$f_{ps} = 270 \text{ ksi} \left(1 - 0.28 \frac{2.20 \text{ in}}{15.34 \text{ in}} \right) = 259 \text{ ksi}$$

$$a = 2.20 \text{ in} \cdot 0.65 = 1.43 \text{ in}$$

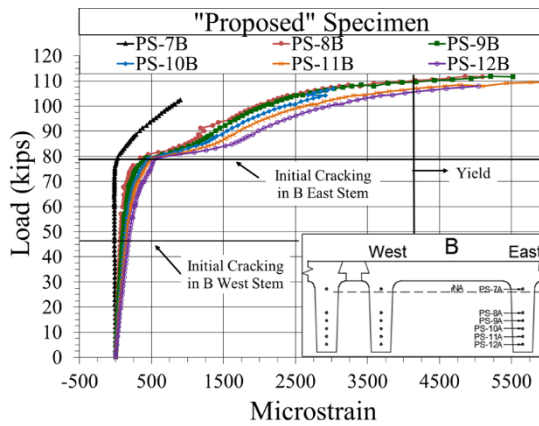
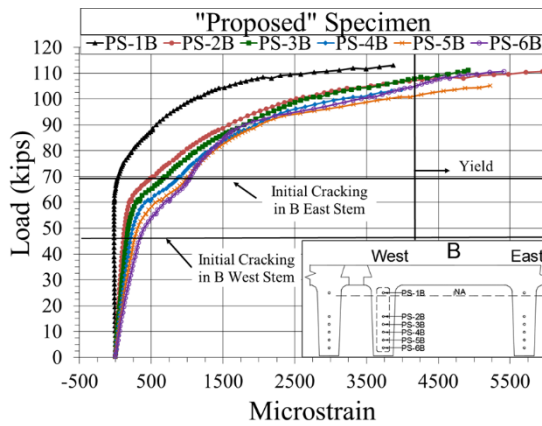
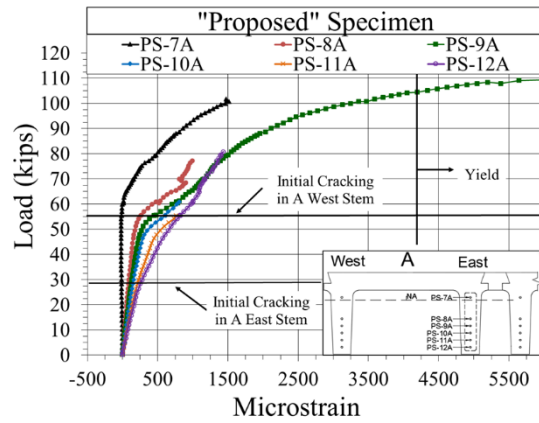
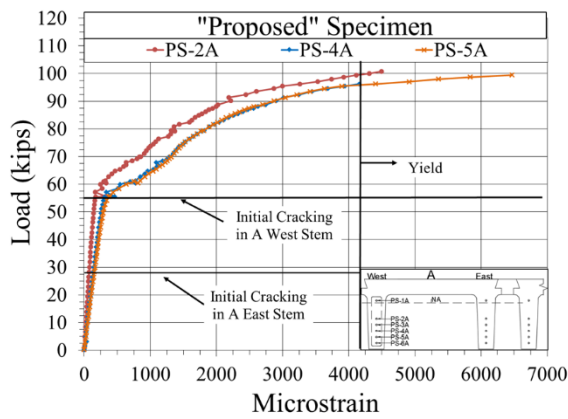
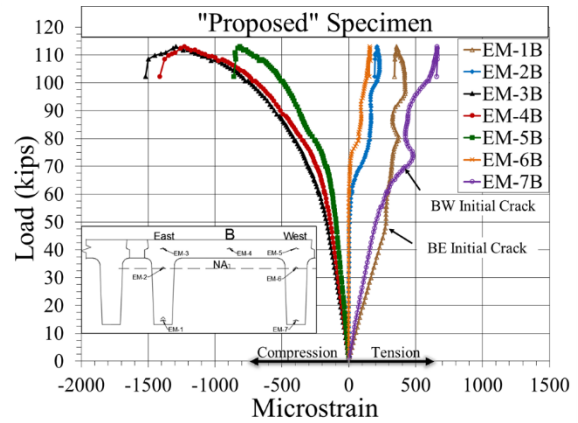
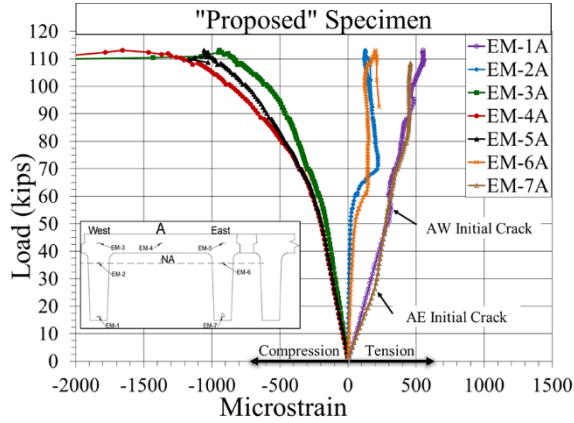
$$M_n = 1.836 \text{ in}^2 \cdot 259 \text{ ksi} \left(15.34 \text{ in} - \frac{1.43 \text{ in}}{2} \right) = 6955 \text{ kip-in or } 580 \text{ kip-ft}$$

APPENDIX G: MEASURED STRAINS

G.1: "Conventional" Specimen



G.2: "Proposed" Specimen



APPENDIX H: FINITE ELEMENT ANALYSIS

The models were constructed to investigate the shear transfer across the longitudinal joints and reaction distribution with varying load placement. The analytical work was performed using the finite element and structural analysis program SAP2000.

H.1: FE Models

The girders of the “Proposed” and “Conventional” specimens were modeled with a combination of solid elements and beam elements. Similar to the full-scale test specimens, a section height of 23 in. and length of 40 ft was used. Beam elements were used to model the stems of the girders and solid elements were used to model the deck of the girder. The slab acted compositely with the beams, thus the section properties matched the theoretical section properties. The beam elements had a section height of 18 in. and were tapered from 5 in. at the bottom to 6.25 in. at the top of the beam section. Reinforcing steel was added to the stem sections to account for the prestressing steel. The deck had cross-sectional dimensions of 46 in. \times 5 in. Figure H-1 shows a 3-dimensional view of the model from SAP2000. A 6-in. \times 6-in. \times 1-in. mesh was used for the solid elements of the deck. Meshes finer than 6 in. \times 6 in. did not yield significantly different results. Thus, a 6-in. \times 6-in. mesh was used to reduce the execution time.

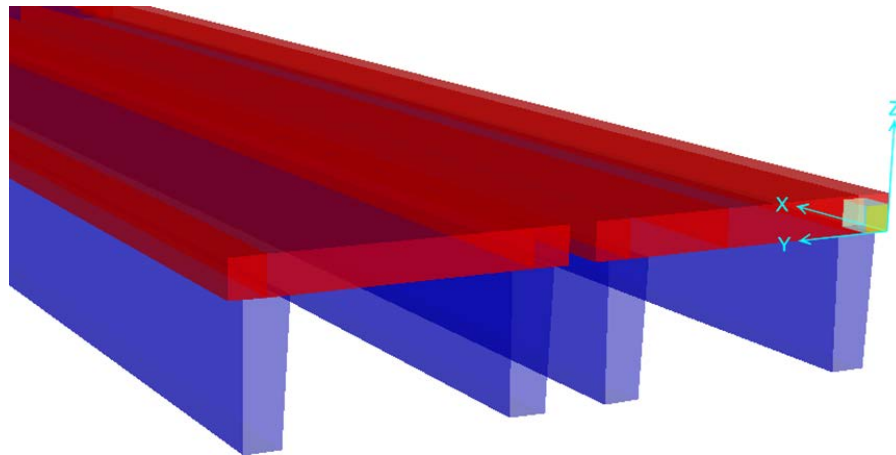


Figure H-1: Extruded View of Finite Element Model

The supports were modeled as linear spring elements with stiffness values in the principal directions based on the elastomeric bearing pads used in the experiment. The stiffness in the U_1 (vertical) direction was 4000 kip/in. The U_1 stiffness was calculated from measured deflections in the elastomeric pads during experimental testing. The stiffness in the U_2 and U_3 (horizontal) directions was calculated based on the shear deformation of the elastomeric pads. This yielded a stiffness of 12 kips/in in the U_2 and U_3 directions.

The longitudinal joint of the “Conventional” specimen was modeled with eight linear spring elements. The spring elements were used to model the welded steel connections between the girders. Figure H-2 shows a schematic of the spring element used to model the welded steel connections between the girders. The gap between the girders is exaggerated in Figure H-2 to show

the spring element. The two girders in the “Conventional” model were spaced with a 3/8-in. gap between the girders which is the typical spacing of double tee girders in the field. The spring elements were spaced 5 ft apart along the longitudinal joint to match the welded steel connections in the “Conventional” specimen. The connections were located at mid-height on the deck.

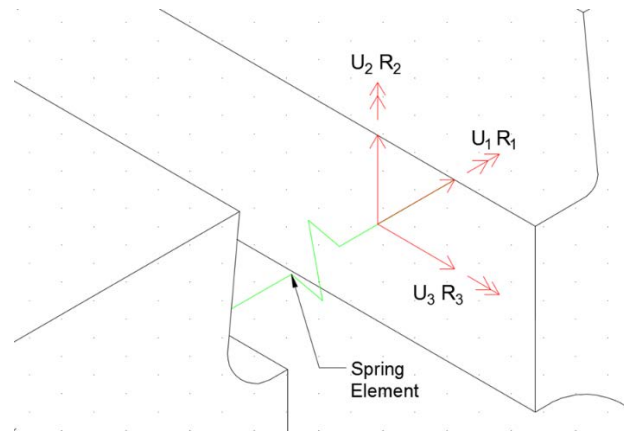


Figure H-2: Spring Element Model for the Welded Connections of the “Conventional” Specimen

The stiffness in the U_1 direction was determined from the axial stiffness of the welded plate joining the connections. The stiffness in the U_2 direction was determined from the double curvature bending of the welded plate in the U_2 direction. The U_3 stiffness was based on the shear deformation of the welded plate in the U_3 direction. The rotational degrees of freedom for R_1 and R_2 were considered fixed since the corresponding stiffness would be relatively high. The R_3 stiffness was based on experimental data from the “Conventional” specimen strength test. Using the load cell data from the strength test, the moments were summed about the longitudinal joint and compared to the measured rotation from the top and bottom LVDTs. This yielded a stiffness of 2,500 kip-in/rad before significant flexural cracking of the sections had occurred. Table H.1 displays the stiffness values used to model the connections of the welded connections. Note that the values shown in Table H.1 are representative of a typical element of the eight linear spring elements used to model the “Conventional” specimen.

Table H.1: Spring Element Stiffness for the “Conventional” Specimen

U_1 (kip/in)	U_2 (kip/in)	U_3 (kip/in)	R_1 (kip-in/rad)	R_2 (kip-in/rad)	R_3 (kip-in/rad)
36,250	2,900	14,375	Fixed	Fixed	2,500

The longitudinal joint of the “Proposed” specimen was modeled with linear spring elements similar to those used with the “Conventional” specimen. However, instead of using eight linear spring elements, 120 linear spring elements were used. Each spring element represented a transverse bar in the longitudinal joint of the “Proposed” specimen. The linear spring elements were spaced at 4 in. along the longitudinal joint and connected to the girders at mid-height on the deck. Because the longitudinal joint of the “Proposed” specimen was 4 in. wider than that of the “Conventional” Specimen, the two girders in the model were spaced 4 inches apart. The U_1 stiffness represented the axial stiffness of one of the transverse bars in the longitudinal joint. The U_2 and U_3 stiffness was fixed

because no significant relative deflection was measured during the “Proposed” strength test. The degrees of freedom for R_1 and R_2 were fixed because rotations in these directions are highly restrained. The R_3 stiffness was calculated with the same technique used for the “Conventional” specimen. The moments resulting from the reactions and applied loads were summed about the longitudinal joint and compared with the measured rotation data. Table H.2 shows the stiffness values used for the “Proposed” specimen with and without the diaphragms. The rotational stiffness in the R_3 direction was much larger when the diaphragms were considered.

Table H.2: Spring Element Stiffness for the “Proposed” Specimen

	U_1 (kip/in)	U_2 (kip/in)	U_3 (kip/in)	R_1 (kip-in/rad)	R_2 (kip-in/rad)	R_3 (kip-in/rad)
With Diaphragm	584	Fixed	Fixed	Fixed	Fixed	3439
Without Diaphragm	584	Fixed	Fixed	Fixed	Fixed	600

H.2: Analytical Results

Linear analyses was performed in SAP2000 for the “Conventional” specimen, the “Proposed” specimen with diaphragms, and the “Proposed” specimen without diaphragms. A surface load of 21 kips was applied on a 20-in. \times 10-in. area and positioned next to the longitudinal joint at mid-span, identical to the load placement for the experimental tests. The stress notations relative to the global X-Y-Z axes shown in Figure H-1 are presented in Figure H-3. The X, Y, and Z axes represent the longitudinal, transverse, and vertical directions of the specimens, respectively. S_{11} is normal stress which is mainly due to a bending moment for the loading setup considered, S_{23} is the shear stress in a longitudinal section, and S_{13} is the shear stress in a transverse section.

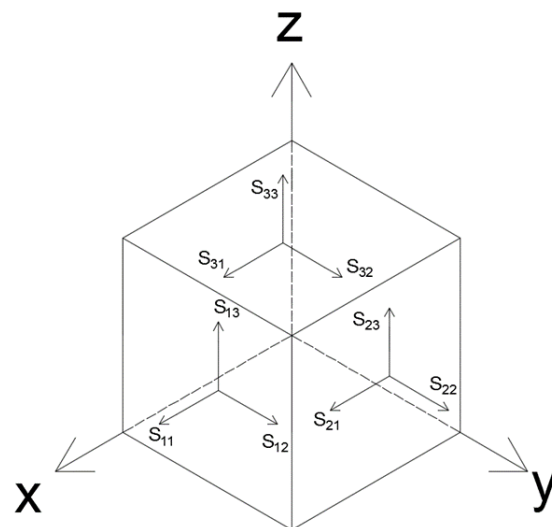


Figure H-3: Stress Notation Relative to the Global System of Axes

H.2.1: “Conventional” Specimen

The S_{11} stress contours for the “Conventional” specimen are shown in Figure H-4. The S_{11} stress contours in Figure H-4 are those stresses resulting from the applied load only, and do not account for

the additional stresses from prestressing and the dead load. The area of highest stress (marked by the red colored area) is on Girder A at mid-span where the load was applied.

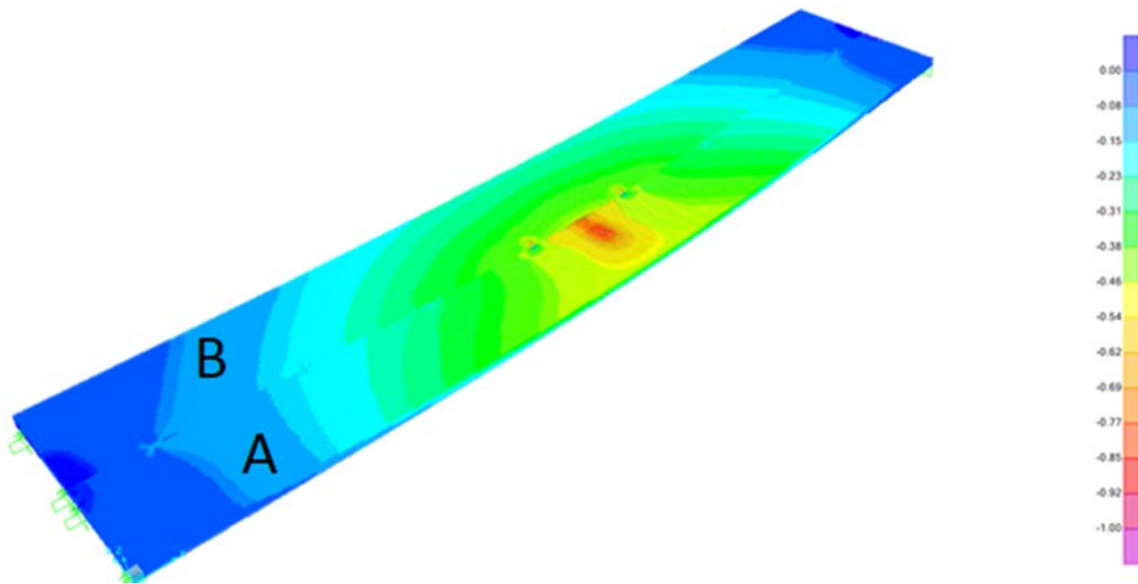


Figure H-4: S_{11} Stress Contours – “Conventional” Specimen

The S_{23} stress contours for the “Conventional” specimen are shown in Figure H-5. The S_{23} stress contours show discrete areas of higher shear stress at the spring elements (connections). The highest S_{23} stresses are at the connections near mid-span.

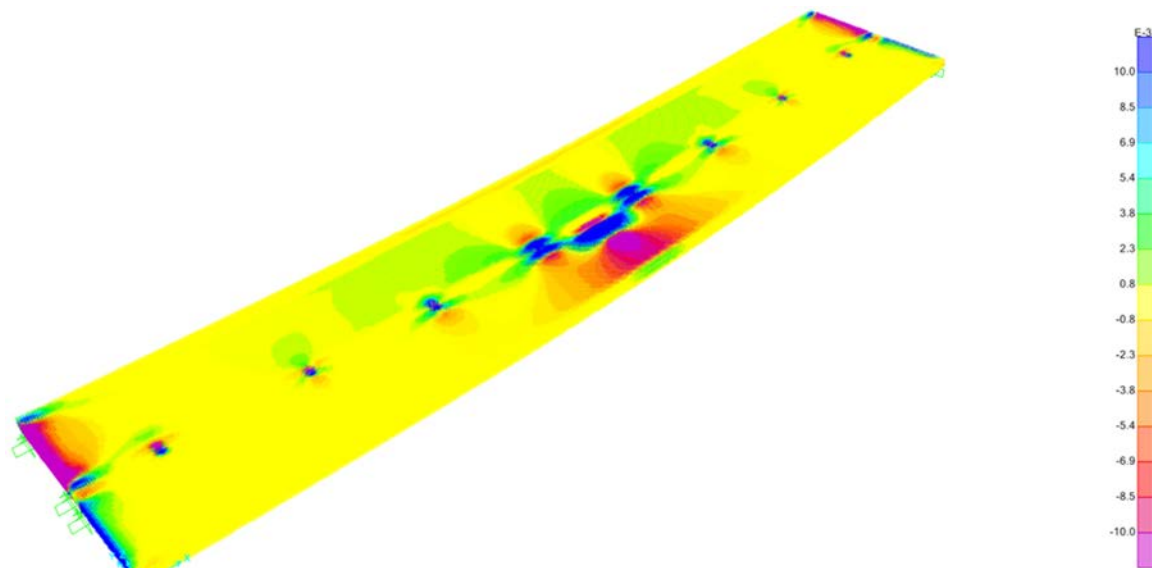


Figure H-5: S_{23} Stress Contours – “Conventional” Specimen

H.2.2: “Proposed” Specimen without Diaphragms

The stress contours for S_{11} is shown in Figure H-6. The maximum stress intensity on Girder B of the “Proposed” without-diaphragm model is larger than that of the “Conventional” model. The higher stress intensity is due to a more rigid longitudinal joint connection. The increased joint stiffness

decreases the rotation and movement between Girder A and Girder B which allows the joint of the “Proposed” specimen to engage the trailing girder (B), resulting in a higher S_{11} stress in Girder B.

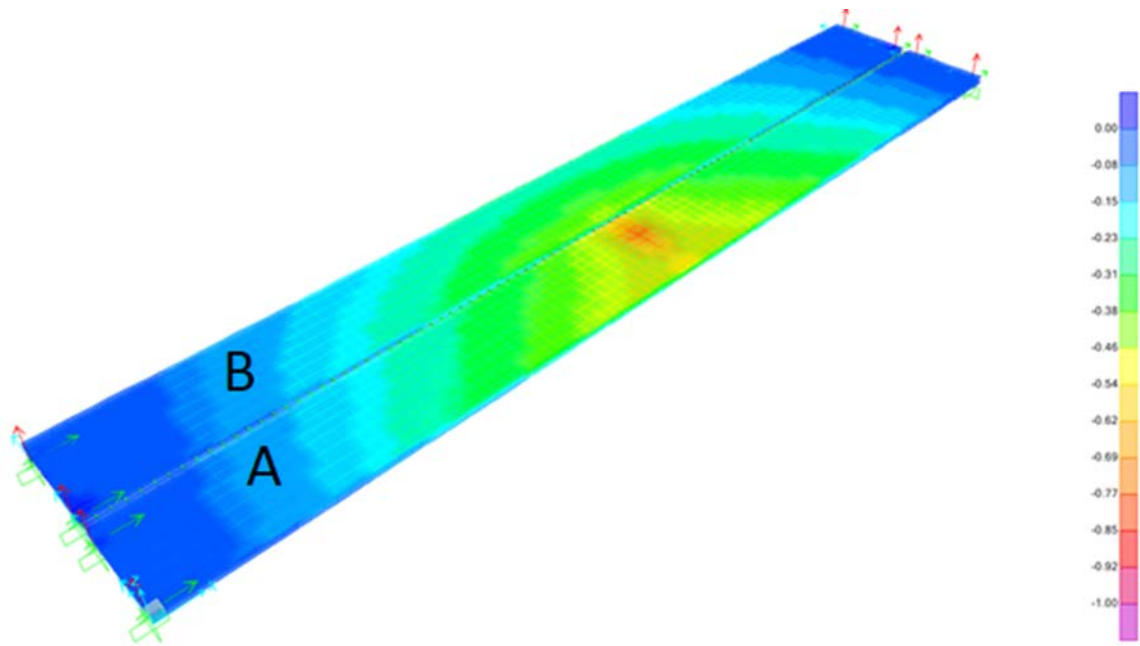


Figure H-6: S_{11} Stress Contours – “Proposed” Specimen with No Diaphragm

The S_{23} stress contours for the “Proposed” specimen with no diaphragms is shown in Figure H-7. The S_{23} stress contours show the highest shear stress along the longitudinal joint to be located in the vicinity of the applied load at mid-span with stress values of approximately 11.5 psi.

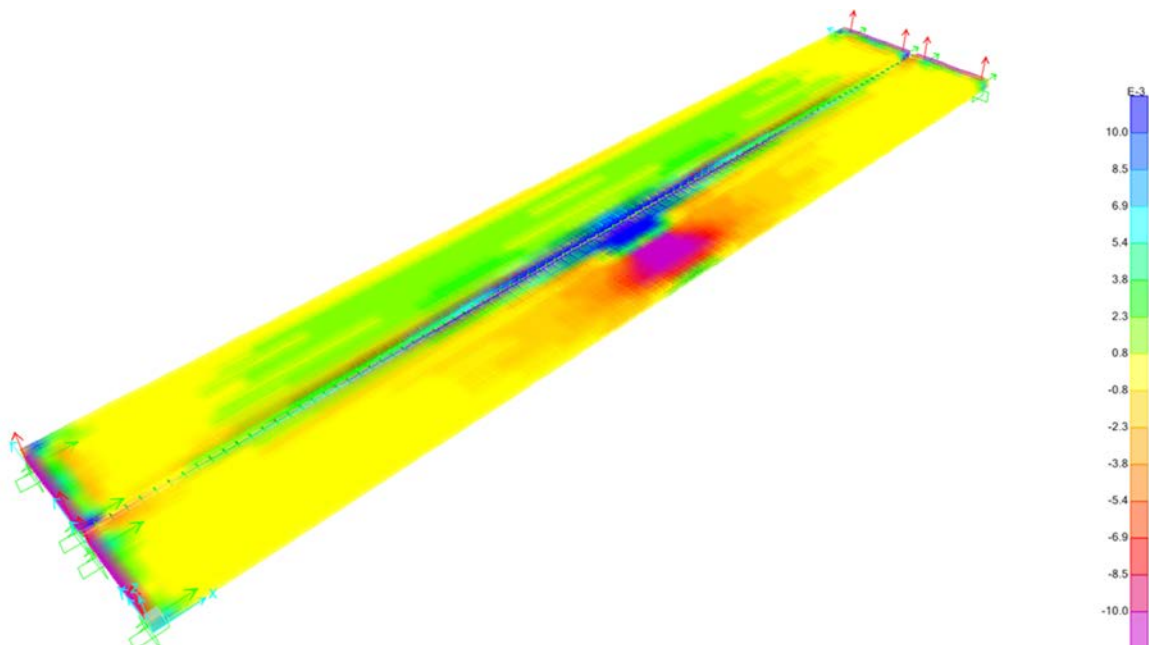


Figure H-7: S_{23} Stress Contours – “Proposed” Specimen with No Diaphragm

H.2.2: “Proposed” Specimen with Diaphragms

The “Proposed” specimen was also modeled with the diaphragms in place. Figure H-8 shows the S_{11} stress contours with an applied load of 21 kips. The S_{11} stress contours for the cases with and without diaphragms are very comparable.

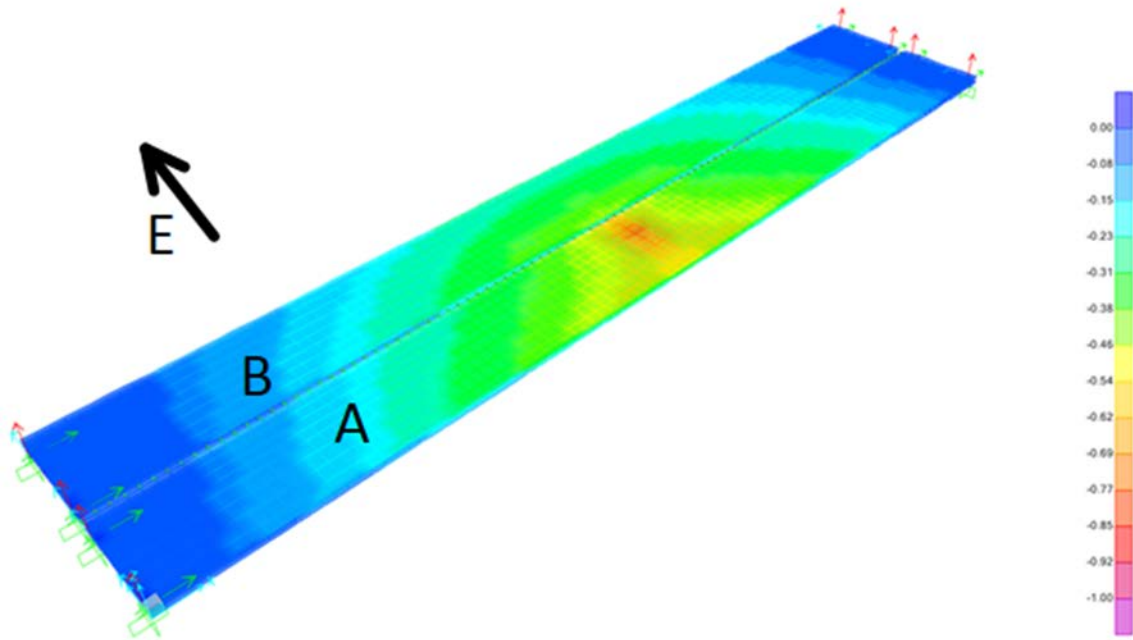


Figure H-8: S_{11} Stress Contours – “Proposed” Specimen with Diaphragms

Figure H-9 shows the S_{23} stress contours for the “Proposed” specimen with diaphragms. The S_{23} stress distribution is very comparable to the stress distribution for the case with no diaphragms.

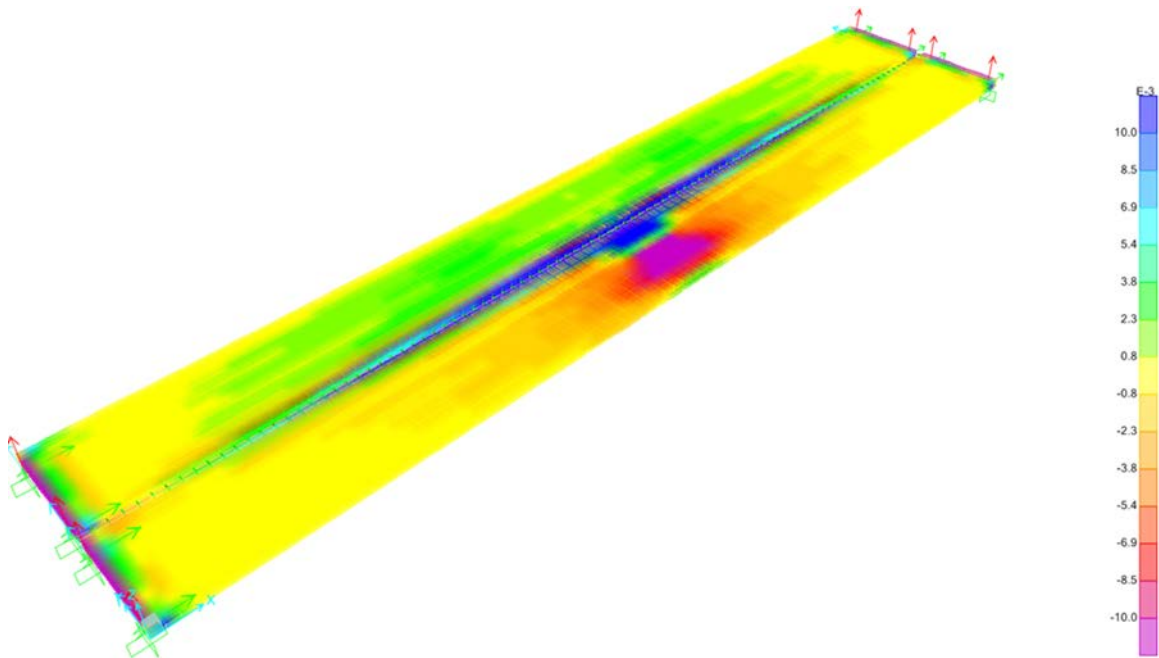


Figure H-9: S_{23} Stress Contours – “Proposed” Specimen with Diaphragms

APPENDIX I: ADDITIONAL LITERATURE REVIEW

I.1: Fatigue Evaluation of Longitudinal U-Bar Joint detail

Zhu, P., Ma, Z., and French, C. (2012). "Fatigue Evaluation of Longitudinal U-Bar Joint Details for Accelerated Bridge Construction." *J. Bridge Eng.*, 17(2), 201–210.

This study is similar to the headed bar joint detail in decked bulb tee girders. For this study continuous longitudinal U-bar joint details are investigated. Four specimens with the U-bar and closure pour detail were tested under static and fatigue loading. The loading demand necessary in the slab fatigue testing was determined on the basis of 3D finite-element study. Test results were evaluated on the basis of flexural capacity, curvature behavior, cracking, and steel strain. The fatigue loading was found to have little influence on the U-bar joint behavior. In general, crack widths were small at the service load level. No debonding between the slab and the joint was noticed. Because the closure-pour material was cast-in-place and had a relatively short curing time for the purpose of accelerated construction, it was very important to control its strength variation. The U-bar joint detail is a viable connection system for the longitudinal joint in bridge decks.

Specimen:

The U-bar detail is shown below in Figure I.1-1 and Figure I.1-2. Four specimens were constructed. Each specimen consisted of two panels. Each panel had dimensions 72 in x 64 in x 6.25 in. The #5 U-bars projected out of the slab to splice with the U-Bars in the adjacent slab. The spacing was 4.5" and the overlap of the U-bars was 6". U-bars near the joint were instrumented with strain gauges.

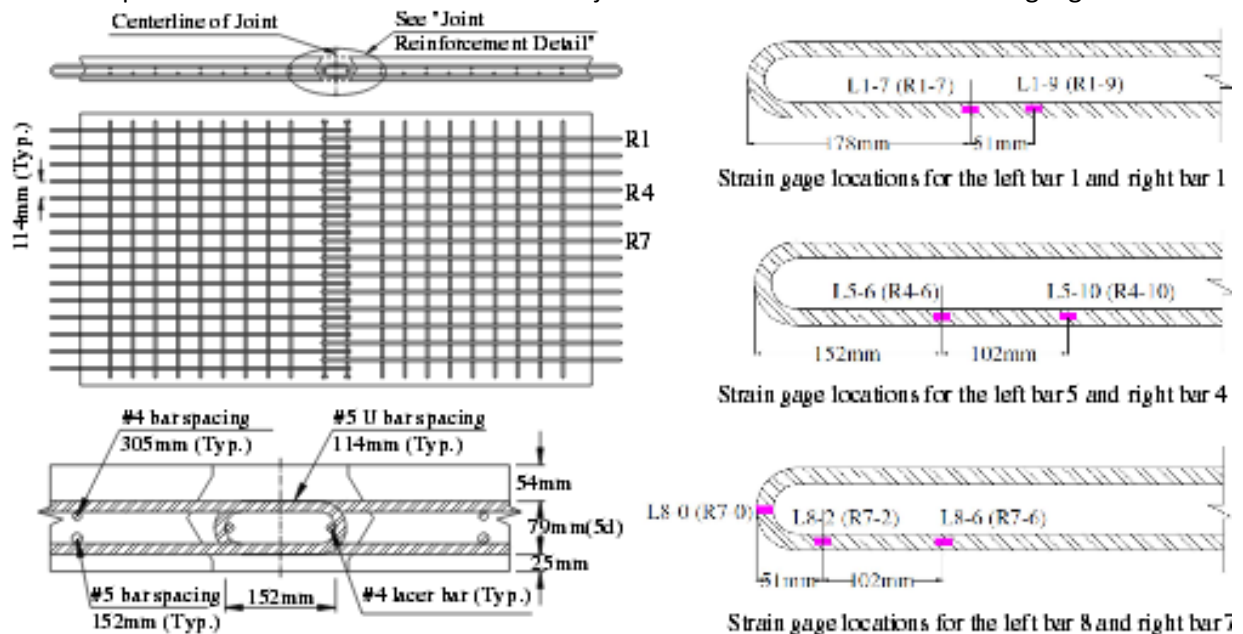


Figure I.1-1 U-Bar detail



Figure I.1-2 U-Bar specimen

Loading:

The author first used a Finite Element Model (FEM) to model the system and determine maximum loads to be used for the specimens.

Four specimens were tested under different loading conditions:

- 1) Pure flexure static load
- 2) Flexure and shear static load
- 3) Pure flexure fatigue load
- 4) Flexure and shear fatigue load

All the specimens were simply supported and LVDTs were used to measure displacement. The static loads were applied in increments. Two million cycles were applied at four Hz. At 0.5, 1, 1.5, and 2 million cycles, static load tests were performed.

Conclusions:

- 1) Fatigue loading had little impact on U-bar joint behavior.
- 2) The U-bar detail performed better than the headed bar detail in terms of moment capacity and service-level crack widths. Also, the U-bar joint zone is less congested than the headed bar detail.
- 3) Cracks were observed at the grouted joint and concrete slab interface. These cracks formed above the service load level and below the service load level depending on the specimen. Cracks were less than 0.15mm at service load. Cracks formed at a smaller rate compared to the headed bar test.
- 4) All specimens exceeded calculated capacity. The U-bar detail is a viable detail for longitudinal joints between decked bulb tee flanges.

I.2: Design, Construction, and Field Testing of an Ultra-High Performance Concrete Pi-Girder Bridge

Rouse, J., Wipf, T., Phares, B., Fanous, F., Berg, O. (2011) "Design, Construction, and Field Testing of an Ultra-High Performance Concrete Pi-Girder Bridge." Iowa State University, Ames, IA.

The Jakway Park Bridge in Buchanan County Iowa was constructed with the second generation "Pi" girder. The precast prestressed pi-girder is composed of Ultra-High Performance Concrete (UHPC). The cross section is shown below in Figure I.2-1. The study explored lab tests and live load field tests to look at the behavior of the beam and compare it to the finite element analysis performed.

Girder:

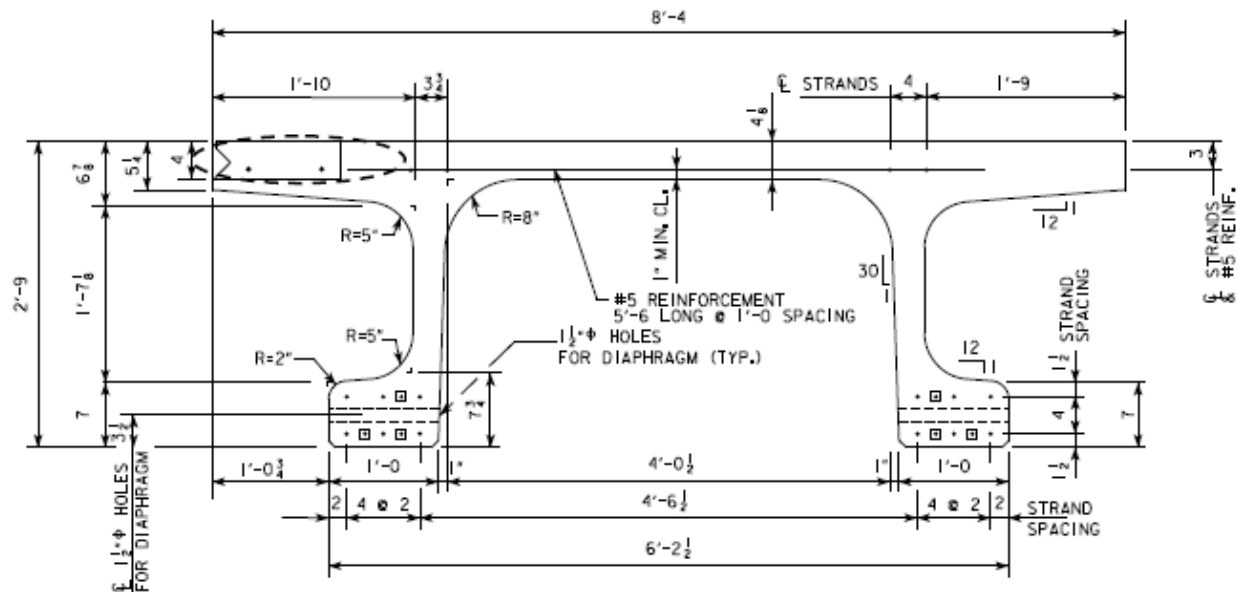
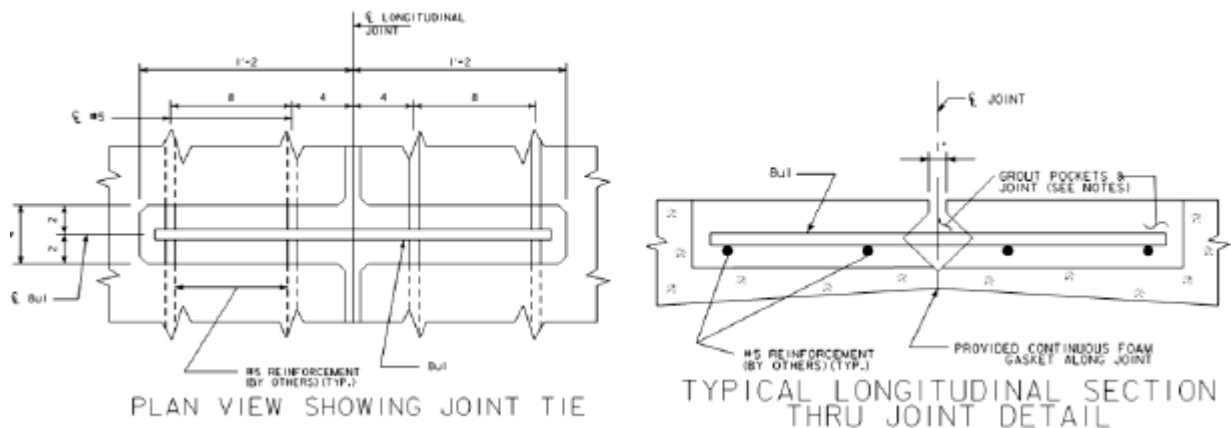


Figure I.2-1 Details of Pi girder

The pi-girders used for the bridge were 50' in length and three 8' 4" wide. The girders had cast-in-place end diaphragms and steel HSS intermediate diaphragms at the quarterspan and midspan. Girders were placed on neoprene bearing pads.

Shear key:

A cast in place shear key was used to connect adjacent girders at the deck level. #8 bars were also placed in "blocked out" grout pockets as shown in Figure I.2-2.



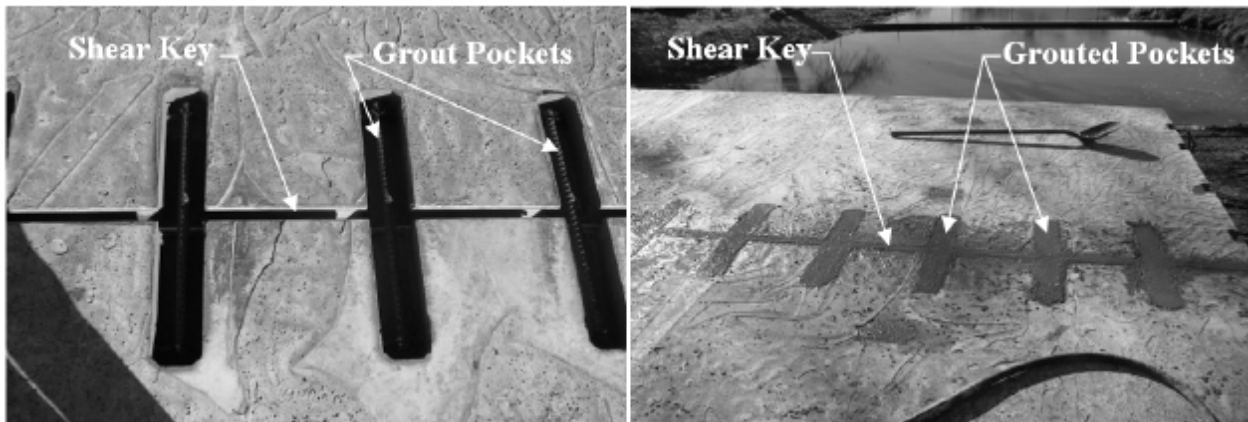


Figure 1.2-2 Grouted shear pockets in Pi girder

Instrumentation:

The girders were tested in the field and instrumented with 32 surface mounted strain gauges and six displacement gauges. Displacement was measured at mid-span.

Testing:

The compressive strength of the concrete and modulus of rupture of the UHPC were tested in the lab and found to be 28,000 psi and 1,800 psi respectively. Field tests were performed in 2008 and then one year later in 2009 to determine if the bridge was behaving similarly. The live load for the test included a 60,000 lb dump truck driven over predetermined paths that varied from edge to edge of the bridge width. For the first set of tests in 2008, the intermediate HSS diaphragms were disconnected and then connected for the second set of tests in 2008 to determine their contribution to live load distribution.

Conclusions:

- The new bridge girder is performing well and is an effective option for medium span bridges with accelerated construction schedules.
- Only very slight changes in structural behavior were noticed in the first year of service.
- Girders have lateral distribution factors of between 0.62 and 0.72.
- Steel diaphragms are not very effective in improving the live load distribution between pi-girders

I.3: Development of the Northeast Extreme Tee (NEXT) Beam for Accelerated Bridge Construction (ABC)

Culmo, M. and Seraderian, R. (2010) "Development of the Northeast Extreme Tee (NEXT) Beam for Accelerated Bridge Construction (ABC)." *PCI Journal*, Summer 2010, Chicago, IL.

The NEXT beam is a regional standard that was developed by the northeast state department of transportations and local precast manufacturers. It is non-proprietary and NEXT Beam was being produced by 4 PCI certified producers as of 2012.

Two different details for the NEXT beam exist, they are the D Beam and the F Beam.

The F Beam (Flange Beam) is a beam with a partial-depth flange which serves as the formwork for a conventional cast-in-place reinforced concrete deck (Figure I.3-1, shown below). F beam has the advantage of a monolithic deck surface at the expense of a few extra days of site construction.

Shown below.

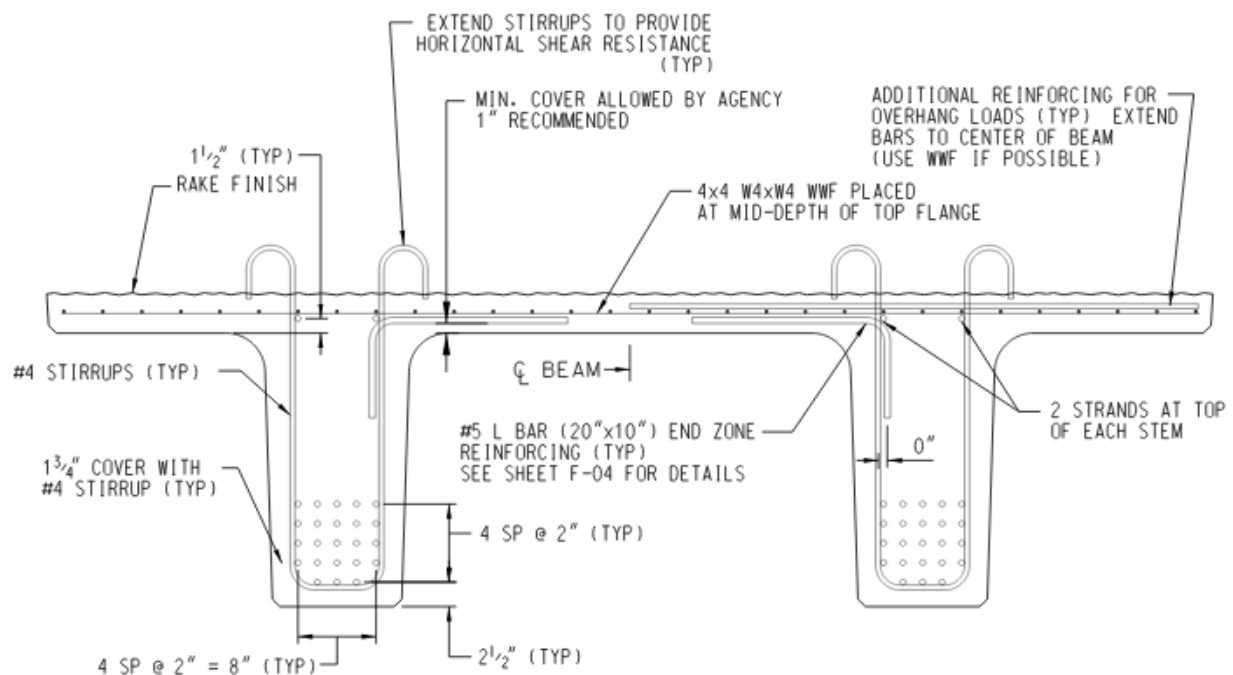


Figure I.3-1 NEXT F Beam

The D Beam (Deck Beam) is a beam with an integral full-depth flange that acts as the structural bridge deck (Figure I.3-2). This allows the bridge to be ready for traffic soon after the beams are placed.

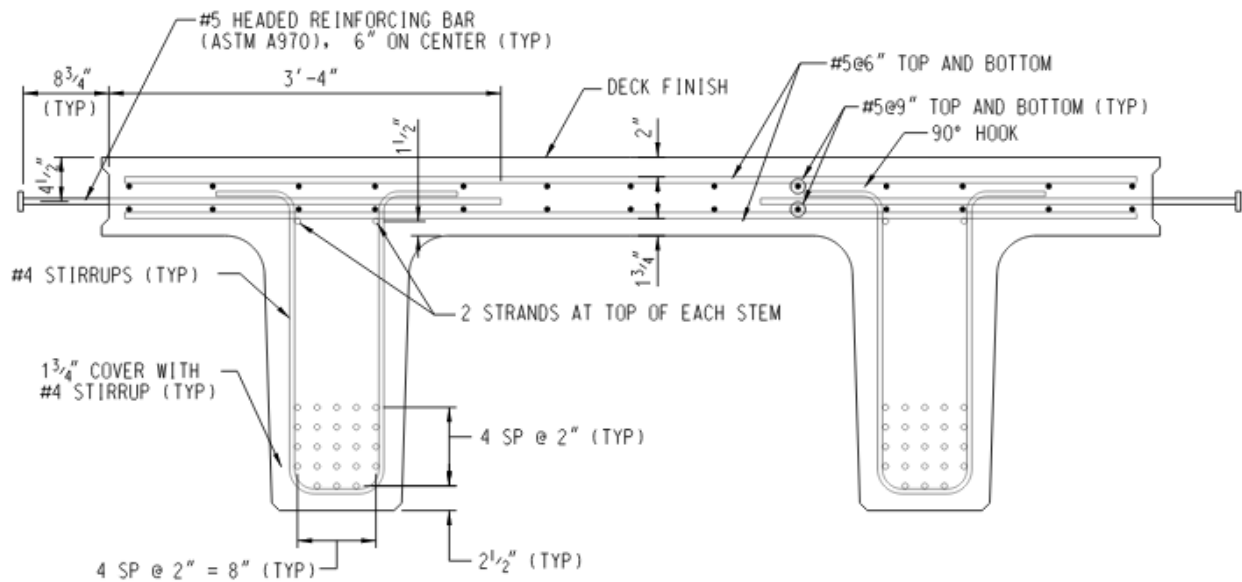
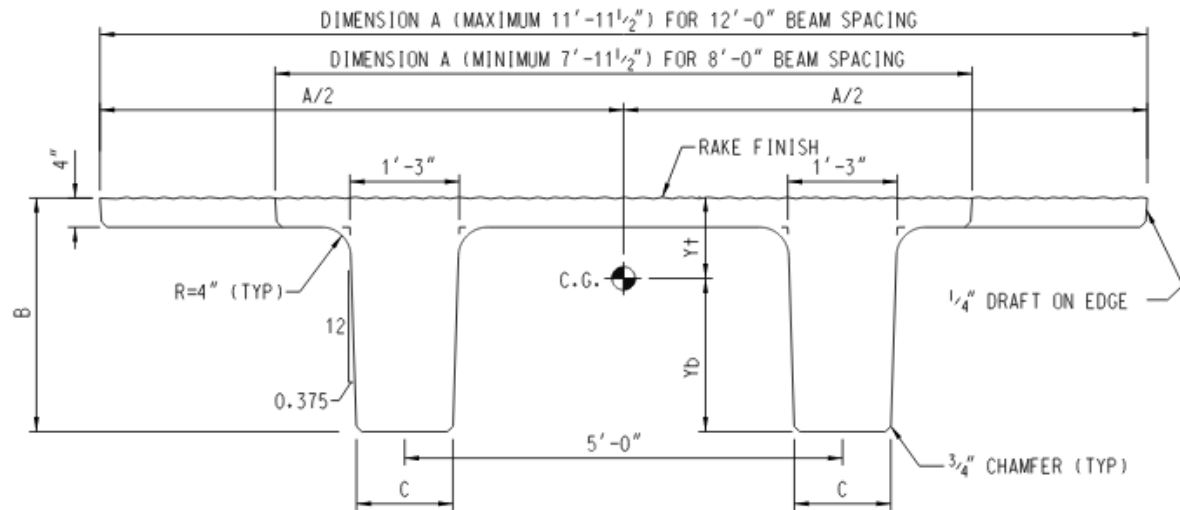


Figure I.3-2 The D Beam

The longitudinal joint between the D Beams was based on research performed on decked bulb tee beams. Headed reinforcement is placed below mid-depth to provide more moment capacity. The joint provides continuity and seal from infiltration. The joint was tested through two million cycles of loading and then successfully subjected to a ponding test.

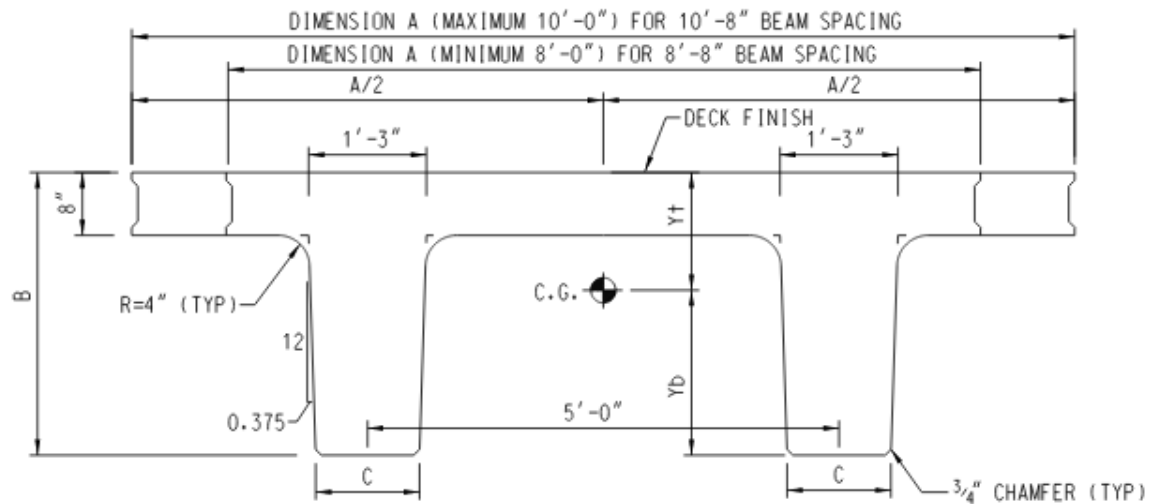
The NEXT Beams have depths ranging from 24" -36" and widths ranging from 8' to 12'. Spans range from 30' to 90'. The NEXT Beam is well suited for accelerated bridge construction.

Section Properties:



NEXT BEAM - SECTION PROPERTIES											
BEAM DESIGNATION	BEAM WIDTH INCHES	BEAM DEPTH INCHES	BASE WIDTH INCHES	STEM WIDTH INCHES	AREA IN ²	I IN ⁴	Yb INCHES	Y+ INCHES	S+ IN ³	Sb IN ³	WEIGHT PLF
	A	B	C				D	E			
MINIMUM WIDTH BEAMS											
NEXT 36 F	95.50	36.00	13.00		1287	160240	21.77	14.23	11261	7361	1341
NEXT 32 F	95.50	32.00	13.25		1182	115813	19.51	12.49	9272	5936	1231
NEXT 28 F	95.50	28.00	13.50		1075	79901	17.24	10.76	7426	4635	1120
NEXT 24 F	95.50	24.00	13.75		966	51823	14.95	9.05	5726	3466	1006
MAXIMUM WIDTH BEAMS											
NEXT 36 F	143.50	36.00	13.00		1479	185525	23.36	12.64	14678	7942	1541
NEXT 32 F	143.50	32.00	13.25		1374	134258	20.98	11.02	12183	6399	1431
NEXT 28 F	143.50	28.00	13.50		1267	92661	18.57	9.43	9826	4990	1320
NEXT 24 F	143.50	24.00	13.75		1158	60045	16.12	7.88	7620	3725	1206

Figure I.3-3 Section Properties for NEXT F Beam



NEXT BEAM - SECTION PROPERTIES										
BEAM DESIGNATION	BEAM WIDTH INCHES	BEAM DEPTH INCHES	BASE WIDTH INCHES	AREA IN ²	I IN ⁴	Y _b INCHES	Y _t INCHES	S _t IN ³	S _b IN ³	WEIGHT PLF
	A	B	C			D	E			
MINIMUM WIDTH BEAMS										
NEXT 40 D	96.00	40.00	13.00	1666	238059	25.47	14.54	16378	9348	1735
NEXT 36 D	96.00	36.00	13.25	1562	176674	23.03	12.97	13624	7671	1627
NEXT 32 D	96.00	32.00	13.50	1455	126111	20.57	11.43	11033	6131	1516
NEXT 28 D	96.00	28.00	13.75	1346	85651	18.06	9.94	8620	4742	1402
MAXIMUM WIDTH BEAMS										
NEXT 40 D	120.00	40.00	13.00	1858	258171	26.55	13.45	19201	9722	1935
NEXT 36 D	120.00	36.00	13.25	1754	191453	24.01	11.99	15973	7973	1827
NEXT 32 D	120.00	32.00	13.50	1647	136502	21.44	10.57	12920	6368	1716
NEXT 28 D	120.00	28.00	13.75	1538	92597	18.80	9.20	10069	4924	1602

Figure I.3-4 Section Properties of NEXT D Beam

I.4: Structural Performance of Precast/Prestressed Bridge Double-Tee Girders Made of High-Strength Concrete, Welded Wire Reinforcement, and 18-mm-Diameter

Maguire, M., Morcos, G. and Tadros, M. (2013) "Structural Performance of Precast/Prestressed Bridge Double-Tee Girders Made of High-Strength Concrete, Welded Wire Reinforcement, and 18-mm-Diameter." *Journal of Bridge Engineering*, Vol. 18, No. 10, pp. 1053-1061.

The high-strength precast prestressed double-tee girders are composed of high-strength concrete (103 MPa). To evaluate the high-strength, two full-scale 15.24 m long, 1.21 m wide, and 0.5 m deep single Tee girders were fabricated and then tested at the University of Nebraska. Transfer length, development length testing, flexural capacity testing and vertical and horizontal shear transfer testing were conducted on each specimen. Preliminary design charts for different girders have been produced already.

The concrete used for the girder was Nebraska high-strength concrete (NUHSC). The NUHSC selected for the double tee was a self-consolidating concrete.

The girders were fabricated as two single tee specimens that were cast in the standard double tee form. A 1.2mm CIP deck was poured on the samples prior to testing. Six tests were conducted:

- 1) Investigate flexural and shear capacity of the girder
- 2) Evaluate the interface shear between girder deck and CIP deck
- 3) Compare transfer and development length of 18 mm strands

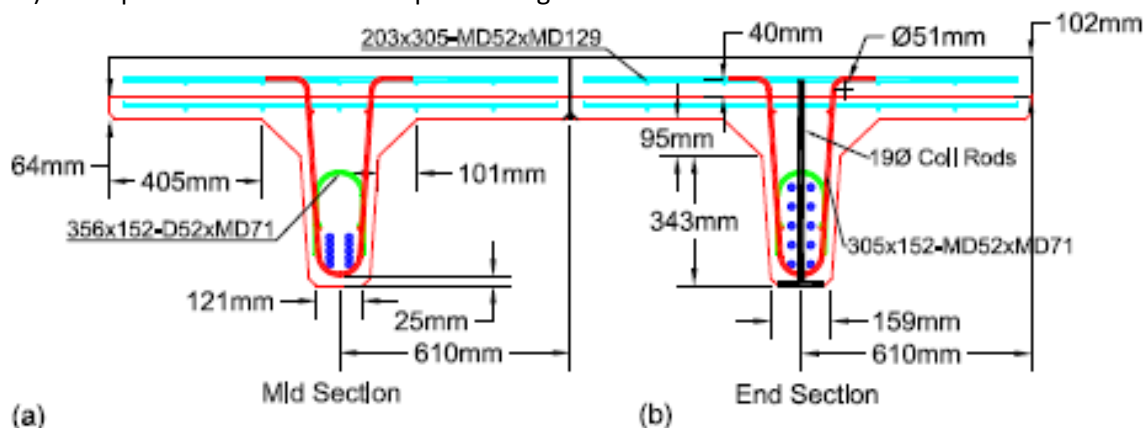


Figure I.4-1 Cross section for double tee

Conclusions

Flexure and shear capacity predicted by AASHTO LRFD specifications are applicable to the proposed bulb double tee girders.

The interface between NUHSC BDT and CIP concrete deck does not contribute to the horizontal shear resistance and should be considered smooth surface unless appropriate interface roughening is achieved.

The BDT girders can result in a span-to-depth ratio of 33 while being economical to fabricate and construct.

I.5: Cast-in-Place Concrete Connections for Precast Deck Systems

French, C., Shield, C., Klaseus, D., Smith, M., Eriksson, W., Ma, Z.J., Zhu, P., Lewis, S., and Cheryl E. Chapman (2011) "Cast-in-Place Concrete Connections for Precast Deck Systems." NCHRP Project 10-71, Report No. 173, Transportation Research Board, Washington, D.C..

Detail U-bar:

The entire project focused on three objectives: 1) a precast composite slab span system (PCSSS) for short to medium bridge spans, 2) Full-depth prefabricated concrete decks, and 3) deck joint closure details for decked-bulb-tee (DBT) flange connections. This summary only focuses on objective three. I did not include objective one because it involves delivering fresh concrete to the site, which has definitely been ruled out. The study also included an extensive investigation of closure pour (grouts) that could be used.

Five different connections were initially proposed in the study, three were ruled out initially and the headed bar and U-bar details were tested further (NCHRP 12-69 tests headed bar detail). The other three details were not discussed extensively, and no details were provided in the report. The issue with the U-bar detail is the tight bend radius to accommodate a bridge deck with proper cover. The minimum radius allowed by ACI is $6d_b$ for conventional reinforcing steel. For the study a bend radius of $3d_b$ was used with a deformed wire reinforcement (DWR), because it is more ductile than conventional steel. Stainless steel was also considered as an alternative material for the U-bar detail but was later ruled out after initial testing due to its higher cost relative to the deformed wire reinforcement.

Closure Pour (grout):

Four overnight cure and four 7-day cure grouts were proposed and studied.

Testing: Freeze/thaw durability, shrinkage, bond, and permeability test.

An overnight cure grout with no extension (aggregate) was used to test the U-bar detail and a 7-day grout with 60% extension was used in the joint of the U-bar detail. Both were non-shrink grout. They also developed a design matrix based on environmental conditions to select joint closure material.



Figure I.5-1 U Bars at Joint